Addis Ababa University

Addis Ababa Institute of Technology (AAiT)

School of Electrical and Computer Engineering

Design and simulation of sensorless control for nine-phase BLDC motor using back-EMF

By

Abraham Mesfin

A thesis submitted to the School of Graduate Studies of Addis Ababa University in partial fulfillment of the requirement for the Degree of Master of Science in Electrical Engineering (Control)

Advisor

Dr. Mengesha Mamo

October, 2017

Addis Ababa, Ethiopia

Addis Ababa University
Addis Ababa Institute of Technology
School of Electrical and Computer Engineering

Design and simulation of sensorless control for nine-phase BLDC motor using back-EMF

By

Abraham Mesfin

Approval by Board of Examiners

Chairman, Department Graduate Committee	Signature	Date
Dr. Mengesha Mamo Advisor's Name	Signature	Date
Internal Examiner	Signature	Date
External Examiner	Signature	Date

Declaration

I declare that this thesis was composed by myself, that the work contained herein is my own except where explicitly stated otherwise in the text, and that this work has not been submitted for any other degree or professional qualification.

Abraham Mesfin _____

Name signature

Addis Ababa, Ethiopia _____

Place Date of Submission

This thesis has been submitted for examination with my approval as a university advisor.

Dr. Mengesha Mamo _____

Advisor's Name Signature

Acknowledgment

Next to the Almighty God, I would like to express my genuine gratitude to my advisor Dr. Mengesha Mamo, I am thankful for his guidance, support and constructive help during my work. His guidance during all phases of this study was invaluable. Besides, I would like to thank all my friends for their encouragement throughout my work. Last but not least, I would like to thank my precious parents for their great support and love during my study.

Table of contents

List of Acronyms

DC	Direct Current
AC	Alternating Current
DSP	Digital Signal Processor
FOC	Field Oriented Control
DTC	Direct Torque Control
VSI	Voltage Source Inverter
PI	Proportional Integral
SVM	Space Vector Modulation
MMF	Magneto motive force
PWM	Pulse Width Modulation
PID	Proportional Integral Derivative
CSI	Current Source Inverter
IGBT	Insulated Gate Bipolar Transistor
PM	permanent magnet
BLDCM	brushless direct current motor
PMSM	permanent magnet synchronous motor
EM	Electro magnetic
EMF	Electromotive force
BEMF	Back electromotive force
PMBLDCM-	permanent magnet brushless direct current motor
ZCD	zero cross detection
EV	Eectric Vehicles
HEV	Hibrid Eectric Vehicles

List of Symbols

ω_r	Rotor speed
ω_e	synchronous speed
ω_a	Arbitrary speed
P	Differential operator
V	Voltage
I	Current
R	Resistance
L	Inductance
M	Mutual inductance
E_{an}, E_{bn}, E_{cn},… E_{in}	Stator-phase Back-EMF
λ	Flux
θ_r	Rotor flux angle
Te	Electromagnetic torque
J	Moment of inertia
B	Frictional coefficient
T_L	Load torque
P	Pole pairs
K_p	Proportional gain
K_i	Integral gain
e(t)	Error signal
u(t)	Actuating signal
V_A,V_B,V_C, V_D, V_E, V_f, V_g	Inverter leg voltages
v_{an}, v_{bn}, v_{cn}, v_{dn},v_{en},v_{fn},v_{gn},	Phase to neutral voltages
V_{Nn}	Voltage between star point of load and negative rail of dc bus
Vdc	DC link voltage
S_1, S_2, S_3,…S_{18}	Switching function

List of Figures

List of Tables

Abstract

The interest in multi-phase machines for high performance applications has been growing in recent years due to their potential advantages over the conventional three-phase machines. Multi-phase machines have advantages of fault tolerance and higher power capacity at low voltages compared to three-phase machines. Nine-phase brushless DC motor has additional advantages of high torque density, high efficiency and reduced stator current per phase without the need to increase the phase voltage. Sensored control of BLDC machine generally requires measuring the speed and position of rotor by using the sensor. The position sensors make the motor system more complicated, mechanically unreliable and expensive. In this thesis, effective sensorless control of nine-phase BLDC motor using Back-EMF waveform sensing is done. Thus, actual implementation of the motor using mathematical model of the machine and nine-phase inverter function based on the back-EMF sequence generated in the stator windings of nine-phase BLDC motor is simulated with the help of MATLAB Simulink software.

For control of the motor PI speed controller is implemented to adjust DC-link voltage based on the error between actual speed and desired speed reference. The controlled gain output of the PI controller is fed to the pulse amplitude modulation controlled DC-link voltage source. The result of the controller is investigated and the speed of the motor for different speed level using MATLAB Simulink software. And the result of the simulated speed response of the controller for different speed has been done and settling time is 0.005sec and rise time is 0.0026sec speed response controller. Phase voltages of the motor controlled based on the back-EMF waveform sequances . switching of nine-phase voltage source inverter controlled has been done efectively based on the back-EMF. The simulation results obtained agree with the design objective.

Keywords: Multiphase machine, eighteen-step inverter, nine phase BLDCM, sensorless control, back-EMF, zero-cross detection, commutation logic.

CHAPTER 1

INTRODUCTION

1.1 Background

The field of multi-phase machines, though not new, is becoming an area of growing interest in recent years due to the wider range of possibilities. The initial motivation for the study of multi-phase machines was the search for a reduction in the machine torque ripple. This is based on the fact that current harmonics that produce torque ripple in three phase machines are reduced or eliminated as the number of phases is increased. Multiphase motors are more fault tolerant comparing with conventional three phases. The motor can be operated normally if one or more phases are failed. [1-3].

BLDC motor have some advantages comparing with brush dc motors and induction motors. The use of strong permanent magnets energy wastage of motor is less so the efficiency will be high. These motors are less weight, volume, high reliability, less noise and less maintenance. Due to these advantages, the use of BLDC motor is growing rapidly in various applications [3]. The BLDC motor is sometimes referred to as an inside out DC motor because its armature is in the stator and the magnets are on the rotor and its operating characteristics resemble those of the dc motor [4], instead of using a mechanical commutator as in the conventional dc motor, the BLDC motor employs electronic commutation which makes it a virtually maintenance-free motor. Thus, multiphase motor drive. can be good choice where high reliability and power density required. In areas such as aerospace, ship propulsion, military applications where requirements are not oppressive when compared with overall demands [2]. The rotor position is dedicated either by position sensors or by sensorless techniques. BLDC motors have many advantages over conventional dc motors, a few of these are [3]:

- Long operating life
- High dynamic response
- High efficiency
- Better speed Vs. torque characteristics
- High speed range
- Higher torque-weight ratio

Permanent magnet machines have been used in the last three decades. They appear in several different stator and rotor structures and can be used in almost all kinds of application where traditional machines are used. Their main features and advantages are: No electrical energy is absorbed by the field excitation system and thus there are no excitation losses which mean substantial increase in efficiency, high torque/volume relationship, better dynamic performance than motors with electromagnetic excitation, simplification of construction and maintenance. Unfortunately, some of these advantages refer only to machines built with high energy magnets, which are still expensive, despite the introduction of new materials and improved production techniques. This feature has restricted the use of permanent magnet machines built with rare earth magnets to applications where cost is of secondary concern [4-5].

Modeling and analysis of multi-phase machines have been an issue for research as early as 1950s [6]. However, they have attracted the attention of many researchers recently due to their fault tolerance and their high-power capability at low voltage as compared to the conventional three-phase machines [7-9]. The interest in multi-phase motor drives has increased in recent years due to several advantages when compared to three-phase drives [6-8]. Some of these advantages are known from the early days of the multiphase drives [8], although they have recently considered with high-level analysis [9]. These advantages are inherent to the own structure of the machine, and include less torque ripple, less acoustic noise and losses, reduced current per phase or increased reliability due to the additional number of phases [8-10]. These advantages make multi-phase drives suitable for high power/current applications such as EV/HEVs, traction or electric ship propulsion. Apart from these benefits, there are further possibilities due to the additional degrees of freedom existing in multi-phase machines. The high torque capability of multi-pole machines by using the higher harmonic currents for torque generation and the desirability of such capability in application such as electric vehicle drive, elevators, and military hardware drives are other impetus for the interest of researchers in this area. The advent of static power converters and microcontrollers have also contributed to the interest, as it is now possible to generate a power supply at any number of phases controlled at a desired waveform and magnitude. In the figure 1.1 n-phase two-level voltage source inverter is given. Where S_1, S_3, S_5, … $S_{(2n+1)}$ are all the upper switches of the n-phase inverter and S_2, S_4, S_6, … S_{2n} are the lower leg switches of the n-phase

inverter. The terminal voltage (Van, Vbn, Vcn…. Vxn) represented the voltage terminal voltage of the inverter leg measured from reference neutral point N.

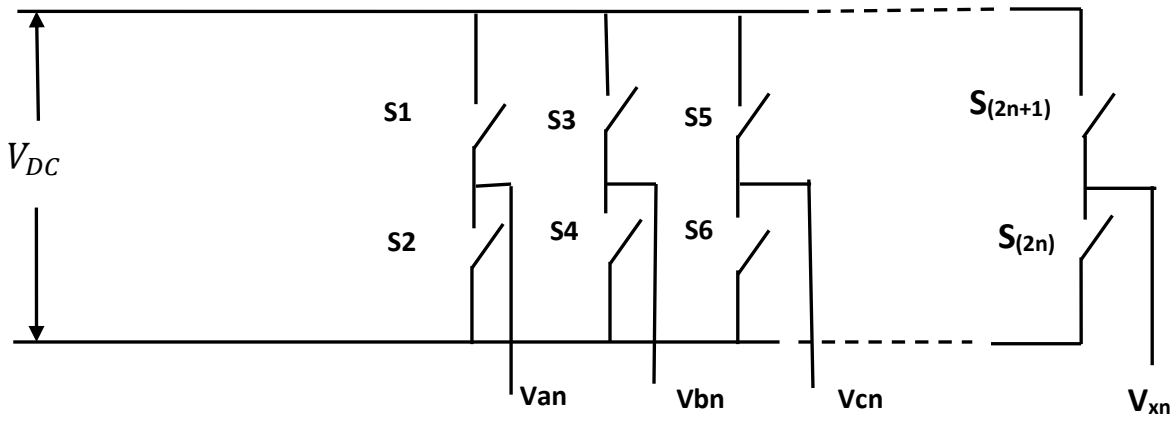

Fig. 1.1 n-phase two-level voltage source inverter

Multiphase machine has high torque capability of multi-pole machines by using the higher harmonic currents for torque generation. In a five-phase machine the third harmonic current can be used to generate an average torque in addition to the fundamental [7]. In the seven-phase machine the third and the fifth harmonic current is controlled to generate the average torque. In the nine-phase machine the third, the fifth and the seventh harmonics can be controlled to generate average torque which add-up with the torque generated by the fundamental component current [7].

1.2 Statement of the Problem and Motivation

Sensored control of BLDC machine generally requires measuring the speed and position of rotor by using the sensor. The position sensors make the motor system more complicated, mechanically unreliable and expensive. Accurate speed information is crucial for a sensorless speed control of permanent magnet synchronous motor drives. This thesis presents sensorless control method based on the fact that the rotor position can be detected by using back-EMF produced in permanent magnet synchronous motors. Instead of using sensors like Hall sensor, the motor itself tell us which phase should be energized. The sensors can also cause problems in terms of reliability as they are sensitive to shock and vibration. A sensor connected through long cables can also be sensitive to disturbances. To reduce cost and improve reliability such position sensors may be eliminated. The question then arises why nine-phase drive required compared to conventional three-phase drive.

The answer lies in the fault tolerant characteristic, reliable and higher efficiency of nine-phase drive compared to the conventional three-phase machine. Specially, in fault tolerance the motor keeps working at good performance even though two or more phases fail which is not possible in three phase motors.

1.3 Objective of the thesis

1.3.1 General objective

The main objective of the thesis is design and simulation of sensorless control for nine-phase BLDC motor using induced back-electromotive force.

1.3.2 Specific objective

These are some of the specific objectives of the thesis

- Study the construction futures of nine-phase BLDC motor.
- Model and develop nine-phase BLDC motor using MATLAB/Simulink software.
- Design nine-phase voltage source inverter based on the orating mode of the motor.
- Design, analyze and simulate the proposed sensorless control based on the back-EMF waveform produced in nine phases stator windings of 9-phase BLDC motor
- Study the result of simulated nine-phase BLDC motor control

1.4 Significance of the Thesis

The main significances of the thesis are listed as follows:

- Shows simple way of controlling sensorless multi-phase BLDC synchronous machine.
- The model and simulation for sensorless control of the BLDC motors based the back-EMF zero cross detection method can be applied for different applications.
- The other significance of this thesis, this work can be used for as reference for future further studies.

1.5 Methodology

- **Literature review:** some related references will be scanned and quoted so that it can be used as the forward stepping movement in the future time. Study model and analysis of the sensorless control of the conventional permanent magnet motor revised.
- **System modeling and analysis:** in this section, first; design futures of nine-phase permanent magnet BLDC synchronous motor analyzed. The model of the nine-phase machine is design in the MATLAB simulation in order to do the major task which is the sensorless control of the machine. From the mathematical mode, the equation of the back-EMF is design. Second; model and analysis of sensorless control of nine-phase BLDC motor based on the back-EMF zero crossing detection (ZCD) present.

1.6 Thesis organization

This thesis is organized in to six chapters including this chapter, Chapter 2, multiphase machines literature reviews different kinds of control technique of multiphase machine are revised. Chapter 3, mathematical modeling of nine phase BLDC motor and derived the mathematical equation of the machine based on the different assumption. Chapter 4, sensorless control of BLDC using back electromotive force produced in the unexcited phase is modeled analyzed and the zero-cross detection(ZCD) of the back-EMF is presented and the switching sequence of the nine phases two-step nine-phase inverter deigned based on the zero-cross sequence of back-EMF. Chapter 5, MATLAB simulation and discussion presented, here in this chapter MATLAB simulation model is presented and prepare block model of the proposed model control in the MATLAB Simulink library and simulation of sensorless control is present and result discussion and observation studied according to the desired output of the machine and the strength of the system and the drawback of the proposed system is mentioned. Chapter 6, conclusion and recommendation of the thesis and, the direction for the future work mentioned and recommended presented.

CHAPTER 2

LITERATURE REVIEW

2.1 Introduction

Variable-speed AC drives are nowadays invariably supplied from power electronic converters. Since the converter can be viewed as an interface that decouples three-phase mains from the machine, the number of machine's phases is not limited to three anymore. Nevertheless, three-phase machines are customarily adopted for variable speed applications due to the wide off-the-shelf availability of both machines and converters. Due to the six-step mode of three-phase inverter operation, one particular problem at the time was the low frequency torque ripple. Since the lowest frequency torque ripple harmonic in an n-phase machine is caused by the time harmonics of the supply of the order 2n±1 (its frequency is 2n times higher than the supply frequency), an increase in the number of phases of the machine appeared as the best solution to the problem. Hence, significant efforts have been put into the development of five phase and six-phase variable-speed drives supplied from both voltage source and current source inverters [12-13].

2.2 Types and advantages of Multiphase machine

The types of multiphase machines are in principle the same as their three-phase counterparts. There are induction and synchronous multiphase machines, where a synchronous machine may be with permanent magnet excitation, with field winding, or of reluctance type. Three phase machines are normally designed with a distributed stator winding that gives near-sinusoidal MMF distribution and is supplied with sinusoidal currents (the exception is the permanent magnet synchronous machine with trapezoidal flux distribution and rectangular stator current supply, known as brushless dc machine, or simply BLDCM). Nevertheless, spatial MMF distribution is never perfectly sinusoidal and some spatial harmonics are inevitably present [15].

Stator winding of an n-phase machine can be designed in such a way that the spatial displacement between any two consecutive stator phases equals $\boldsymbol{\alpha = \frac{2\pi}{n}}$, in which case a symmetrical multiphase machine results. This will always be the case if the number of phases is an odd prime number. However, if the number of phases is an even number or an odd number that is not a prime number, stator winding may be realized in a different manner, windings having a sub-phase each (where

n=a·k). Typically, a=3 (although a=5exists as well) and k=2,3,4, 5, … In such a case, the spatial displacement between the first phases of the two consecutive a sub-phase winding is $\boldsymbol{\alpha = \frac{\pi}{n}}$,, leading to an asymmetrical distribution of magnetic winding axes in the cross section of the machine (asymmetrical multiphase machines). In this multiphase machine type, there are k neutral points and these are typically kept isolated, for the reasons discussed later on [14].

Some of the advantages of multiphase machines, when compared to their three-phase counterparts, are valid for all stator winding designs while others are dependent on the type of the stator winding. Machines with sinusoidal winding distribution are characterized with the following [16-18].

- Fundamental stator currents produce a field with a lower space-harmonic content.
- The frequency of the lowest torque ripple component, being proportional to 2n, increases with the number of phases.
- Due to a larger number of phases, multiphase machines are characterized with much better fault tolerance than the three-phase machines. Independent flux and torque control requires means for independent control of two currents. This becomes impossible in a three-phase machine if one phase becomes open-circuited, but is not a problem in a multiphase machine as long as no more than (**n-3**) phases are faulted.

2.3 Multiphase machine control

High quality information about the rotor flux angle is crucial in field oriented control systems. The most common way to attain this information has been to add a dedicated sensor to the rotor shaft. This has a few disadvantages especially in drive systems used in automotive applications. Its physical size is a large drawback when designing the motor. The length of the machine is often critical due to constraints in the powertrain. This makes it sometimes impossible to fit a standard mechanical sensor. The sensors can also cause problems in terms of reliability as they are sensitive to shock and vibration. A sensor connected through long cables can also be sensitive to disturbances. A sensor fulfilling all requirements is often expensive. While, removing it would constitute an important cost reduction. A control system that not has to rely on a mechanical position sensor would therefore be favorable, a so called sensorless control system. Research on this has been done for many years and a lot of methods have been proposed. Many of them have been based on detection of the speed dependent back electromotive force (EMF). This work

satisfactory for medium and high speed but fails at low and zero speed. This as the back EMF is reduced with speed and is gradually lost.

Researchers have reported different models and control strategies for multi-phase machines. Authors of reference [13] have reported a nine-phase machine to be controlled as three independent three-phase machines. They assumed balanced system and used the model of conventional three-phase motors and have not used the advantage of controlling the higher harmonics for torque generation. Authors of reference [14] have generated a general model of a nine-phase synchronous machine with a cylindrical rotor and stator. A lot of works have focused on five-phase machine, probability, due to its relative simplicity next to three-phase machine. In reference [15], the authors have worked out the model of five phase machine. They have also indicated that their approach can be used for any number of phases. Reference [16] also has presented an analysis of a five-phase asymmetrical connected induction machine. Multi- Phase machines have advantages of fault tolerance and higher power capacity at low voltages compared to conventional three-phase machines. The methods of speed control of multiphase machines are in principle the same as for three-phase machines. Constant V/f control is nowadays of relatively little interest, since the cost of implementing more sophisticated control algorithms is negligible compared to the cost of multiphase power electronics and the multiphase machine itself (neither is available on the market). The emphasis is therefore placed further on vector control and DTC [17].

As long as a symmetrical multiphase machine with sinusoidally distributed stator winding is under consideration, the same vector control schemes as for a three-phase machine are directly applicable regardless of the number of phases [18]. The only difference is that the coordinate transformation has to produce an n-phase set of stators current references, depending on whether current control is in the stationary or in the synchronous rotating reference frame. If current control is in the stationary reference frame, $(n - 1)$ stationary current controllers (assuming stator winding with a single neutral point) are required. Either phase currents or phase current components in the stationary reference frame can be controlled and here the standard ramp-comparison current control method offers the same quality of performance as with three-phase drives [19]. Assuming that indirect vector control is used, basic rotor-flux-oriented control scheme of an n-phase induction or synchronous machine with sinusoidal MMF distribution is of the form shown in

Figure 2.1 The block "vector controller" is identical to the one for the three-phase machine of the same type and the value of the stator d-axis current reference depends on the machine type. For example, "vector controller" for a surface-mounted permanent magnet synchronous machine is just a speed controller, stator d-axis current reference is zero and transformation angle is the rotor position angle. In the case of an induction machine, stator d-axis current reference is the rated magnetizing current, while "vector controller" includes a speed controller, calculation of the angular slip speed and calculation of the transformation angle by summation of the slip angle and rotor position angle [15].

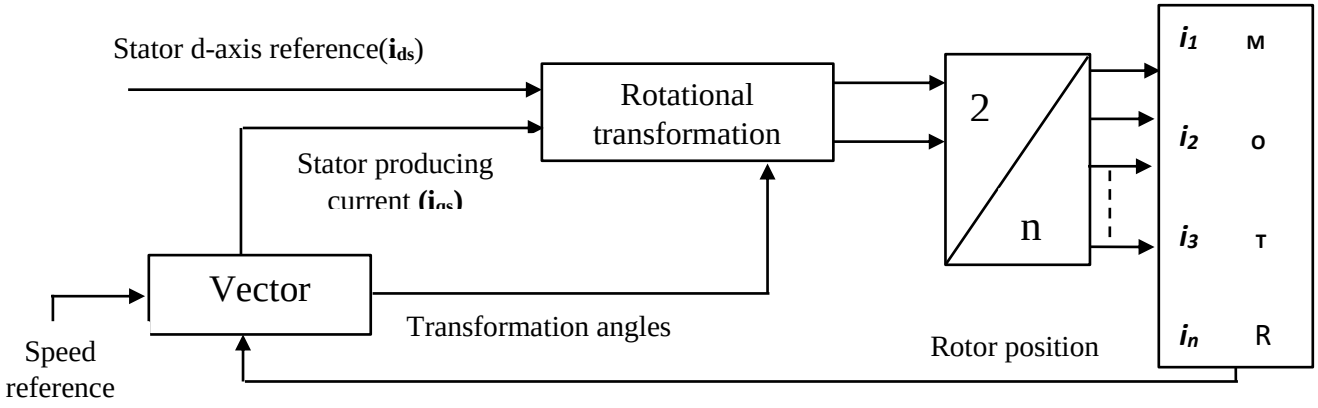

Fig. 2.1 Basic rotor flux oriented control scheme for multiphase machine with current control in the stationary reference frame [15]

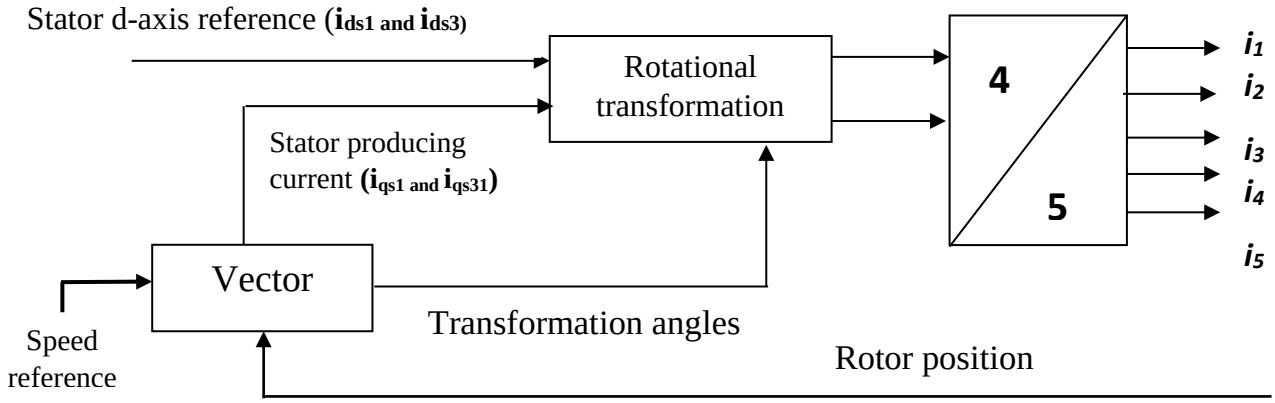

Fig. 2.2 Basic rotor flux oriented control scheme for five-phase machine with concentrated winding and with control in the stationary reference frame (indexes 1 and 3 stand for the first and the stator current harmonic reference) [15]

If a concentrated winding machine is used, torque can be enhanced using low-order stator current harmonic injection [20]. Hence, the vector control scheme has to be modified accordingly [21]. The injected low-order stator current harmonics are firmly tied to the fundamental in terms of magnitude, frequency and phase and the major modification of the vector control scheme consists in calculating the references for these harmonics on the basis of the fundamental and on utilization of the modified rotational transformation. Vector control schemes have to utilize again $(n - 1)$ current controllers. Vector control of concentrated winding machines is well-documented in literature for five-phase induction, permanent magnet synchronous, and synchronous reluctance machines, where torque enhancement is provided by the third harmonic injection. Similarly, third harmonic injection can be used in asymmetrical six-phase machines [22]. In a seven-phase machine both the third and the fifth harmonic can be used to improve torque per ampere characteristic [23], while with a nine-phase machine injection of the third, the fifth, and the seventh harmonic is possible [24]. A conceptual block diagram of a rotor flux oriented control scheme for a five-phase machine, assuming again current control in the stationary reference frame, is shown in Figure 2.2. The block "vector controller" now additionally includes partitioning of the overall torque reference (obtained at the output of the speed controller) into the stator *q*-axis current references for the first and the third stator current harmonic, as well as the calculation of the transformation angles for the first and the third harmonic.

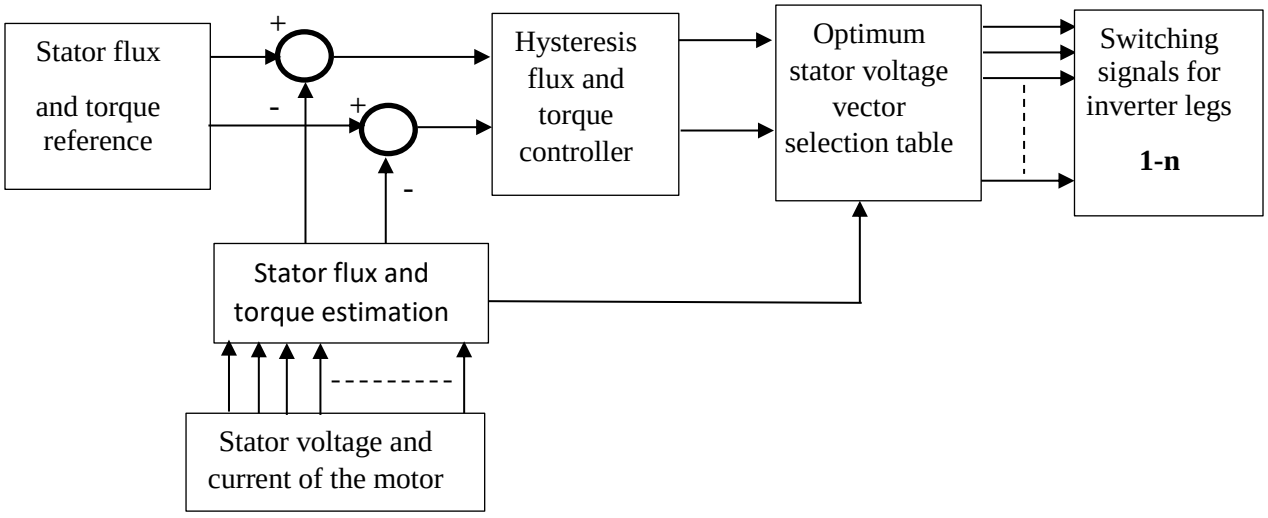

Fig. 2.3 illustration of DTC schemes for multiphase machines using switching table based DTC

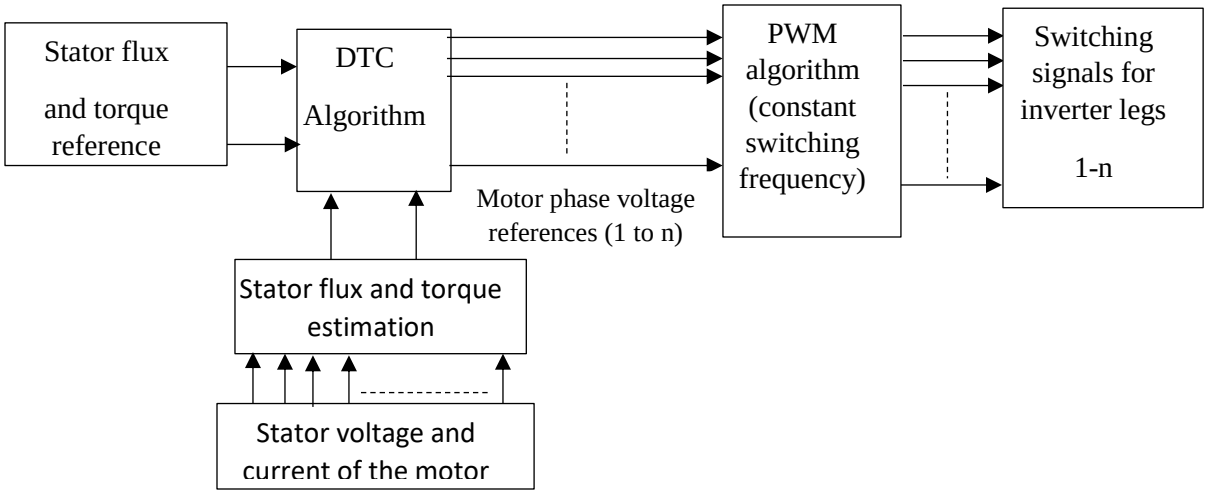

Fig. 2.4 DTC schemes for multiphase machines using constant switching frequency DTC [25]

Notice that the "rotational transformation" block in Figure 2.2 is different from the corresponding one in Figure 2.1. The outputs of this block are now four stator current components shown in Figure 2.2, which reflect the desired first and the third stator current harmonic. There are two basic approaches to DTC of three-phase machines. Hysteresis stator flux and torque controllers can be used in conjunction with an optimum stator voltage vector selection table, leading to a variable switching frequency. Alternatively, the inverter switching frequency can be kept constant by applying an appropriate method of inverter PWM control. In principle, both approaches are also applicable to multiphase machines [25] and are shown in Figure 2.4.

A problem that is encountered in hysteresis-based DTC schemes for sinusoidal multiphase machines is that optimum stator voltage vector selection table, designed in the same manner as for a three-phase induction machine, dictates application of a single space vector in one (variable) switching period. However, each individual inverter output voltage space vector inevitably leads to generation of unwanted low-order harmonics, which excite $x-y$ stator circuits and lead to large unwanted stator current low-order harmonics. This problem has so far not been solved completely although a significant improvement has been reported for an asymmetrical six-phase induction machine in [25]. A more detailed description of the control schemes shown in Figure. 2.4 and their detailed outlay for multiphase induction motor drives is available in [15] for asymmetrical six-phase and five-phase induction machines, respectively.

2.4 Multiphase voltage source inverter (VSI) Control

By and large, the existing research related to PWM control of multiphase inverters applies to two-level inverters [27]. The most straightforward approach is undoubtedly utilization of the carrier-based PWM methods. Similar to the carrier-based PWM with third harmonic injection for a three-phase VSI, it is possible to improve the dc bus utilization in multiphase VSIs by injecting the appropriate zero sequence harmonic (or adding the offset) into leg voltage references. Carrier based PWM is also suitable for control of concentrated winding machines, where in addition to the fundamental and zero sequence voltage, references also need to contain a certain amount of specified low-order harmonic(s) aimed at providing torque enhancement. In principle, carrier-based PWM can be used without any problems for generation of multi-frequency output voltages with any number of components. figure 2.5 shows nine-phase multiphase inverter

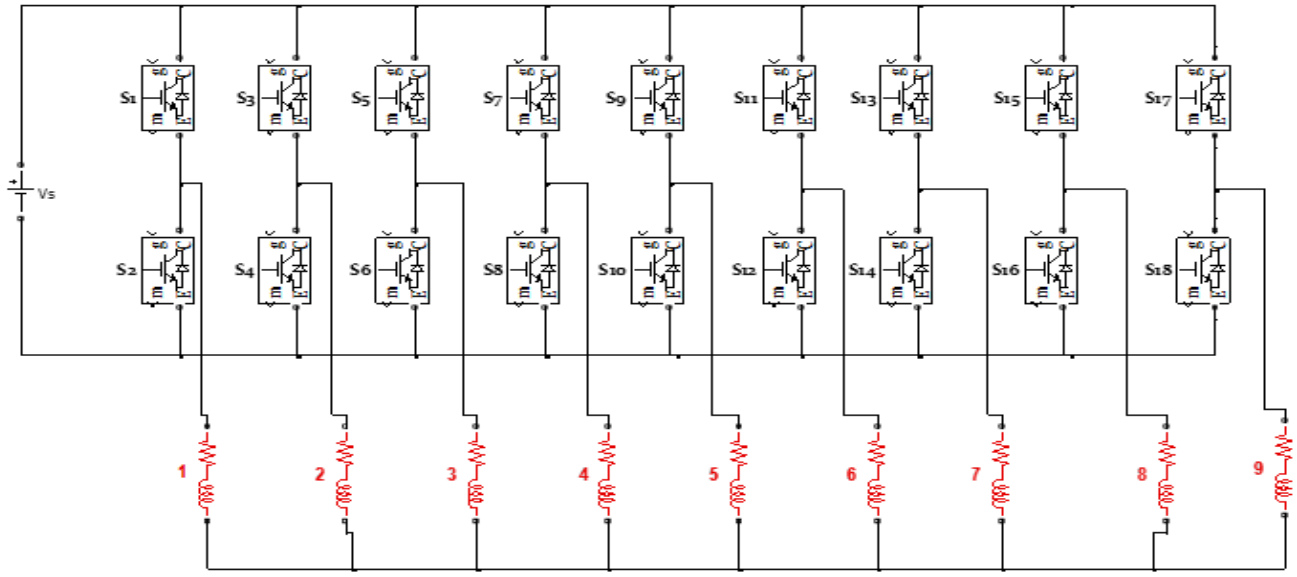

Fig. 2.5 nine-phase inverter connected to stator winding of the nine-phase BLDC motor

Space-vector PWM is undoubtedly the most popular method as far as the three-phase inverters are concerned. However, as the number of phases of the inverter increases, the available number of inverter output voltage space vectors changes according to the law $\mathbf{2^n}$**,** since there are $\mathbf{2^n}$ different switching configurations.

2.5 Review of control of BLDC motor

A BLDC motor is driven by voltage strokes coupled with the rotor position. These strokes must be properly applied to the active phases of the three-phase winding system so that the angle between the stator flux and the rotor flux is kept close to 90° to get the maximum generated torque. There are two methods of controlling BLDC motor one using rotor position sensor and the second one is sensorless control, in the following sub-topics explained these two methods are explained.

2.5.1 Sensored control of BLDC motor

Permanent magnet BLDC motor drives require a rotor position sensor to properly perform phase commutation. These motor is driven by voltage strokes coupled with the rotor position. These strokes must be properly applied to the active phases of the three-phases windings sequentially so that the angle between the stator flux and the rotor flux is kept close to 90° to get the maximum generated torque. Therefore, the controller needs some means of determining the rotor's orientation or position relative to the stator coils, such as Hall-effect sensors, which are mounted in or near the machine's air gap to detect the magnetic field of the passing rotor magnets. Each sensor outputs a high level for 180° of an electrical rotation for three-phase BLDC motor, and a low level for the other 180°. The three sensors mounted in the rotor of the three phase BLDC motor have a 120° relative offset from each other.

The process of switching the current to flow through only eight phases for every 60-electrical degree rotation of the rotor is called electronic commutation**.** The motor is supplied from a three-phase inverter, and the switching actions can be simply triggered by the use of signals from position sensors that are mounted at appropriate points around the stator. Similarly, to that of three phase BLDC motor in case of nine phase BLDC motor, when we mounted at 40 electrical degree intervals and aligned properly with the stator phase windings these Hall switches deliver digital pulses that can be decoded into the desired nine-phase switching sequence [27]. Such a drive usually also has a current loop to regulate the stator current, and an outer speed loop for speed control [28].

In summary, permanent magnet motor drives require a rotor position sensor to properly perform phase commutation, but there are several drawbacks when such types of position sensors are used.

The main drawbacks are the increased cost and size of the motor, and a special arrangement needs to be made for mounting the sensors. Further, Hall sensors are temperature sensitive and hence the operation of the motor is limited, which could reduce the system reliability because of the extra components and wiring [27].

2.5.2 Sensorless control using back-EMF

The second methods for proper control of BLDC motor is sensorless control. Here in this method instead of using sensors we can extract the rotor position from the motor itself. To reduce cost and improve reliability such position sensors may be eliminated. These disadvantages of using Hall sensors, lots of research is being done in sensorless drives. Position sensors can be completely eliminated, thus reducing further cost and size of motor assembly, in those applications in which only variable speed control (i.e., no positioning) is required and system dynamics is not particularly demanding (i.e., slowly or, at least, predictably varying load). A PM brushless drive that does not require position sensors but only electrical measurements is called a sensorless drive [27]. Since back-EMF is zero at standstill and proportional to speed, the measured terminal voltage that has large signal-to-noise ratio cannot detect zero crossing at low speeds. That is the reason why in all back-EMF-based sensorless methods the low-speed performance is limited, and an open-loop starting strategy is required [29].

The voltage for 3-phase BLDC motor is provided by a 3-phase power stage controlled by a DSP. Why Sensorless Control? As explained in the previous section, the rotor position must be known in order to drive a Brushless DC motor. If any sensors are used to detect rotor position, then sensed information must be transferred to a control unit (see Figure 2.6) [35].

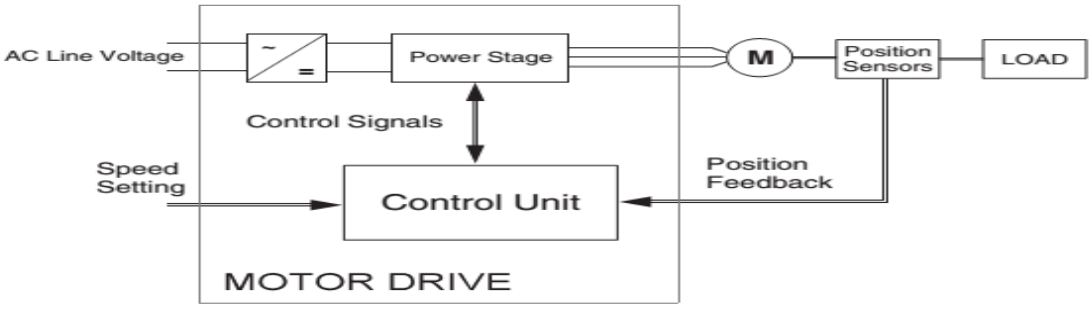

Fig. 2.6 Sensored control drive for BLDC motor diagram

Therefore, additional connections to the motor are necessary. This may not be acceptable for some applications.

2.5.2.1 Three phase Power Stage for three-phase BLDC motor

In order to explain and simulate the idea of Back-EMF sensing techniques a simplified mathematical model based on the basic circuit topology (see Figure 2.7) has been created. The second goal of the model is to find how the motor characteristics depend on the switching angle. The switching angles the angular difference between a real switching event and an ideal one (at the point where the phase to phase Back-EMF crosses zero). The motor-drive model consists of a normal three phase power stage plus a Brushless DC motor. The power for the system is provided by a voltage source (Vdc). Six semiconductor switches (S1, S2, S3, ... S6), controlled elsewhere, allow the rectangular voltage waveforms (see Figure 2.8) to be applied. The semiconductor switches and diodes are simulated as ideal devices. The natural voltage level of the whole model is put at one half of the dc-bus voltage (see figure 2.7). This simplifies the mathematical expressions. [35]

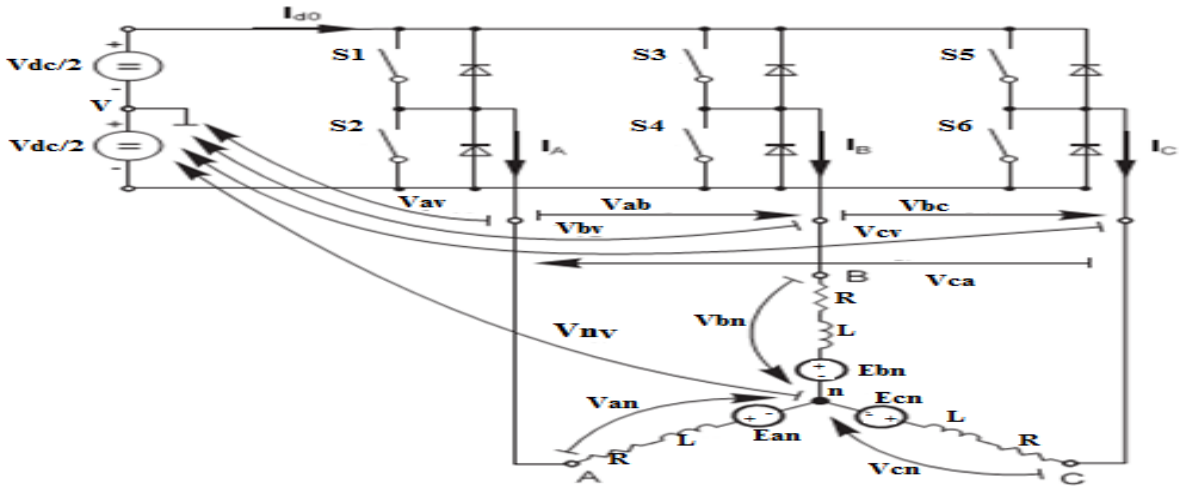

Fig. 2.7 power stage motor topology for three phase BLDC motor [35]

where:

$Vav, Vbv, and\ Vcn$ are “branch” voltages; the voltages between one power stage output and its virtual zero.

$Van, Vbn, and\ Vcn$ are motor phases winding voltages?

$Ean, Ebn\ and\ Ecn$ are phase Back-EMF voltages induced in the stator winding.

Vnv is the voltage between the central point of the star of motor winding and the power stage natural zero

$Ia, Ib\ and\ Ic$ are phase currents

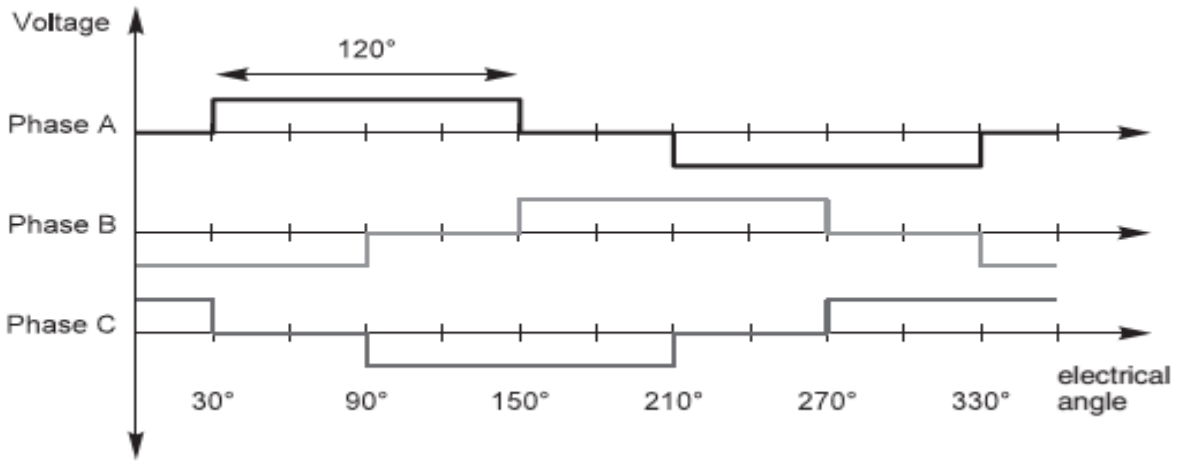

Fig. 2.8 Voltage applied based on the ZCD of back-EMF for three phase BLDC motor

2.5.2.2 Speed control of BLDC motor

Speed control of BLDC motors are very crucial. Many of the power electronic circuits used for this are subjected to very high switching losses ending up with reduced overall system efficiency. A speed control of BLDC motor based on pulse amplitude modulation control drive techniques, for brushless DC (BLDC) motor is investigated and verified by a series of simulation studies. It is well known that the BLDC motor can be driven by either Pulse-Width Modulation (PWM) techniques with a constant DC-link voltage or Pulse-Amplitude Modulation (PAM) techniques with an adjustable DC-link voltage. Therefore, the detailed theoretical analysis of the PAM control for high-speed BLDC motor is first given. Then a conclusion that the PAM control is superior to the PWM control at high speed is obtained because of decreasing the commutation delay and high frequency harmonic wave. The cost for PAM control has to pay is requiring variable DC-link voltage level control. This can be easily realized by the off-self DC/DC converter controller. for high speed range applications, such as air conditioner and refrigerator, PAM controls recommended since it provides higher efficiency [36].

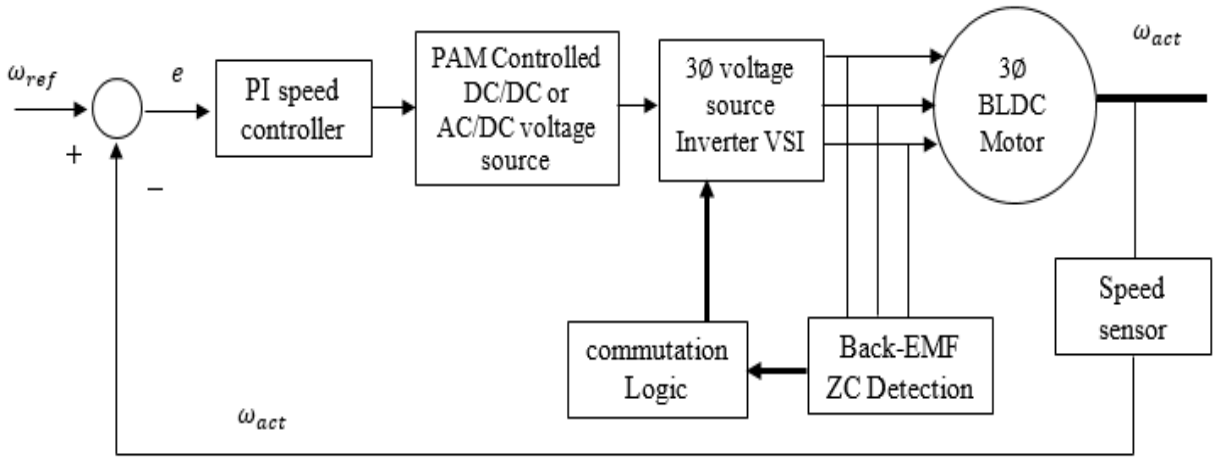

Fig. 2.9 PAM based closed loop speed controller for 3Ø BLDC motor [36]

Speed control of BLDC motors are very crucial in this attire. Many of the power electronic circuits used for this are subjected to very high switching losses ending up with reduced overall system efficiency. DC-DC converters are used in a wide range as the front-end converter to obtain a regulated dc output voltage. Since the back-EMF of the motor is directly proportional to rotor speed and field strength of the motor, any change in one of the parameter cause the other to modify accordingly.

In multiphase machine variable speed control is a must the most common classical method is used in speed control of motor is using proportional-integrator-differentiator (PID) controller. PID controller has been used widely for processes and motion control system in industry. The transfer function of PID controller is shown in Fig. 5. The control system performs poorly in characteristics and even it becomes unstable, if improper values of the controller tuning constants and used. So it becomes necessary to tune the controller parameters to achieve good control performance with the proper choice of tuning constants [31].

2.5.3 PID Design Concept

The proportional-integral-derivative (PID) controller is about the most common and useful algorithm in control system engineering. In most case, feedback loops are controlled using the PID algorithm. The main reason why feedback is very important in systems is to be able to attain a set

point irrespective of the disturbances or any variation of any form. The PID controller always designed to correct error(s) between measured proses value(s) and set value(s) in a system.
A simple illustration on how PID works is given below. Consider the characteristics of parameters-proportional(P), integral(I), and derivative(D) controls, as applied to the figure 2.10.

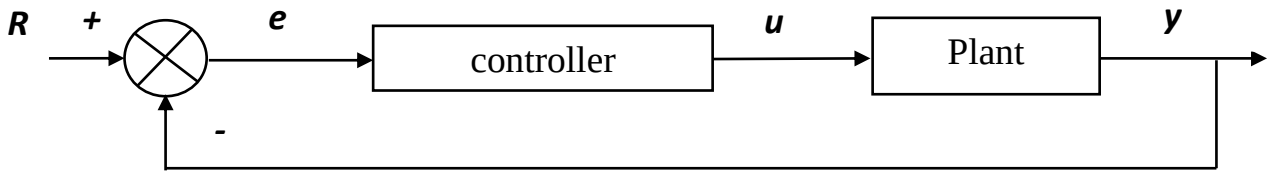

Fig. 2. 10 A typical closed loop controller of system

The controller provides the excitation needed by the system and it is deigned the overall behavior of the system. The PID controller has several categories of structural arrangements. the most common of this are the series and parallel structures and in some cases, there are hybrid form of the series and the parallel structure. The following shows the typical illustrative common PID controller structures.

$$K_p + \frac{K_I}{s} + K_d.s = \frac{K_d s^2 + K_p s + K_I}{s}$$

Where:
K_p=Proportional gain
K_I=Integral gain
K_d=Derivative gain

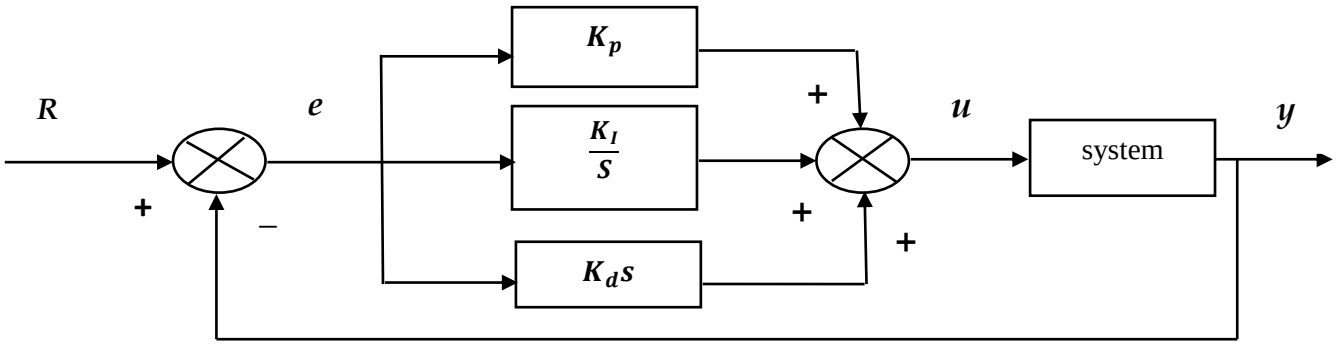

Fig. 2.11 Closed-loop PID controller block of system

Considering the figure 2.11, variable, e is the sample error, and it is the difference between the desired input value(R) and the actual output(Y). In closed loop, **e** will be sent to the controller, and the controller will perform the integral and derivative computation on the error signal. Thereafter, the signal, u which the output of the controller is now equal to the sum of [the product of proportional gain, K_p and magnitude of the error(e)], [the product of the integral gain, Ki and the integral of the error(e)] and [the product of the derivative gain, K_d and the derivatives of the error(e)].

$$U=K_p e+K_i \int e dt + K_d \frac{de}{dt}$$

The signal value, **u** is the set continuously to the plant with every corresponding new output, **Y** being obtained as the prosses continues. The output, **Y** is set back and subsequently new error signal, **e** is found and the same process repeats itself on and on. Also, it is very typical to have the **PID** transfer function written in several forms depending on the arrangement structure. The following equation shows one of these (a parallel structure):

$$K_p + \frac{K_I}{s} + K_d.s = K_p \times (1 + \frac{1}{S.T_I} + T_d.s)$$

Where

K_p= Proportional gain

T_I= Integral time or rest time = $\frac{K_p}{K_I}$

T_d = Derivative time rate time

2.5.4 Some characteristic effects of PID parameters

The proportional gain **K_p**, will may reduce rise time and might reduce or remove study state error of the system. The integral gain **K_I** it eliminates the study state error but it has a negative effect on the transient response (a worse response may happen in this case). And the derivative gain **K_d**, will tend to increase stability of the system, and reduces overshoot percentage, and improving the transient response of the system. In all, the table below will give a comprehensive effect of each of the controllers on a typical closed-loop system.

Table 2.1 PID controller parameter characteristics on atypical system

Parameters	Rise time	Overshoot	Settling time	Study-state error
K_p ↑	decreases	increase	small change	decreases
K_I ↑	decreases	increase	increases	eliminate
K_d ↑	small change	decrease	decreases	small change

Legend=↑ increases

The ability bled these three parameters will make a very efficient and stable system. It should be noted that the relationship between the three controller parameters may not exactly be correct because of the inter dependency. Therefore, it is possible to compute particular parameters which effects would be noticed on the other two.

CHAPTER 3

MATHEMATICAL MODEL OF NINE-PHASE BLDC MOTOR

3.1 Construction Futures of Nine-phase BLDC Motor

The Brushless DC motor is also referred to as an electronically commuted motor. There are no brushes on the rotor and the commutation is performed electronically at certain rotor positions. The stator magnetic circuit is usually made from magnetic steel sheets. The stator phase windings are inserted in the slots as shown in Figure 3.1 or it can be wound as one coil on the magnetic pole. The magnetization of the permanent magnets and their displacement on the rotor are chosen such a way that the Back-EMF shape is trapezoidal. This allows the nine-phase voltage system with a rectangular shape, to be used to create a rotational field with low torque ripples.

The operation of the BLDCM is based on the simple force interaction of between the rotor PM flux force and the stator electromagnetic force. Therefore, the nine phase stator windings are feed from the nine-phase voltage source inverter. The stator winding produces electromagnetic force and the instruction of this force with the rotor permanent magnetic force produces rotor rotation and resultant toque. The stator windings are symmetrically distributed with 40-degree electrical angles from each other. for n phase machine the winding distribution will be 2π/n electrical angle. A typical nine-phase, two-poles BLDC motor with concentrated stator windings and with permanent magnet rotor shown in figure 3.1. And the schematic representation of the stator winding is shown in figure 3.2.

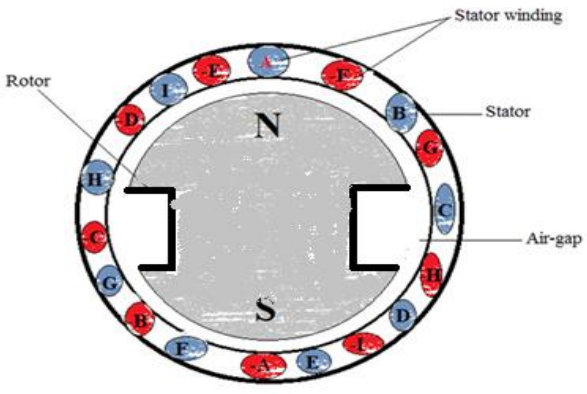

Fig. 3.1 nine-phase BLDC motor diagram

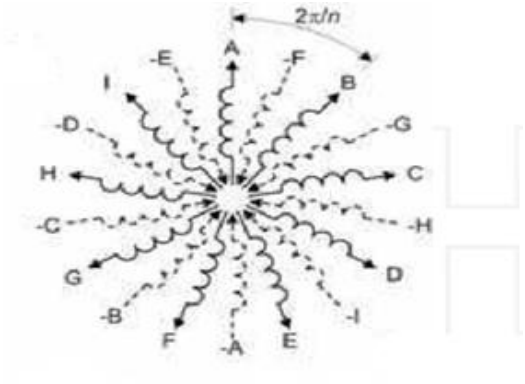

Fig.3.2 schematic dual-stator windings of nine-phase BLDC motor

The shape of the back-EMF wave form distinguishes the concentrated stator winding BLDC motor from the conventional PMSM. The conventional PMSM has a sinusoidal back-EMF waveform. The nine-phase BLDC motor has a permanent magnet rotor and stator windings are wound in such a way that the trapezoidal back-electromotive force. Therefore, no particular advantage in transforming the machine equation into well-known two axis rotating frame equations. Which are done in case of machines with sinusoidal back-EMF [31-32]. Here in order to control the machine we should have to know the rotor position to produces the desired torque and speed.

3.2 Voltage Equation of Nine-phase BLDC Motor

For the effectiveness of the work the following assumptions are made for sensorless control of the machine using back-EMF detection;

- Magnetic saturation is negligible
- No saliencies of the poles
- Hysteresis and eddy current loss is not considered
- Self, mutual and resistance of the stator are all equal

For the sensorless control model equivalent circuit of the given phase for nine phases BLDC motor is given by the figure 3.3.

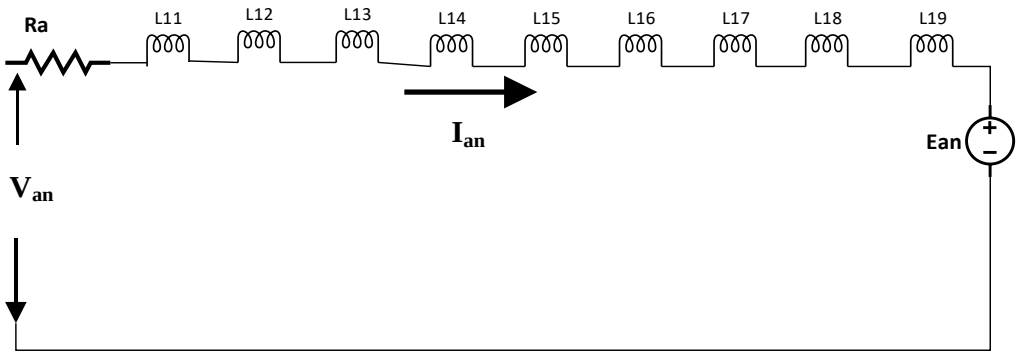

Fig. 3.3 Equivalent circuit of nine-phase BLDCM for phase- a

From the equivalent circuit diagram we can drive the phase voltage V_{xn} (stator x winding voltage with respect to the neutral point n) is given by;

$$V_{an} = R_a i_a + L_{11}\frac{di_a}{dt} + L_{12}\frac{di_b}{dt} + L_{13}\frac{di_c}{dt} + L_{14}\frac{di_d}{dt} + L_{15}\frac{di_e}{dt} + L_{16}\frac{di_f}{dt} + L_{17}\frac{di_g}{dt} + L_{18}\frac{di_h}{dt} + L_{19}\frac{di_i}{dt} + e_{an} \quad (3.1)$$

Similarly, the other eight phases voltage equation is given by:

$$V_{bn} = R_b i_b + L_{21}\frac{di_a}{dt} + L_{22}\frac{di_b}{dt} + L_{23}\frac{di_c}{dt} + L_{24}\frac{di_d}{dt} + L_{25}\frac{di_e}{dt} + L_{26}\frac{di_f}{dt} + L_{27}\frac{di_g}{dt} + L_{28}\frac{di_h}{dt} + L_{29}\frac{di_i}{dt} + e_{bn} \quad (3.2)$$

$$V_{cn} = R_c i_c + L_{31}\frac{di_a}{dt} + L_{32}\frac{di_b}{dt} + L_{33}\frac{di_c}{dt} + L_{34}\frac{di_d}{dt} + L_{35}\frac{di_e}{dt} + L_{36}\frac{di_f}{dt} + L_{37}\frac{di_g}{dt} + L_{38}\frac{di_h}{dt} + L_{39}\frac{di_i}{dt} + e_{cn} \quad (3.3)$$

$$V_{dn} = R_d i_d + L_{41}\frac{di_a}{dt} + L_{42}\frac{di_b}{dt} + L_{43}\frac{di_c}{dt} + L_{44}\frac{di_d}{dt} + L_{45}\frac{di_e}{dt} + L_{46}\frac{di_f}{dt} + L_{47}\frac{di_g}{dt} + L_{48}\frac{di_h}{dt} + L_{49}\frac{di_i}{dt} + e_{dn} \quad (3.4)$$

$$V_{en} = R_e i_e + L_{51}\frac{di_a}{dt} + L_{52}\frac{di_b}{dt} + L_{53}\frac{di_c}{dt} + L_{54}\frac{di_d}{dt} + L_{55}\frac{di_e}{dt} + L_{56}\frac{di_f}{dt} + L_{57}\frac{di_g}{dt} + L_{58}\frac{di_h}{dt} + L_{59}\frac{di_i}{dt} + e_{en} \quad (3.5)$$

$$V_{fn} = R_f i_f + L_{61}\frac{di_a}{dt} + L_{62}\frac{di_b}{dt} + L_{63}\frac{di_c}{dt} + L_{64}\frac{di_d}{dt} + L_{65}\frac{di_e}{dt} + L_{66}\frac{di_f}{dt} + L_{67}\frac{di_g}{dt} + L_{68}\frac{di_h}{dt} + L_{69}\frac{di_i}{dt} + e_{fn} \quad (3.6)$$

$$V_{gn} = R_g i_g + L_{71}\frac{di_a}{dt} + L_{72}\frac{di_b}{dt} + L_{73}\frac{di_c}{dt} + L_{74}\frac{di_d}{dt} + L_{75}\frac{di_e}{dt} + L_{76}\frac{di_f}{dt} + L_{77}\frac{di_g}{dt} + L_{78}\frac{di_h}{dt} + L_{79}\frac{di_i}{dt} + e_{gn} \quad (3.7)$$

$$V_{hn} = R_h i_h + L_{81}\frac{di_a}{dt} + L_{82}\frac{di_b}{dt} + L_{83}\frac{di_c}{dt} + L_{84}\frac{di_d}{dt} + L_{85}\frac{di_e}{dt} + L_{86}\frac{di_f}{dt} + L_{87}\frac{di_g}{dt} + L_{88}\frac{di_h}{dt} + L_{99}\frac{di_i}{dt} + e_{hn} \quad (3.8)$$

$$V_{in} = R_i i_i + L_{91}\frac{di_a}{dt} + L_{92}\frac{di_b}{dt} + L_{93}\frac{di_c}{dt} + L_{94}\frac{di_d}{dt} + L_{95}\frac{di_e}{dt} + L_{96}\frac{di_f}{dt} + L_{97}\frac{di_g}{dt} + L_{98}\frac{di_h}{dt} + L_{99}\frac{di_i}{dt} + e_{in} \quad (3.9)$$

From the assumption above all self and mutual inductance are equal

$L_{11}=L_{22}=L_{33}=\ldots=L_{99}$ ⟶ Self inductance

$L_{xy}=L_{yx}$ for $x\neq y$ were (x,y=1,2,3,4…..9) ⟶ Mutual inductance

$R_a=R_b=R_c\ldots\ldots R_i = R$ ⟶ stator winding resistance

And the machine stator windings are connected star symmetrical and balanced connection manner. Therefore;

$$i_a + i_b + i_c + i_d + i_e + i_f + i_g + i_h + i_i = 0 \quad (3.10)$$

Therefore, the phase **a** stator winding current can be given by:

$$i_a = -i_b - i_c - i_d - i_e - i_f - i_g - i_h - i_i \quad (3.11)$$

$$V_{an} = R_a i_a + L_{11}\frac{di_a}{dt} + M\left(\frac{di_b}{dt} + \frac{di_c}{dt} + \frac{di_d}{dt} + \frac{di_e}{dt} + \frac{di_f}{dt} + \frac{di_g}{dt} + \frac{di_h}{dt} + \frac{di_i}{dt}\right) + e_{an} \quad (3.12)$$

Using equation (3.11) the bracket in equation (3.12) became

$$\frac{di_a}{dt} = -\left(\frac{di_b}{dt} + \frac{di_c}{dt} + \frac{di_d}{dt} + \frac{di_e}{dt} + \frac{di_f}{dt} + \frac{di_g}{dt} + \frac{di_h}{dt} + \frac{di_i}{dt}\right) \quad (3.13)$$

Therefore, the simplified equivalent circuit based on the assumptions above became as follows

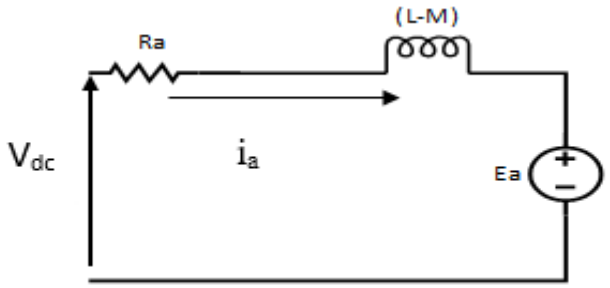

Fig. 3.4 Simplified Equivalent circuit of phase-a for the nine-phase BLDC motor

Therefore, using equation (3.13) and substituting in equation (3.12) so we will get the most simplified equation (3.14)

$$V_{an} = R_a i_a + (L - M)\frac{di_a}{dt} + e_{an} \quad (3.14)$$

Similarly using the same procedures as shown above from equation 3.10 to equation 3.14 above we can get all the simplified voltage equation for the rest of the stator phases. Therefore, the simplified form of the voltage equation can be given as follows:

$$V_{an} = R_a i_a + (L - M)\frac{di_a}{dt} + e_{an} \quad (3.15)$$

$$V_{bn} = R_b i_b + (L - M)\frac{di_b}{dt} + e_{bn} \quad (3.16)$$

$$V_{cn} = R_c i_c + (L - M)\frac{di_c}{dt} + e_{cn} \quad (3.17)$$

$$V_{dn} = R_d i_d + (L - M)\frac{di_d}{dt} + e_{dn} \quad (3.18)$$

$$V_{en} = R_e i_e + (L - M)\frac{di_e}{dt} + e_{en} \quad (3.19)$$

$$V_{fn} = R_f i_f + (L - M)\frac{di_f}{dt} + e_{fn} \quad (3.20)$$

$$V_{gn} = R_g i_g + (L - M)\frac{di_g}{dt} + e_{gn} \quad (3.21)$$

$$V_{hn} = R_h i_h + (L - M)\frac{di_h}{dt} + e_{hn} \quad (3.22)$$

$$V_{an} = R_i i_i + (L - M)\frac{di_i}{dt} + e_{in} \quad (3.23)$$

Using the simplified equation (3.15) to (3.24) of the nine-phase BLDC motor the equivalent circuit of the machine can be given by fig 3.4.

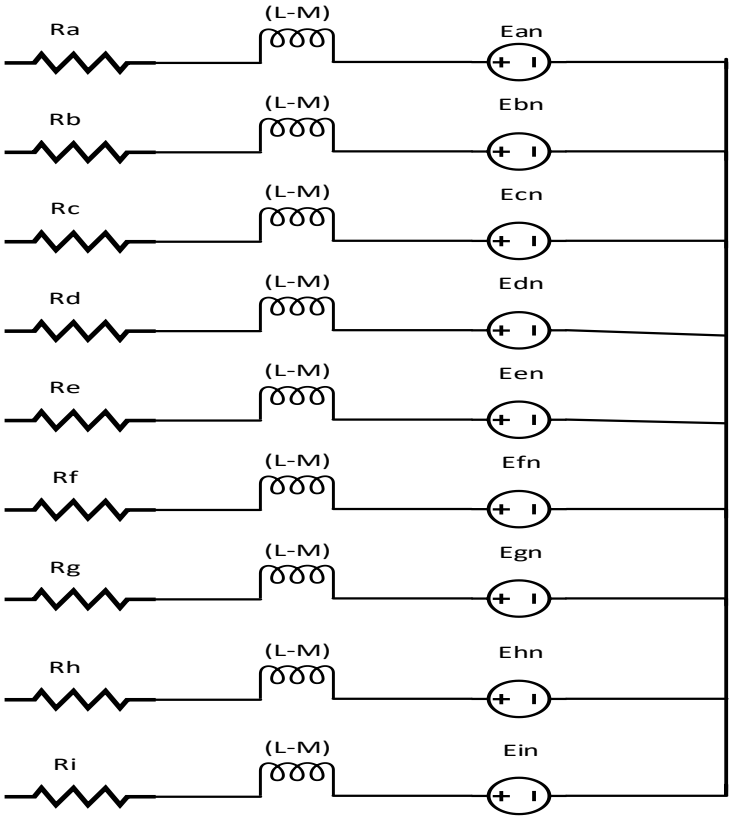

Fig. 3.5 simplified equivalent circuit of the nine-phase BLDC motor

3.3 Back-EMF Equation of Nine-phase BLDC Motor

BLDC motor acts as a generator when it rotates, creating voltage. the nine- phase produce nine-voltages 40-degrees apart. the voltage generated by the motor is called Back Electro-Motive Force. When BLDC motor rotates, according to the lens's law, each winding generates back-electromotive force. Which opposes the main voltage supplied to the windings. The polarity of this back-EMF opposes the energizing voltage polarity. Here, under consideration for this thesis

work concentrated stator winding nine-phase permanent magnet brushless DC motor is used for sensorless control of the machine based on back-EMF zero-cross sequences from table algorithm. As the rotor rotates, the wave form of the voltage induced in each phase with respect to time is an exact replica of the air-gap flux-density wave form with respect to rotor position. But because of the fringing effect on the wave from the back-EMF wave form takes on trapezoidal shape.

From faraday's law term of voltage equation, we can get back-EMF of the machine due to the permanent magnet flux-linkage in the phase winding which is given by equation;

$$e(t)_{ui} = \frac{d\lambda_{ui}}{dt} \tag{3.24}$$

where; e_{ui} is the back-EMF in phase u_i phase winding due to the permanent magnet in the rotor, λ_{ui} is the flux-linkage in phase u_i due to the rotor permanent magnet and i various 1,2,3….,9. And the expression of the flux-linkage (λ_{ui}) is given in equation (3.24a)

$$\begin{bmatrix}\lambda_{u1}\\ \lambda_{u2}\\ \lambda_{u3}\\ \lambda_{u4}\\ \lambda_{u5}\\ \lambda_{u6}\\ \lambda_{u7}\\ \lambda_{u8}\\ \lambda_{u9}\end{bmatrix} = lrN\left(B\begin{bmatrix}\cos(\theta_r)\\ \cos(\theta_r-\delta)\\ \cos(\theta_r-2\delta)\\ \cos(\theta_r-3\delta)\\ \cos(\theta_r-4\delta)\\ \cos(\theta_r-5\delta)\\ \cos(\theta_r-6\delta)\\ \cos(\theta_r-7\delta)\\ \cos(\theta_r-8\delta)\end{bmatrix}\right) \tag{3.24a}$$

so, by substitute equation (3.24a) in equation (3.24) the expression for nine phases back-EMF given by equation (3.25)

$$\begin{bmatrix} e_{u1} \\ e_{u2} \\ e_{u3} \\ e_{u4} \\ e_{u5} \\ e_{u6} \\ e_{u7} \\ e_{u8} \\ e_{u9} \end{bmatrix} = lrN\omega_m \left(B \begin{bmatrix} \sin(\theta_r) \\ \sin(\theta_r - \delta) \\ \sin(\theta_r - 2\delta) \\ \sin(\theta_r - 3\delta) \\ \sin(\theta_r - 4\delta) \\ \sin(\theta_r - 5\delta) \\ \sin(\theta_r - 6\delta) \\ \sin(\theta_r - 7\delta) \\ \sin(\theta_r - 8\delta) \end{bmatrix} \right) \quad (3.25)$$

Where;

$\boldsymbol{\theta_r}$ -is the rotor angel refers to the rotor flux,

$\boldsymbol{\delta}$ -is the stator winding distribution angle $\boldsymbol{(\delta = \frac{2\pi}{9} = 40^0)}$,

N- number of turns per phase winding,

r- is the mean-radius of the air gap and

l - is the effective axial length of stator winding,

B- is the magnetic-flux density of the machine. For more simplified form let us put

$$k_e = \text{lrNB}$$

Where, k_e = is known as the back-EMF constant

therefore, the above equation came be written us follows: -

$$\begin{bmatrix} e_{u1} \\ e_{u2} \\ e_{u3} \\ e_{u4} \\ e_{u5} \\ e_{u6} \\ e_{u7} \\ e_{u8} \\ e_{u9} \end{bmatrix} = k_e\omega_m \left(B \begin{bmatrix} \sin(\theta_r) \\ \sin(\theta_r - \delta) \\ \sin(\theta_r - 2\delta) \\ \sin(\theta_r - 3\delta) \\ \sin(\theta_r - 4\delta) \\ \sin(\theta_r - 5\delta) \\ \sin(\theta_r - 6\delta) \\ \sin(\theta_r - 7\delta) \\ \sin(\theta_r - 8\delta) \end{bmatrix} \right) \quad (3.25a)$$

Where;

θ_r-is the rotor angel referred to the rotor flux,

Ke-is the back-EMF constant of the motor

B-is magnetic flux density

The back-EMF are displaced by 40 electrical degrees from one phase to another, and the above equation (3.25a) can be put more simplifies form as shown below;

$$e_a = k_e\omega_m[f(\theta_e)]$$

$$e_b = k_e\omega_m[f(\theta_e - \delta)]$$

$$e_c = k_e\omega_m[f(\theta_e - 2\delta)]$$

$$e_d = k_e\omega_m[f(\theta_e - 3\delta)]$$

$$e_e = k_e\omega_m[f(\theta_e - 4\delta)] \quad (3.25b)$$

$$e_f = k_e\omega_m[f(\theta_e - 5\delta)]$$

$$e_g = k_e\omega_m[f(\theta_e - 6\delta)]$$

$$e_h = k_e\omega_m[f(\theta_e - 7\delta)]$$

$$e_i = k_e\omega_m[f(\theta_e - 8\delta)]$$

Where;

ω_m-mechanical rotor speed [rad/sec]

K_e – back-EMF constant [v/rad.s^{-1}]

$f(\theta_e)$- trapezoidal function

θ_e- electrical angle of the rotor

$f(\theta_e) = Asin(\theta_e)$, where $f(\theta_e)$ is trapezoidal ac signal

3.4 Torque Equation

Once we got the back-EMF and the stator phase current then, we can calculate the torque developed by the machine. During any 40^0 intervals, the instantaneous power being converted from electrical to mechanical is the sum of the contribution from eight phases in series and is given by;

$$p_T = \omega_m T_e \tag{3.24}$$

Where;

p_T - Total power output,

T_e - Total output torque

Therefore, the electromagnetic torque produced by the nine phase BLDC motor can be expressed as;

$$T_e = \frac{e_{mu1}\, i_{u1} + e_{mu2}\, i_{u2} + e_{mu3}\, i_{u3} + e_{mu4}\, i_{u4} + e_{mu5}\, i_{u5} + e_{mu6}\, i_{u6} + e_{mu7} i_{u7} + e_{mu8}\, i_{u8} + e_{mu9}\, i_{u9}}{\omega_m} \tag{3.25}$$

Equation can also rewrite as in equation below such as (3.25-a)

$$T_e = \frac{1}{\omega_m} \sum_{X=a}^{i} (e_{xn} i_x) \tag{3.25-a}$$

And also the back-EMF can be replaced by the derivatives of the flux produced in the motor and equation (3.25-a) can be rewritten follows in equation (3.25-b)

$$T_e = \sum_{X=a}^{i} \left(\frac{d\Psi_x}{d\theta} i_x\right) \tag{3.25-b}$$

where:

Te =internal motor torque (no mechanical losses)

ω, θ= rotor speed, rotor position

x =phase index, it stands for a, b, c, d, e, f, g, h, i

Ψ_x= magnetic flux of phase winding x

It is important to understand how the Back-EMF can be sensed and how the motor behavior depends on the alignment of the Back-EMF to commutation events. This is explained in the next chapter. And from the equation of motion a simple system with moment of inertia J, friction force B and load torque T_l, the electromagnetic torque produced counter balanced by load torque, inertia torque and friction torque is given by equation (3.26);

$$T_e = J \frac{dw_m}{dt} + B w_m + T_l \tag{3.26}$$

Where;

J – Inertia of the rotor and coupled shaft [kg.m^2]

B – Friction constant [Nm.rad^{-1}]

T_l – Load torque [Nm]

w_m - Mechanical rotor speed [rad.sec^{-1}]

The electrical rotor angle is equal to the mechanical rotor angle multiplied by the number of pole pairs which is given by;

$$\boldsymbol{\theta_e = \frac{p}{2}\theta_m} \tag{3.27}$$

And the mechanical rotor speed (ω_m) can be found using (12a)

$$\boldsymbol{\omega_m = \frac{d\theta_m}{dt}} \tag{3.28}$$

Where; θ_m is mechanical rotor angle [rad.]

3.5 Open loop s-domain analysis of Nine-phase BLDC motor

Typically, the mathematical model of BLDC motor is totally no difference with the conventional DC motor. The major thing addition is the phase involved which effects the overall result of the BLDC motor model. The phases peculiarly affect the resistive and inductive of the BLDC motor arrangement. For example, a simple arrangement with a symmetrical 9-hase and "wye" internal connection could give the illustration of the whole phase concept. Consider one of the single phase equivalent circuit of the nine-phase machine

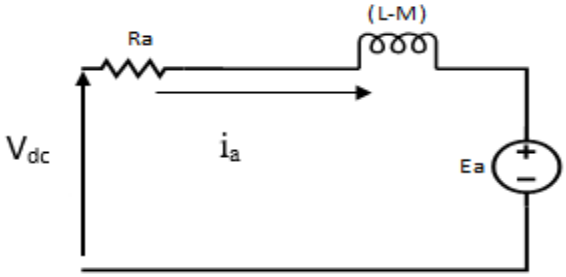

Fig. 3.6 simplified single-phase equivalent circuit of the nine-phase BLDC motor

The basic component of each of the nine-phase windings are armature resistance R, winding inductance L**,** mutual inductance M and the back-electromotive force(back-EMF). Using Kirchhoff's voltage low (KVL) in the above equivalent circuit the following equation obtained.

$$V_{an}=R_a i_a + (\text{L-M})\frac{dia}{dt} + e_{an} \tag{3.29}$$

From the above equation (3.39) we can calculate the back-EMF

$$e_{an} = -R_a i_a - (\text{L-M})\frac{dia}{dt} + V_{an} \tag{3.30}$$

Where;

V_{an} =The stator phase winding voltage

i_a = stator phase winding current

e_{an} = back-EMF produced in the phase a winding

Similarly, considering the mechanical properties of the motor, from the Newton's second law of motion, the mechanical properties relative to the torque of the system arrangement would be the product of the inertia load, J and the rate of angular velocity ω_m is equal to the sum of all torques; these follow with equation 3.31 and 3.32 accordingly;

$$\boldsymbol{J\frac{d\omega_m}{dt} = \sum T_i} \tag{3.31}$$

$$T_e = J\frac{d\omega_m}{dt} + B\omega_m + T_L \tag{3.32}$$

Where,

T_e =The electrical torque produced by the motor

J = The moment of inertia of the motor

B = air gap friction constant

ω_m = angular speed of the motor

$T_L =$ The supposed load torque applied

Where, the back-EMF produced in each stator winding phase is directly proportional with the rotor speed and it can be written as follows;

$$e_{an} = k_e \omega_m \tag{3.33}$$

Where, k_e is the back-EMF constant which is the function of the motor PM flux linkage (λ_m)

And also, the electrical torque produced is also a direct relation with the stator phase current applied and given by the following relation;

$$T_e = k_t i_a \tag{3.34}$$

Where, k_t is the torque constant which is dependent on the mass of the shaft and the radius.

Therefore, re-writing equations (3.29) and (3.30) then equations (3.35) and (3.36)

$$\frac{dia}{dt} = -i_a \frac{R_a}{(L-M)} - \frac{k_e}{(L-M)} \omega_m + \frac{1}{(L-M)} V_{an} \tag{3.35}$$

$$\frac{d\omega_m}{dt} = i_a \frac{k_t}{J} + \frac{B}{J} \omega_m + \frac{1}{J} T_L \tag{3.36}$$

Using Laplace transfer to evaluate equations (3.35) and (3.36), the following are obtained approximately (all initial conditions are all assumed to be zero)

From equation (3.35)

$$L\{\frac{dia}{dt}\} = \mathrm{L}\{-i_a \frac{R_a}{(L-M)} - \frac{k_e}{(L-M)} \omega_m + \frac{1}{(L-M)} V_{an}\} \tag{3.37}$$

This implies;

$$si_a = -i_a \frac{R_a}{(L-M)} - \frac{k_e}{(L-M)} \omega_m + \frac{1}{(L-M)} V_{an} \tag{3.38}$$

Similarly, the Laplace transform of equation (3.36)

$$L\{\frac{d\omega_m}{dt}\} = L\{i_a \frac{k_t}{J} + \frac{B}{J} \omega_m + \frac{1}{J} T_L\} \tag{3.39}$$

$$S\omega_m = i_a \frac{k_t}{J} - \frac{B}{J}\omega_m + \frac{1}{J}T_L \tag{3.40}$$

At no load (for $T_L = 0$), equation (3.40) becomes;

$$S\omega_m = i_a \frac{k_t}{J} - \frac{B}{J}\omega_m \tag{3.41}$$

From equation (3.41) the stator-phase current (i_a) cn be found, then we obtained equation (3.42)

$$i_a = \frac{S\omega_m + \frac{B}{J}\omega_m}{\frac{k_t}{J}} \tag{3.42}$$

Then, substitute equation (3.42) in equation (3.40)

$$\frac{S\omega_m + \frac{B}{J}\omega_m}{\frac{k_t}{J}}\left(s + \frac{R_a}{(L-M)}\right) = \frac{-k_e}{(L-M)}\omega_m + \frac{1}{(L-M)}V_{an} \tag{3.43}$$

After, some simplification (3.42) finally resolved equation (3.43)

$$V_{an} = \left(\frac{s^2J(L-M) + sB(L-M) + sRJ + BR_a + k_e k_t}{k_t}\right)\omega_m \tag{3.44}$$

The transfer function G(s) is therefore, obtained as follows using the ratio of and the angular velocity, ω_m to the voltage source V_{an} .

That is,

$$G(s) = \frac{\omega_m}{V_{an}} = \frac{k_t}{s^2J(L-M) + sB(L-M) + sRJ + BR_a + k_e k_t} \tag{3.45}$$

Considering, the following assumptions;

1) The friction constant is very small ($B \approx 0$) tends to zero, that implies that
2) $R_aJ \gg B(L-M)$ and
3) $k_e k_t \gg R_a B$

And the negligible values zeroed, the transfer function is finally written as;

$$G(s) = \frac{\omega_m}{V_{an}} = \frac{k_t}{s^2J(L-M) + sRJ + k_e k_t} \tag{3.46}$$

So, by re-arrangement and mathematical manipulation on "J(L-M)", by multiplying top and bottom of the equation (3.46)

$$\frac{R_a}{k_e k_t} \times \frac{1}{R_a}$$

Equation (4.19) is obtained after the manipulation;

$$G(s) = \frac{\omega_m}{V_{an}} = \frac{1/k_t}{\frac{JR_a}{k_e k_t} \times \frac{(L-M)}{R_a} s^2 + \frac{JR_a}{k_e k_t} s + 1} \tag{3.47}$$

From equation (3.47) the following constants are gotten,

The mechanical time constant (T_m) which is given by;

$$\tau_m = \frac{JR_a}{k_e k_t} \tag{3.48}$$

The electrical time constant (T_e) which is given by;

$$\tau_e = \frac{(L-M)}{R_a} \tag{3.49}$$

Substituting, equations (3.48) and (3.49) in equation (3.47), it yields;

$$G(s) = \frac{\omega_m}{V_{an}} = \frac{1/k_t}{\tau_m \tau_e s^2 + \tau_m s + 1} \tag{3.50}$$

Similarly, each winding phases of the nine phase windings of the BLDC motor will have similar equations, and the total torque and speed is a contribution of each phases.

However, the thesis is sensorless control of the motor each time eight-phase is contributed as it is discussed the previous chapter based on the back-EMF wave sensorless control the model of the BLDC motor also various as follows;

The whole phases (the nine) will affect primarily the mechanical and electrical time constants as they are important part of modeling parameters. Based on the assumption below,

- All the stator windings of the nine phases of BLDC motor is constant and equal which is represented by (R)

- All the difference inductance (L-M) in each phase of the nine phase windings are all equal and represented by ℓ.

For the mechanical time constant (with symmetrical star stator winding arrangement), equation (3.49) becomes;

$$\tau_m = \sum \frac{JR}{k_e k_t} \tag{3.51}$$

Where, $k_e, k_t \; and \; J$ are constant and τ_m (the mechanical time constant) is dependent only the sum of the active phase winding

$$\tau_m = \frac{J}{k_e k_t} \sum R \tag{3.52}$$

Similarly, the electrical time constant also (τ_e) is given by the sum of all phases ratio of the $\frac{l}{R}$ which is given by;

$$\tau_e = \sum \frac{l}{R} \tag{3.53}$$

The electrical time constant is also depending on the sum of all the phase resistor and the single phase inductance of the stator winding. Therefore, τ_e becomes as follows;

$$\tau_e = \frac{l}{\sum R} \tag{3.54}$$

Therefore, since for asymmetrical arrangement and nine phase BLDC motor, the mechanical and electrical constants for sensorless control using back-EMF becomes can be calculated as follows, since for sensorless control from the previous chapter that only eight phases uses at each time of commutation. Therefore, the mechanical and the electrical time constant of the machine can be modified as follows;

First the mechanical time constant (τ_m) equation (3.47) for nine phase machine becomes

$$\tau_m = \frac{9\mathrm{RJ}}{k_e k_t} \tag{3.55}$$

Similarly, the electrical time constant, τ_e (3.54) becomes given by as follows;

$$\tau_e = \frac{l}{9R} \tag{3.56}$$

Considering the phase effects,

$$\tau_m = \frac{9RJ}{\frac{k_{e(L-L)}}{\sqrt{9}} k_t} \tag{3.57}$$

Where, $k_{e(L-L)}$ is the line to line phase back-EMF constant

Equation (3.50) now becomes

$$\tau_m = \frac{9RJ}{K_e k_t} \tag{3.58}$$

Where, K_e is the phase values of the EMF (voltage) constants;

$$K_e = \frac{k_{e(L-L)}}{\sqrt{9}} \tag{3.59}$$

And, also there is relationship between K_e and k_t; by equating the electrical power and mechanical power the following equation can be extracted;

$$\sqrt{9} \times e_{pn} \times I_p = \frac{2\pi}{40} \times \omega_m \times T_e \tag{3.60}$$

Where;

e_{pn} = Back-EMF voltage produced in each phase

I_p =the stator phase current

$\frac{2\pi}{40}$ = commutation sequence of the nine-phase inverter

ω_m = rotor angular speed

T_e = torque produced

Simplify the equation above,

$$\frac{e_{pn}}{\omega_m} = \frac{T_e}{I_p} \times \frac{2\pi \times 1}{40 \times \sqrt{9}} \tag{3.61}$$

But, $e_{pn} = K_e\omega_m$ and $T_e = k_t I_p$ substitute these two equations on the above equation (3.61) and after some cancelation the result will be

$$K_e = k_t \times \frac{2\pi \times 1}{40 \times \sqrt{9}} \tag{3.62}$$

Therefore, K_e becomes after evaluating equation (3.62)

$$K_e = k_t \times 0.0523 \tag{3.63}$$

$K_e = \left[\frac{V.sec}{rad}\right]$, the electrical Back-EMF constant

$k_t = \left[\frac{N.m}{A}\right]$, the electrical torque constant

The equation for the nine-phase BLDC motor can now be obtained as follow from the equation (3.22) by considering the effects of the constants and the phase accordingly,

$$G(s) = \frac{\omega_m}{V_{an}} = \frac{1/K_e}{\tau_m \tau_e s^2 + \tau_m s + 1} \tag{3.64}$$

After now, we can use the parameters of the machine. The parameters used in the modeling are extracted from the "the datasheet" of the motor with corresponding relevant parameters used.

Table 3.1 the nine phase BLDC motor parameters

Motor parameters	**Values**
Per phase resistance (R)	0.7 ohm
Per phase inductance (L)	0.52mH
Per mutual inductance (M)	0.21mh
Factious constant (B)	0.0005Nm/rad/sec
Moment of inertia (J)	0.00025 kgm^2
Number of poles(P)	2
Back-EMF constant (Ke)	0.0175 V.rad/sec
Torque constant (Kt)	1.2 Nm/A
DC-bus voltage(Vdc)	300V

Based on the given parameter, in the table 3.1 and substituting and evaluating of the transfer function of the motor will yields;

From the equation (3.64)

$$G(s) = \frac{\omega_m}{V_{an}} = \frac{1/K_e}{\tau_m \tau_e s^2 + \tau_m s + 1} \quad (3.64)$$

So that, the valve of all the coefficients of the nominator and the dominators hast be find first,

From equation (3.36) the back-EMF constant (K_e) using the table value of torque constant (k_t) becomes;

$$K_e = k_t \times 0.0523 = 1.2 \times 0.0523 = 0.0628\ \text{V.rad/sec}$$

And, similarly the time constants can also find using the tabulated data and equations (3.29) and (3.58) as follows; First using (3.56) for torque time constant (τ_e) $\tau_e = \frac{l}{9R}$

Where, l is the difference between the self-inductance phase winding (L) and mutual inductance (M). therefore,

$l = L - M$ =0.00052H-0.00021H=0.00031H=0.31mH

Then, $\tau_e$can now be calculate as follows;

$$\tau_e = \frac{0.00031H}{9 \times 0.7\Omega} = 4.92 \times 10^{-5}$$

And, the mechanical time constant (τ_m) can also calculate using equation (3.58)

$$\tau_m = \frac{9\text{RJ}}{K_e k_t} = \frac{9 \times 0.7 \times 0.00025 kg.m/s}{0.0628 \times 1.2} = 0.0251$$

Therefore, substituting all the given parameters and evaluated parameters (K_e, τ_m and τ_e) in equation (3.64) the transfer function, $G(s)$ of the motor can be calculated as follows;

$$G(s) = \frac{\omega_m}{V_{pn}} = \frac{\frac{1}{K_e}}{\tau_m \tau_e s^2 + \tau_m s + 1} = \frac{\frac{1}{0.0628}}{0.0251 \times 4.92 \times 10^{-5} \times s^2 + 0.0251 \times s + 1}$$

Therefore, the open loop transfer function $G(s)$) of the Nine-phase BLDC motor using s-domain is obtained

$$G(s) = \frac{\omega_m(s)}{V_{pn}(s)} = \frac{15.9236}{1.235 \times 10^{-6} \times s^2 + 0.0251 \times s + 1} \quad (3.64)$$

The next chapter, talks about nine-phase BLDC sensorless motor modeling of the motor and closed loop PI speed control design of the motor is discussed.

CHAPTER 4

SENSORLESS CONTROL OF NINE-PHASE BLDC MOTOR USING BACK-EMF

4.1 The general overview of sensorless control of nine-phase BLDC motor using back-EMF method

The overall system configuration of the nine phase BLDCM sensorless control using back EMF drive is shown in Figure 4.1 The commutation logic controlled inverter and sensorless position detection based on back-EMF are used. In this thesis, a concentrated stator winding nine-phase BLDC motor operates eight phases on mode is used. Eight phases which produces maximum torque are exited leaving the reaming three phase open, therefore the back-EMF in open phases is sensed to determine the switching sequence of the inverter. The nine-phase machine is fed by nine-phase invertors as shown in the figure 4.8. stator phases of the machine are operated by means of electronic eighteen-step commutation system.

The overall sensorless control of nine phases BLDC motor using Back-EMF consists of the following basic blocks

- Nine-phase motor mathematical model (voltage equation) block
- Nine-phase Voltage source inverter block
- Back-EMF zero crossing detection block
- commutation logic block

The shape of the back-EMF wave form distinguishes the concentrated stator winding BLDC motor from the conventional PMSM (i.e. the conventional PMSM has a sinusoidal back-EMF wave form). The nine-phase BLDC motor has a permanent magnet rotor and stator windings are wound in such a way that the back-electromotive force trapezoidal waveform. Therefore, no particular advantage in transforming the machine equation into well-known two axis rotating frame equations. Which are done in case of machines with sinusoidal back-EMF [15]. Here in order to control the machine we should have to know the rotor position to produces the desired torque and speed. Here, under consideration for this thesis work concentrated stator winding nine-phase permanent magnet synchronous motor is used for sensorless control using back-EMF of the

machine. As the rotor rotates, the wave form of the voltage induced (i.e. back-EMF) in each phase with respect to time is an exact replica of the air-gap flux-density wave form with respect to rotor position. But because of the fringing effect on the wave from the back-EMF waveform takes on trapezoidal shape.

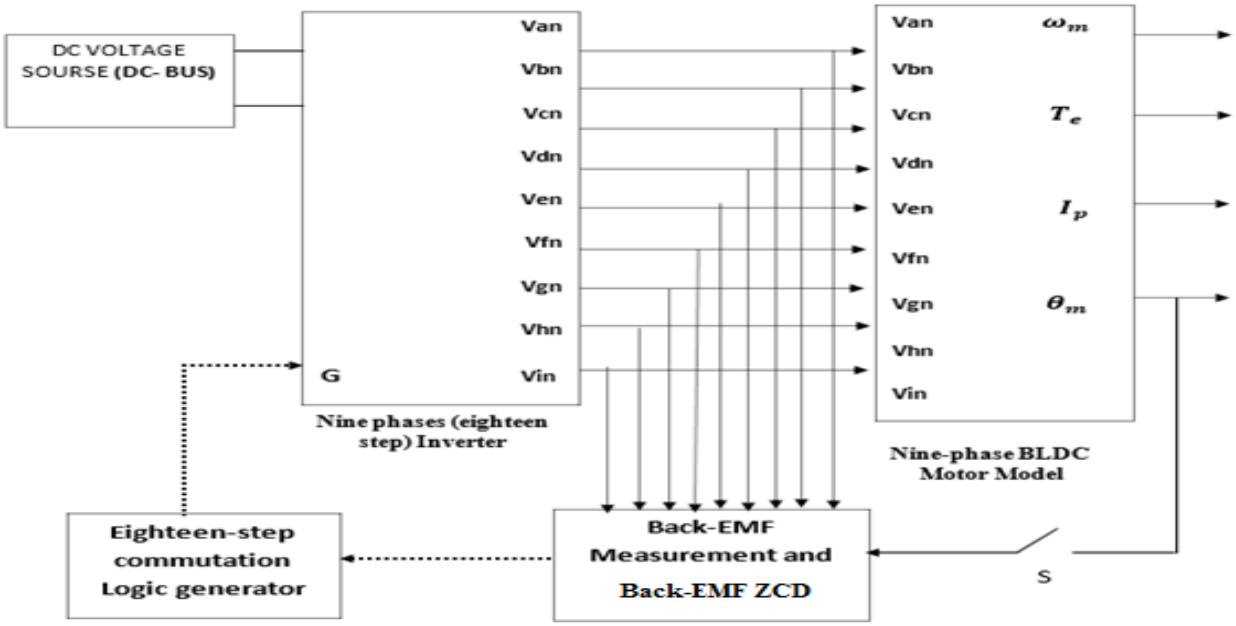

Fig. 4.1 Overall sensorless control of BLDC motor block diagram

The Back-EMF zero crossing detection enables position recognition. The rectangular, easy to create, shape of applied voltage ensures the simplicity of control and drive. But the rotor position must be known at certain angles in order to align the applied voltage with the back-EMF. The alignment between back-EMF and commutation events is very important. In this condition the motor behaves as a DC motor and runs at the best working point.

In BLDC motor control theory, the stator's flux should be 90 electrical degrees ahead of the rotor's flux for maximum torque generation. As a consequence, for maximum torque, the phase current needs to be in phase with the phase back-EMF voltage. For the 9-phase BLDC motors considered, the phases are shifted $\frac{2\pi}{9}$ =40° from each other, so a convenient method for having a rotating rotor flux in the stator is the eighteen-step commutation scheme previously described, commutating each of the nine-phase voltages 20 electrical degrees.

The sequence of distribution of the gate signals to the nine phases VSI depends on the rotor position and rotor speed feedback from BLDC motor. The position of the rotor is estimated in sensorless back-EMF method using the zero-cross detection and the point which the back-EMF cross zero or the sequence is used to trigger the switches as the timer for during every ($\frac{2\pi}{18} = 20^0$) electrical degrees. Therefore, according to the rotor position pulses to 18 switches, driving the nine phases BLDC motor will be developed using back-EMF wave form sequences. Therefore, equation for back-EMF from chapter 3 is given in equation (3.24) and rewritten here in equation (4.1)

$$\begin{bmatrix} e_{mu1} \\ e_{mu2} \\ e_{mu3} \\ e_{mu4} \\ e_{mu5} \\ e_{mu6} \\ e_{mu7} \\ e_{mu8} \\ e_{mu9} \end{bmatrix} = k_e \omega_m \left(\begin{bmatrix} \sin(\theta_r) \\ \sin(\theta_r - \delta) \\ \sin(\theta_r - 2\delta) \\ \sin(\theta_r - 3\delta) \\ \sin(\theta_r - 4\delta) \\ \sin(\theta_r - 5\delta) \\ \sin(\theta_r - 6\delta) \\ \sin(\theta_r - 7\delta) \\ \sin(\theta_r - 8\delta) \end{bmatrix} \right) \tag{4.1}$$

The back-EMF are displaced by 40^0 electrical degrees from one phase to another, and the above equation (3.24) can be put more simplifies form as shown below;

$$\mathbf{e_a = k_e \omega_m [f(\theta_e)]}$$

$$\mathbf{e_b = k_e \omega_m [f(\theta_e - \delta)]}$$

$$\mathbf{e_c = k_e \omega_m [f(\theta_e - 2\delta)]}$$

$$\mathbf{e_d = k_e \omega_m [f(\theta_e - 3\delta)]}$$

$$\mathbf{e_e = k_e \omega_m [f(\theta_e - 4\delta)]} \tag{4.1b}$$

$$\mathbf{e_f = k_e \omega_m [f(\theta_e - 5\delta)]}$$

$$\mathbf{e_g = k_e \omega_m [f(\theta_e - 6\delta)]}$$

$$\mathbf{e_h = k_e \omega_m [f(\theta_e - 7\delta)]}$$

$$\mathbf{e_i = k_e \omega_m [f(\theta_e - 8\delta)]}$$

Where;

ω_m-mechanical rotor speed [rad/sec]

K_e – back-EMF constant [v/rad.s^{-1}]

$f(\theta_e)$-trapezoidal function

θ_e-electrical angle of the rotor

δ – displaced or lag angle= $\frac{2\pi}{9} = 40^0$

In this type of machine in order to develop the maximum torque the back-EMF and current in each phase must be in phase.

4.2 Nine-phase BLDC motor control using back-EMF

The performance and reliability of BLDC motor drivers have been improved because the conventional control and sensing techniques have been improved through sensorless technology. In this thesis sensorless control of nine-phase BLDC motor based on Back-EMF method is used in order to control the machine for maximum resultant torque. These types of motor had advantage to use sensorless control of the rotor position because the motor has trapezoidal back-EMF wave form. For maximum toque output out of the nine-phase stator winding machine eight of the nine phases are conducted and one is an exited. This is because of maximum toque can be achieved when the stator electromagnetic (EM) force is perpendicular to the rotor permanent magnet.

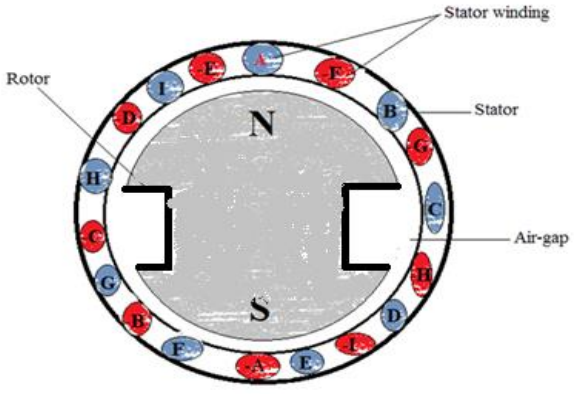

Fig. 4.2 2-pole nine-phase dual stator winding BLDC motor

The sequence of taking the current from one phase to another phase is called commutation sequence. In case of nine phases motor back-EMF control for maximum torque control, the commutation is based on the back-EMF waveform of the motor is based on the following steps:

1. If positive current in a particular stator winding $(a, b, c \ldots i)$ that commutation interval results appositive torque, then leave it without doing nothing.
2. If positive current in a particular nine phase stator winding $(a, b, c \ldots i)$ that commutation interval results a negative torque, then flip the current over (change the polarity) for a particular commutation interval.
3. If positive current in a particular nine phase stator winding $(a, b, c \ldots i)$ that commutation interval results a transition of torque (torque from high to low or low to high) then turn off the applied current though that winding in that particular commutation interval.

The above rule is based on the back-EMF of the motor and for maximum torque generation. And we can see the commutation sequence from the motor back-EMF wave form sequence and then we can develop a truth table (Table 4.1) for the eighteen steps commutation sequence by looking the back-EMF wave sequence and the current of each phase.

After we apply the above rule the resultant electrical torque output the machine, is given by: -

$$Te = Ta + Tb + Tc + Td + Te + Tf + Tg + Th + Ti \quad (4.2)$$

The figure 4.2(a, b, and c) below shows the sequential rotor position of the three (A, B, and C phases) phases out of nine phases. For the rest of the phases similarly we can show likewise.

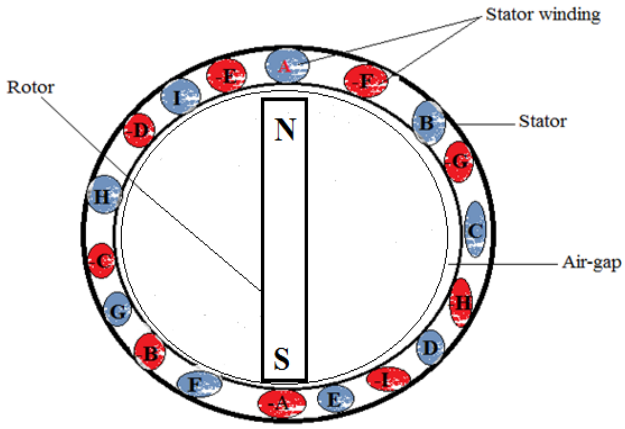

Fig. 4.2 (a) Nine-phase BLDC motor when the rotor PM reached phase A stator winding

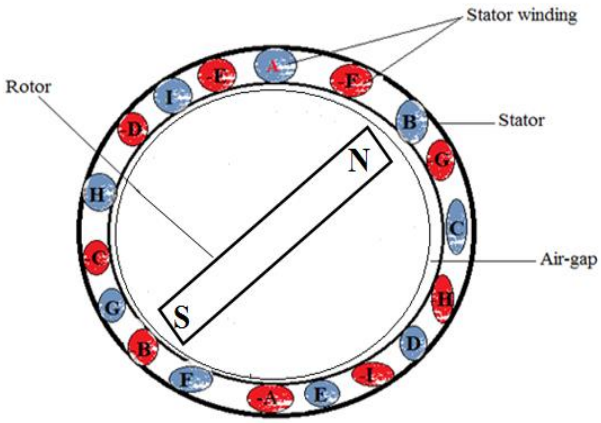

Fig. 4.2 (b) Nine-phase BLDC motor when the rotor PM reached phase B stator winding

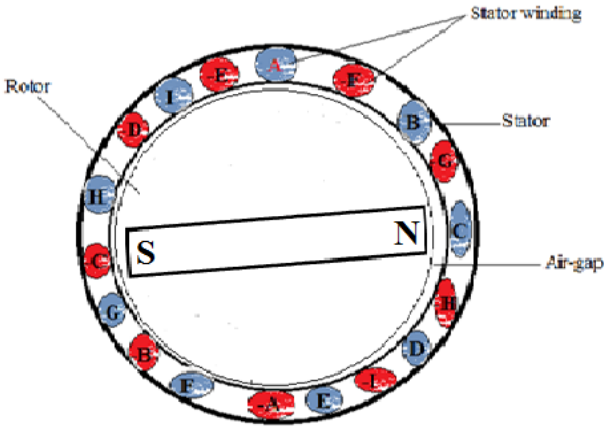

Fig. 4.2 (c) Nine-phase BLDC motor when the rotor PM reached phase C stator winding

From, the above principle of rotation the back-EMF produced in the stator winding shown in the figure 4.4 the graph plotted below is for one complete cycle (rotation) of the motor for 360^0 the horizontal axis represents the position of the rotor and the vertical axis represent the back-EMF produced in the nine-phase stator winding.

4.3 Sensorless control of nine-phase BLDC motor Using back-EMF ZCD

Based the operating modes of this BLDC motor principle the sensorless control of the motor can be 160^0 conduction mode in this case the effects of stator winding are negligible and the back-EMF produced in each winding phase angle difference between each phase is 40^0 depending on the winding arrangement of the motor. In ideal cases, this happens on zero-crossing of back EMF, when the rotor moves, the Back-EMF is acquired so the position is known and back-EMF zero

crossing can be used to calculate the position of the rotor and processing of the commutation in the Running state. Therefore, for every instance of commutation out of nine phases 8 phases are conduct and one phases remains unpowered. maximum torque generation for trapezoidal n-phase motor n-1 phases is conducted and reaming one phase is unexcited or unpowered. Each semi converter device in the nine-phase inverter drive conduct for duration of 160^0 electrical angle.

Here the fig.4.4 is the nine-phase permanent magnet BLDC motor induced voltage (Back-EMF), fig 4.5 show as the nine phase voltage waveform. And also, figure 4.5 shows the waveform of BEMF and the stator phase current for one complete cycle (360^o). and also the tables below show that, detection of the rotor position according to the waveform of the machine and the stator phase voltage in each sequence. The figure 4.3 blow shows that the schematic stator phase winding arrangement of the nine-phase BLDC motor and the angle between each phases is 40^0.

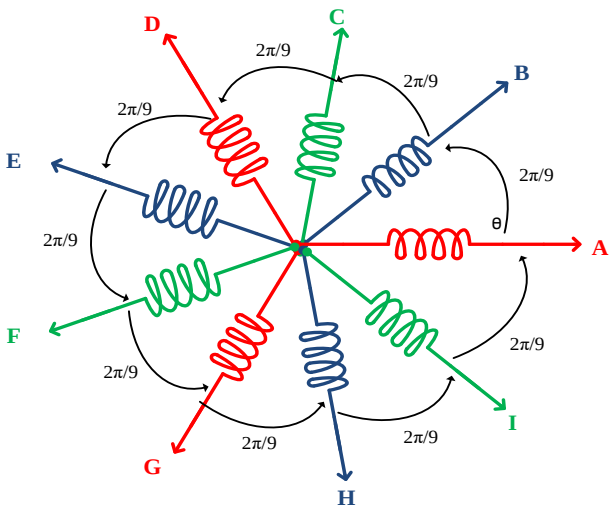

Fig. 4.3 Nine-phase stator winding equivalent schematic diagram

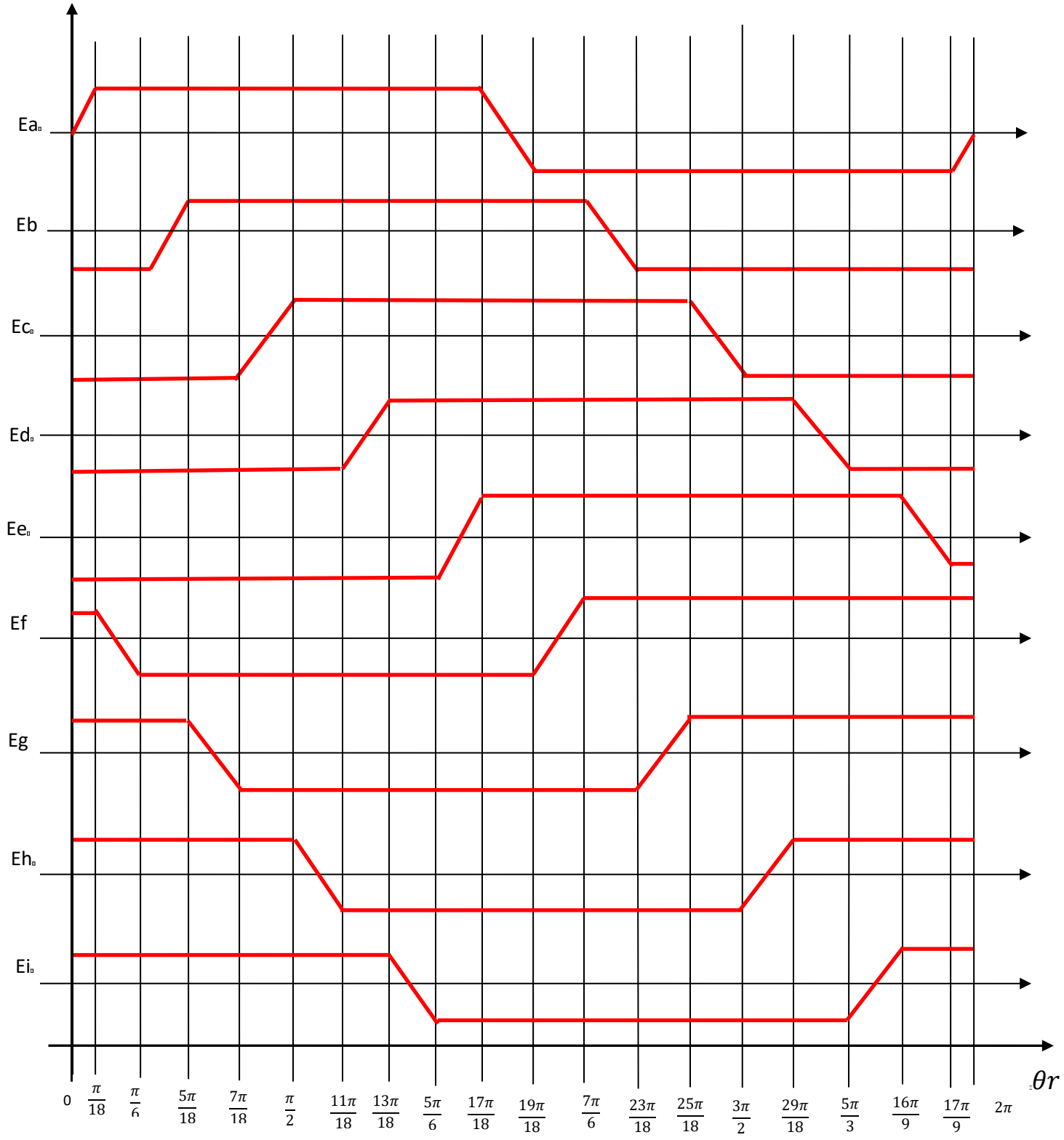

Fig. 4.4 Back-EMF volteges waveform of the nine-phase of BLDC motor for one complet cycle(360^0)

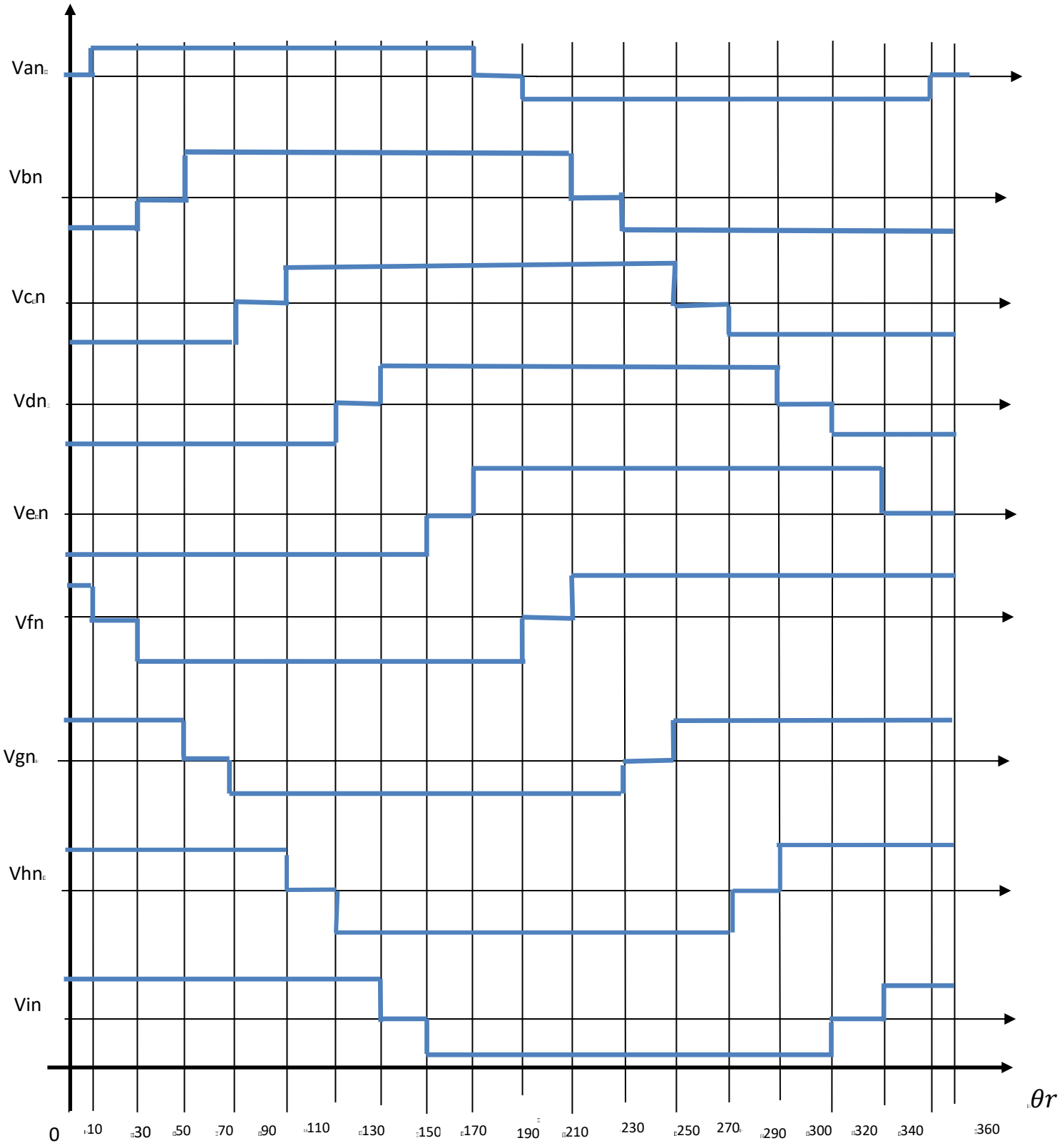

Fig. 4.5 Nine phase voltages waveforms for one complet cycle[2]

Based on the distribution of the winding and each phase windings separated by $\frac{2\pi}{9} = 40°$, the back-EMF produced in the nine-phase stator phase wave form for one complete cycle is given as following figure below and the each phase back-EMF exactly 40^0.

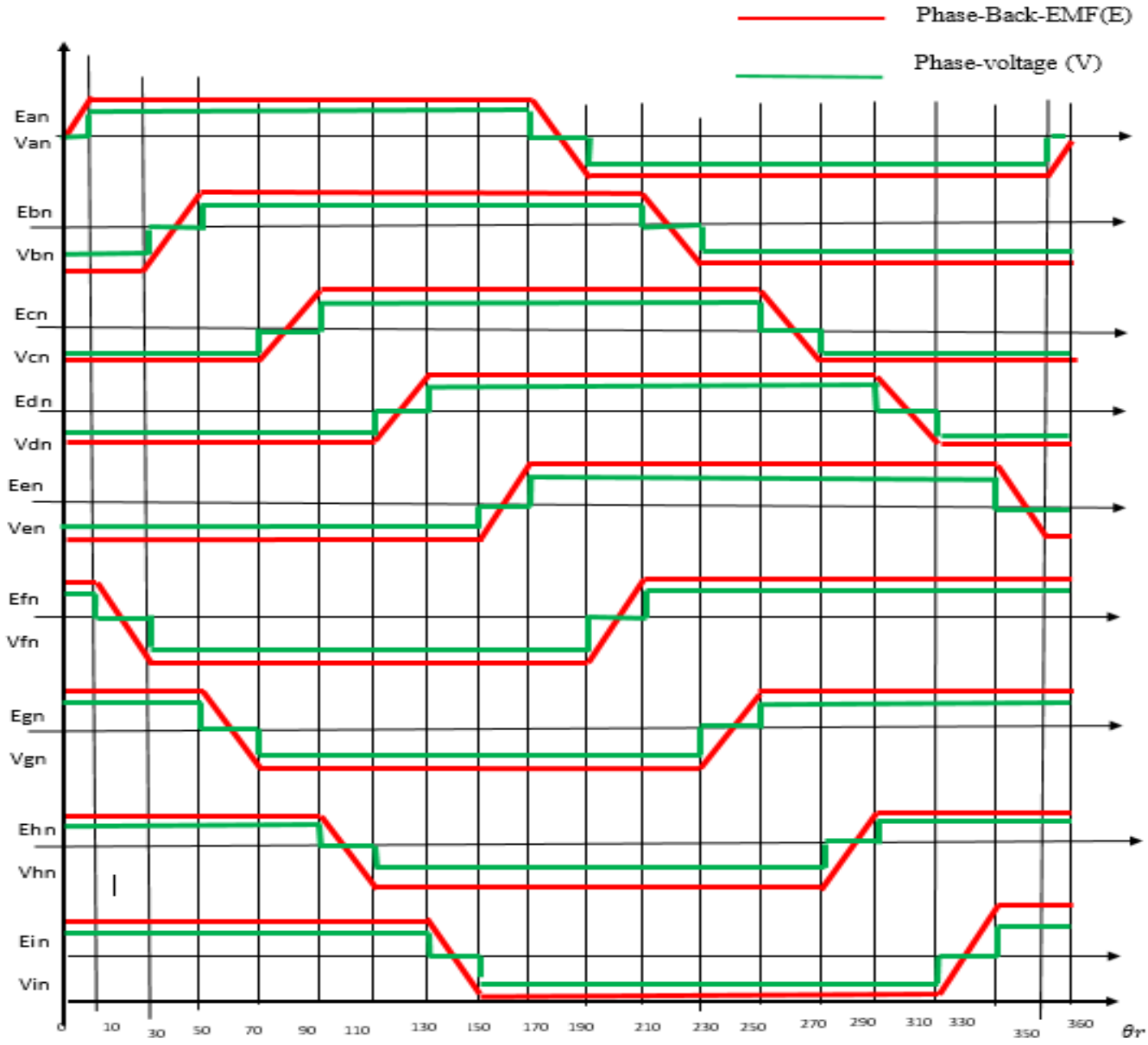

Fig. 4.6 Back-EMF and phase current wave form of the nine-phase BLDC motor [2]

And the following table shows the whole position detection of the rotor based on the back-EMF zero crossing point and the polarity of phase currents based on the back-EMF produced in stator winding. Based on the back-EMF graph figure 4.6 above the following tabulated summarization was developed.

Table 4.1 Summarized sensorless rotor position detections and states of the nine-phase VSI switches based on back-EMF

Back-EMF Zero-crossing occur in Phase	back-EMF waveform phases or polarities for the 110^0 elec.dgrees rotation									Rotor angle position in Ele. degrees	conducting switches of nine-phase **VSI**
	e_a	e_b	e_c	e_d	e_e	e_f	e_g	e_h	e_i		
A	0	-1	-1	-1	-1	+1	+1	+1	+1	-10^0-10^0	S_{11}, S_{13}, S_{15}, S_{17}, S_4, S_6, S_{10}, S_{12}
F	+1	-1	-1	-1	-1	0	+1	+1	+1	10^0-30^0	S_1, S_{13}, S_{15}, S_{17}, S_4, S_6 , S_8, S_{10}
B	+1	0	-1	-1	-1	-1	+1	+1	+1	30^0-50^0	S_1, S_{13}, S_{15}, S_{17}, S_6, S_8,S_{10}, S_{12},
G	+1	+1	-1	-1	-1	-1	0	+1	+1	50^0-70^0	S_1, S_3, S_{15}, S_{17}, S_6, S_8, S_{10}, S_{12}
C	+1	+1	0	-1	-1	-1	-1	+1	+1	70^0-90^0	S_1, S_3, S_{15}, S_{17}, S_8, S_{10}, S_{12}, S_{14}
H	+1	+1	+1	-1	-1	-1	-1	0	+1	90^0-110^0	S_1, S_3, S_5, S_{17}, S_8, S_{10}, S_{12}, S_{14}
D	+1	+1	+1	0	-1	-1	-1	-1	+1	110^0-130^0	S_1, S_3, S_5, S_{17}, S_{10}, S_{12}, S_{14}, S_{16}
I	+1	+1	+1	+1	-1	-1	-1	-1	0	130^0-150^0	S_1, S_3, S_5, S_7, S_{10}, S_{12}, S_{14}, S_{16}
E	+1	+1	+1	+1	0	-1	-1	-1	-1	150^0-170^0	S_1, S_3, S_5, S_7, S_{12}, S_{14}, S_{16}, S_{18}
A	0	+1	+1	+1	+1	-1	-1	-1	-1	170^0-190^0	S_3, S_5, S_7, S_9, S_{12}, S_{14}, S_{16}, S_{18}
F	-1	+1	+1	+1	+1	0	-1	-1	-1	190^0-210^0	S_3, S_5, S_7, S_9, S_2, S_{14}, S_{16}, S_{18}
B	-1	0	+1	+1	+1	+1	-1	-1	-1	210^0-230^0	S_5, S_7, S_9, S_{11}, S_2, S_{14}, S_{16}, S_{18}
G	-1	-1	+1	+1	+1	+1	0	-1	-1	230^0-250^0	S_5, S_7, S_9, S_{11}, S_2, S_4, S_{16}, S_{18}
C	-1	-1	0	+1	+1	+1	+1	-1	-1	250^0-270^0	S_7, S_9, S_{11}, S_{13}, S_2, S_4, S_{16}, S_{18}
H	-1	-1	-1	+1	+1	+1	+1	0	-1	270^0-290^0	S_7, S_9, S_{11}, S_{13}, S_2, S_4, S_6, S_{18}
D	-1	-1	-1	0	+1	+1	+1	+1	-1	290^0-310^0	S_9, S_{11}, S_{13}, S_{15}, S_2, S_4, S_6, S_{18}
I	-1	-1	-1	-1	+1	+1	+1	+1	0	310^0-330^0	S_9, S_{11}, S_{13}, S_{15}, S_2, S_4, S_6, S_8
E	-1	-1	-1	-1	0	+1	+1	+1	+1	330^0-350^0	S_{11}, S_{13}, S_{15}, S_{17}, S_2, S_4, S_6, S_8

Therefore, using back-EMF zero crossing point and the polarity we can control the position of the motor easily and also the switching sequence of the nine-phase VSI based on the position of the rotor extracted from the back-EMF generated inside the stator winding. From the table the polarities of the current indicate that which switches should be turn on which are not and the polarity of the phase sequence helps which switch the top or the lower leg switch turned on. If the polarity is negative with that period, the lower leg of the particular phase is turned on similarly if the polarity is positive the upper leg of that phase is on for that particular period. Using the back-EMF waveform for one complete cycle (360^0), the terminal voltage of the nine-phase inverter for the eighteen-step commutation sequences for an interval of 20^0 period summarized in the following table 4.2. Phase current polarities for the first 180^0 elec. degrees based on the back-EMF waveform also given in the table.

Table 4.2 Nine phases terminal voltage according to 160^0 operating mode for the half cycle

Steps	Switching interval Electrical degree	The nine-phase stator Phase voltage w.r.t neutral point N during each state								
		V_{an}	V_{bn}	V_{cn}	V_{dn}	V_{en}	V_{fn}	V_{gn}	V_{hn}	V_{in}
1	350^0-10^0	0	$\frac{-Vdc}{2}$	$\frac{-Vdc}{2}$	$\frac{-Vdc}{2}$	$\frac{-Vdc}{2}$	$\frac{+Vdc}{2}$	$\frac{+Vdc}{2}$	$\frac{+Vdc}{2}$	$\frac{+Vdc}{2}$
2	10^0-30^0	$\frac{+Vdc}{2}$	$\frac{-Vdc}{2}$	$\frac{-Vdc}{2}$	$\frac{-Vdc}{2}$	$\frac{-Vdc}{2}$	0	$\frac{+Vdc}{2}$	$\frac{+Vdc}{2}$	$\frac{+Vdc}{2}$
3	30^0-50^0	$\frac{+Vdc}{2}$	0	$\frac{-Vdc}{2}$	$\frac{-Vdc}{2}$	$\frac{-Vdc}{2}$	$\frac{Vdc}{2}$	$\frac{+Vdc}{2}$	$\frac{+Vdc}{2}$	$\frac{+Vdc}{2}$
4	50^0-70^0	$\frac{+Vdc}{2}$	$\frac{+Vdc}{2}$	$\frac{-Vdc}{2}$	$\frac{-Vdc}{2}$	$\frac{-Vdc}{2}$	$\frac{-Vdc}{2}$	0	$\frac{+Vdc}{2}$	$\frac{+Vdc}{2}$
5	70^0-90^0	$\frac{+Vdc}{2}$	$\frac{+Vdc}{2}$	0	$\frac{-Vdc}{2}$	$\frac{-Vdc}{2}$	$\frac{-Vdc}{2}$	$\frac{-Vdc}{2}$	$\frac{+Vdc}{2}$	$\frac{+Vdc}{2}$
6	90^0-110^0	$\frac{+Vdc}{2}$	$\frac{+Vdc}{2}$	$\frac{+Vdc}{2}$	$\frac{-Vdc}{2}$	$\frac{-Vdc}{2}$	$\frac{-Vdc}{2}$	$\frac{-Vdc}{2}$	0	$\frac{+Vdc}{2}$
7	110^0-130^0	$\frac{+Vdc}{2}$	$\frac{+Vdc}{2}$	$\frac{+Vdc}{2}$	0	$\frac{-Vdc}{2}$	$\frac{-Vdc}{2}$	$\frac{-Vdc}{2}$	$\frac{-Vdc}{2}$	$\frac{+Vdc}{2}$
8	130^0-150^0	$\frac{+Vdc}{2}$	$\frac{+Vdc}{2}$	$\frac{+Vdc}{2}$	$\frac{+Vdc}{2}$	$\frac{-Vdc}{2}$	$\frac{-Vdc}{2}$	$\frac{-Vdc}{2}$	$\frac{-Vdc}{2}$	0
9	150^0-170^0	$\frac{+Vdc}{2}$	$\frac{+Vdc}{2}$	$\frac{+Vdc}{2}$	$\frac{+Vdc}{2}$	0	$\frac{-Vdc}{2}$	$\frac{-Vdc}{2}$	$\frac{-Vdc}{2}$	$\frac{-Vdc}{2}$
10	170^0-190^0	0	$\frac{+Vdc}{2}$	$\frac{+Vdc}{2}$	$\frac{+Vdc}{2}$	$\frac{+Vdc}{2}$	$\frac{-Vdc}{2}$	$\frac{-Vdc}{2}$	$\frac{-Vdc}{2}$	$\frac{-Vdc}{2}$

Based on the back-EMF and current waveforms for one complete revolution of the motor the following tables are developed. Based on the above truth table a block diagram is designed to generate appropriate commutation signal which will be simulate and verify using MATLAB/Simulink in chapter 5. Based on the truth table a MATLAB function *y=emfE (u)* developed code to generate the eighteen pulse commutation logic Appendix-B.

4.3.1 Torque Equation

Based on the operating system of the motor and the sensorless control of the motor summarized in the table 4.5 above we can have developed the torque equation for the motor for each commutation sequence as we see from the table at each periods of the commutation the polarity of the back-EMF and phase currents are the same in order to get maximum torque. From the previous chapter 3 the electrical torque developed by the motor can be given as follows:

Once we got the back-EMF and the stator phase current then, we can calculate the torque developed by the machine. During any 40^0 intervals, the instantaneous power being converted from electrical to mechanical is the sum of the contribution from eight phases in series and is given by;

$$p_T = \omega_m T_e \tag{4.3}$$

And electrical power produced by the motor in each phase also given by (4.3a)

$$p_T = e_{pn} i_p \tag{4.3a}$$

And the total electrical power produced

$$p_T = \sum_{x=a}^{i} e_{xn} i_x \tag{4.3b}$$

Where;

p_T - Total power output,

T_e - Total output torque

e_{pn}- phase back-EMF

i_p- phase current

x= any phases (a, b, c, d, e, f, g, h, i)

Therefore, the electromagnetic torque produced by the nine phase BLDC motor can be expressed as;

Using the above equation and by equating 4.3 and 4.3b following electrical torque equation can be derived.

$$T_e = \frac{e_{an}\, i_a + e_{bn}\, i_b + e_{cn}\, i_c + e_{dn}\, i_d + e_{en}\, i_e + e_{fn}\, i_f + e_{gn} i_g + e_{hn} i_h + e_{in}\, i_i}{\omega_m} \quad (4.4)$$

Using sensorless control of the motor we don't have the speed of the motor at the beginning therefore, we have to cancel out the rotor speed in equation above. Where, e is back-EMF in each-winding phase due to the rotation of the rotor given as follows:

$$e_{xn} = lNrB\omega_m \quad (4.5)$$

N- number of turns per phase winding,
r- is the mean-radius of the air gap and
l - is the effective axial length of stator winding,
B- ***is*** the magnetic-flux density of the machine. For more simplified form let us put
x= any phase

$$k_e = \text{lrNB} \quad (4.6)$$

Where, k_e = is known as the back-EMF constant
Therefore, the electrical torque given in equation 4.3 can be express by substituting the back-EMF equation given in equation 4.5 and after cancelation of rotor speed (ω_m) torque equation become

$$T_e = \frac{p}{2}\left(lNrBi_a + lNrBi_b + lNrBi_c + lNrBi_d + lNrBi_e + lNrBi_f + lNrBi_g + lNrBi_h + lNrBi_i\right) \quad (4.7)$$

Where, $l, N, r, p, and\ B$ all are constant and,

i.e. $$T_p = k_t i_p \quad (4.8)$$

N- number of turns per phase winding,
r- is the mean-radius of the air gap and
l - is the effective axial length of stator winding,
B- is the magnetic-flux density of the machine.
For more simplified form substituting of equation 4.8 in to equation 4.7 becomes,

$$T_e = K_t i_a + K_t i_b + K_t i_c + K_t i_d + K_t i_e + K_t i_f + K_t i_g + K_t i_h + K_t i_i \quad (4.9)$$

Now, the torque produced by the motor in every commutation sequence can be calculated using equation (4.6), from the table 4.5 we can see that each switching periods eight phases conducts and one phase is not or not energized. now let us see the torque produced for some commutation sequences,

Sequence-1 (0^0-10^0) all phases are contributing torque except **phase-a** therefor, the torque produced by the motor given as follows. i.e. $i_a = 0$,

$$T_e = K_t i_b + K_t i_c + K_t i_d + K_t i_e + K_t i_f + K_t i_g + K_t i_h + K_t i_i \quad (4.10)$$

All the conducting phases produces equal current (i_p) and the torque constant also constant everywhere,

Therefore, the resultant torque produced equation (4.7) can be simplified

$$T_e = 8K_t i_p \quad (4.10a)$$

Sequence-2 (10^0-30^0) all phases are contributing torque except **phase-f** therefor, the torque produced by the motor given as follows. i.e. $i_f = 0$,

$$T_e = K_t i_a + K_t i_b + K_t i_c + K_t i_d + K_t i_e + K_t i_g + K_t i_h + K_t i_i \quad (4.11)$$

Similarly, sequence-1 torque produced in this period is contributions of 8 phases,

$$T_e = 8K_t i_p \quad (4.11a)$$

Sequence-3 (30^0 -50^0) all phases are contributing torque except **phase-b** therefor, the torque produced by the motor given as follows. i.e. $i_b = 0$,

$$T_e = K_t i_a + K_t i_c + K_t i_d + K_t i_e + K_t i_f + K_t i_g + K_t i_h + K_t i_i \quad (4.12)$$

$$T_e = 8K_t i_p \quad (4.12a)$$

Similarly, the torque produced for the rest of the sequence can be done and by doing that using back-EMF sensing and controlling the nine-phase VSI maximum constant torque can be achieved. And each time of commutation eight phases out of nine is used and the total torque amplitude produced is eight times the torque produced by each phase.

Fig. 4.7 resultant electrical torque produced for 20^0 commutation

4.4 Nine-phase Inverter design for nine-phase BLDC motor

The power electronic convertor coverts DC supply to AC output is called inverter. Nowadays using this power electronic convertor, we can get more than three phase electrical supply. The nine-phase BLDC motor need an electronic inverter to control the rotation of the motor and to commutate the stator current one winding phase to the other phase winding. Depending on the type of DC source supplying the inverter; it can be classified as voltage source inverters (VSI) and current source inverters (CSI). The DC source is usually rectified from the three-phase AC-input power. There is a DC link connected between the rectifier and the inverter. A capacitive-output DC link is used for a VSI and an inductive output link is employed in CSI. The circuit diagram for a two-level nine-phase voltage source inverter for power applications is shown in figure 4.8.

Here in this thesis nine-phase inverter is used for the nine-phase BLDC motor. The inverter has DC power supply (usually from rectifiers) and 18 electrical switches and each switch is conducting for 160 electrical degrees for sensorless control. Each switches are conducting seat has the eight-cycles and each cycle has 20 electrical degrees and at each cycle a commutation is takes place. Commutation means switching current from one conducting stage to another not conducting stage. The switches are controlled by eighteen-pulse logic gate generator according to the rotor position. The rotor position information is crucial for controlling the machine. If we have the rotor position information we can do proper commutation for controlling the machine. Here is schematic diagram of nine-phase inverter switches. In the figure 4.8; V_{dc} represent DC source the numbers (1, 2, 3, 4…9) indicates the nine phase winding of the motor and (S_1, S_2, S_3…. S_{18}) represents the eighteen semi-inverter switches to control inverter outputs. For operation of nine-phase BLDC motor, the phase current and back-EMF should be aligned to generate constant torque. The commutation sequence point here in this thesis can be detected using sensorless method based on back-EMF waveform sequence. And a 20^0 phase shift, using 18-step commutation scheme through a nine-

phase inverter for driving the nine-phase BLDC motor. And the conducting interval for each phase is 160^0 electrical angle. Therefore, only eight phases are conducting current at any time, leaving reaming last phase floating or unexcited. In order to produce maximum torque, the inverter should be commutated every 20^0 by detecting zero crossing of the back-EMF on the floating phase coil of the motor, so that current is in phase with the back-EMF waveform. The terminal voltage of the floating phase is directly proportional to the back-EMF. The ZCP can be detected by comparing terminal voltage of floating phase with the half of DC link voltage or the virtual neutral voltage.

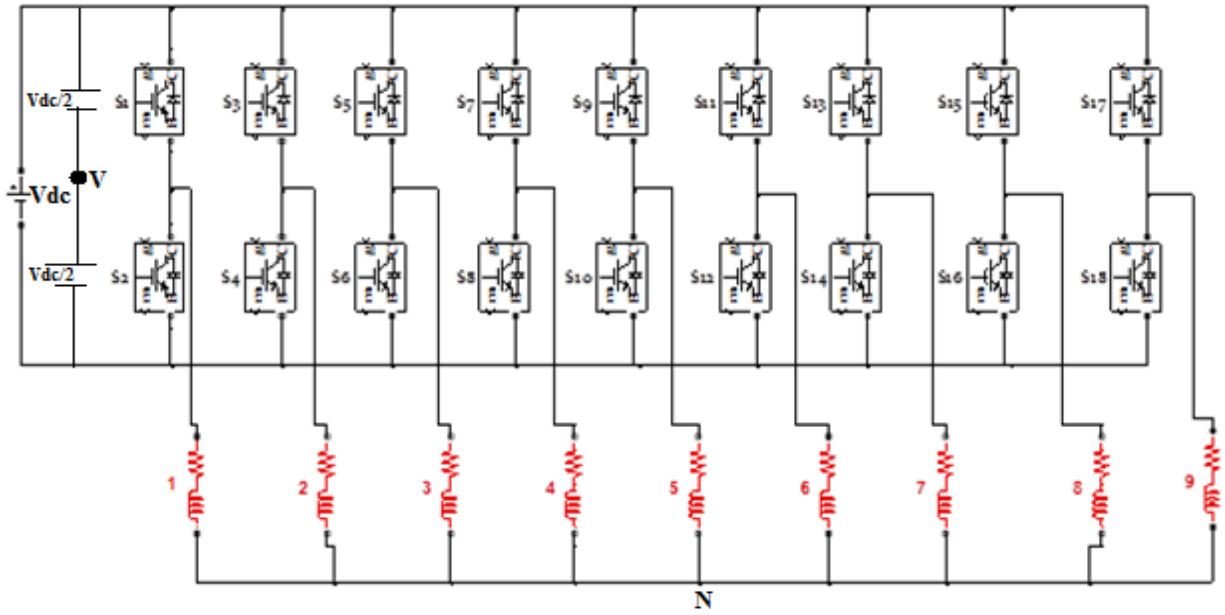

Fig. 4.8 schematic diagram of Nine-phase VSI's for nine-phase BLDC motor

The switching sequences of the eighteen-step inverter is based on the back-EMF waveform is determined from the truth table of the back-EMF waveforms. During each commutation sequence ($\frac{2\pi}{18} = 20$) the back-EMF wave-form is detected and the sequence leads us to determine which switches are ON and which switches are turned OFF. Therefore, from the back-EMF waveform we can get the switching sequence and the eighteen step sequences are given to the nine-phase inverter and the inverter supply the appropriate signal (input voltage) to the nine-phase stator winding of the machine for maximum torque operation.

A basic nine-phase VSI is an eighteen-step bridge inverter, consisting of eighteen power electronics switches. Each switch in the circuit consists of two power semiconductor devices,

connected in anti-parallel. One of these is a fully controllable semiconductor, such as a IGBT, while the second one is a diode. A step can be defined as the change in firing from one switch to the next switch in proper sequence. For a eighteen-step inverter each step (commutation sequence) ($\frac{2\pi}{18} = 20^{\circ}$) intervals for one cycle of 360^0. That means the switches would be gated at regular intervals of $\mathbf{20}^{\circ}$ in proper sequence to get a nine-phase AC output voltage at the output terminal of VSI. The eighteen switches are divided into two groups; upper nine switches as positive group (i.e. S_1, S_3, S_5, S_7, S_9, S_{11}, S_{13}, S_{15}, S_{17}) and lower five as negative group of switches (i.e. S_2, S_4, S_6, S_8, S_{10}, S_{12}, S_{14}, S_{16}, S_{18}). There are two conductions mode to the switches the nine-phase inverter switches for one complete cycle (360^0) such as [28]:

1) 180^0 conduction mode and
2) 40^0 conduction mode.

4.4.1 Nine-phase 180^0 Degree Conduction Mode VSI

By referring to figure 4.2, each switch conducts for 160^0 of a cycle. Switch pair in each leg, i.e. S_1-S_2; S_3-S_4; S_5-S_6; S_7-S_8; S_9-S_{10}; S_{11}-S_{12}; S_{13}-S_{14}; S_{15}-S_{16}; S_{17}-S_{18} are turned on with a time interval of 180^0. It means that S_1 conducts for 160^0 and off for 20^0 then, S_2 starts conduct and its state is for the first 20^0 not conduct and for the next 160^0 conduct for the application of the inverter for nine-phase BLDC motor.

In the eighteen-step 180^0 conduction mode of operation, eight switches are on at a time, four from positive group and four from negative group or vice versa, each switch conducts for 160^0 of a cycle and two switches of the same leg should be turned on simultaneously in both cases as this condition would short circuit the DC source and in each period of 180^0 conduction two switches. The upper and lower switches of only one leg of the nine-phase inverter is not conduct at each time in the case of eighteen-step commutation of the BLDC motor.

4.4.2 Nine-phase 40^0 Degree Conduction Mode VSI

The nine-phase BLDC winding of motor is constructed with angle between each other is $\left(\frac{2\pi}{9} = 40^{\circ}\right)$ using the lag-angle of the winding and using the switching of the this nine phase in order to proper commutation. The power circuit diagram of this inverter is the same as shown in figure

4.9 for the 40° mode VSI, each switch conducts for $40^{\circ 0}$ of a cycle. Like 180^{0} mode, 40° mode inverter also require eighteen-steps, each of $\frac{2\pi}{18} = 20^{\circ}$ duration for completing one cycle of the output AC voltage.

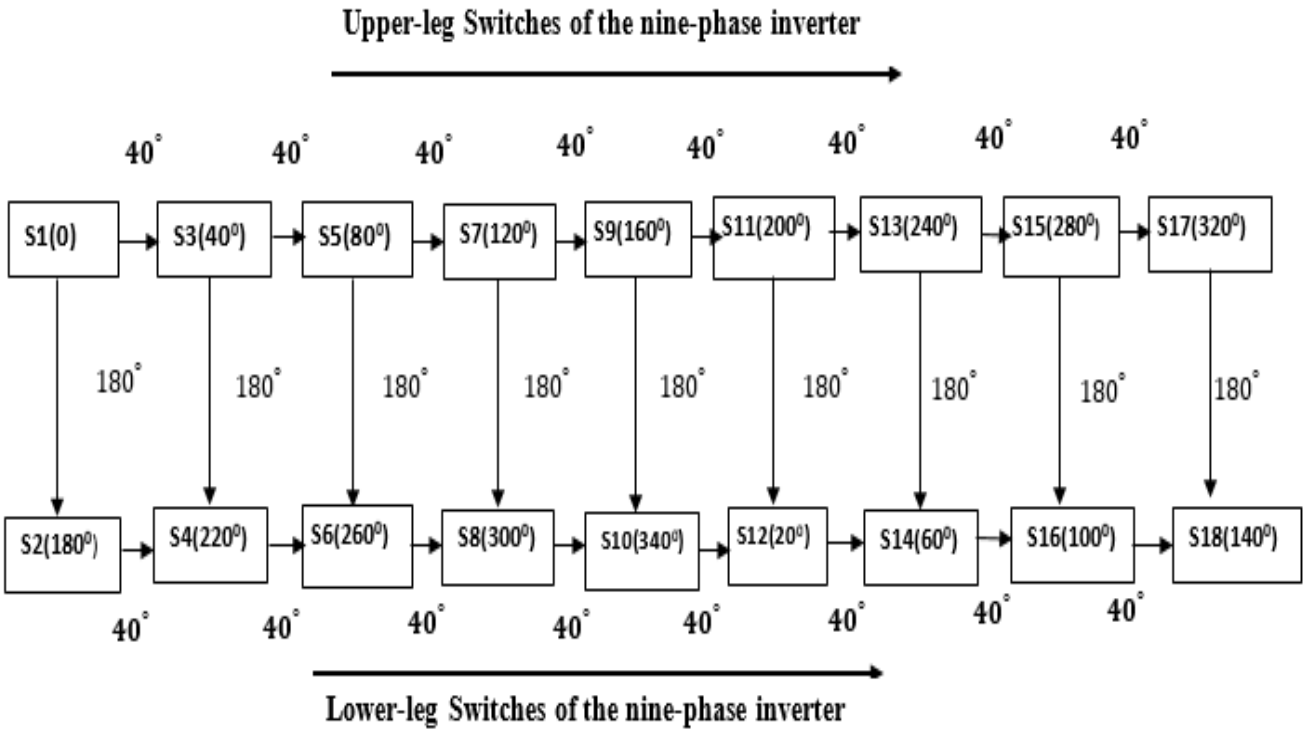

Fig. 4.9 Nine-Phase 40^{0} operating mode VSI

As shown in figure 4.2; in 40^{0} mode conduction S_1 conducts with S_{12} for 20^{0} then S_{14} for the next 20^{0} conducts with S_3 conduct with S_{12} for another first 20^{0} and conduct with S_{14} for the next 20^{0}, like, wise every 20^{0} the switching is takes place for all the rest of the switches of the nine-phase inverters using this note and the above figure 4.2 conduction mode sequences of the switches based on the period of sequence can be written as follows S_{12} S_1, S_{12} S_3, S_3 S_{14}, S_{14} S_5, S_5 S_{16}, S_{16} S_7, S_7 S_{18}, S_{18} S_9, S_9 S_2, S_2 S_{11}, S_{11} S_4, S_4 S_{13}, S_{13} S_6, S_6 S_{15}, S_{15} S_8, S_8 S_{17} and S_{17} S_1, this sequence is also known as the eighteen-step computation sequence. In this conduction mode the chances of short circuit of the DC link voltage source is avoided as each switch conduct for 40^{0} in one cycle, so there is an interval of 20^{0} in each cycle when no switch is in conduction mode and the output voltage at this time interval is zero.

4.4.3 Nine-phase Inverter function modeling

For each commutation sequence using the back-EMF waveform sequences and the switching sequence of the machine develop the nine-phase inverter phase output voltage. The output voltage of the inverter to the stator windings of the machine can be modeled as follows as function of switching sequence of the inverter and the DC-bus voltage shown as below using equation (4.13).

$$\left.\begin{array}{l} ½(S_1V_{dc}-S_4V_{dc}) \\ ½(S_3V_{dc}-S_2V_{dc}) \\ ½(S_5V_{dc}-S_6V_{dc}) \\ ½(S_7V_{dc}-S_8V_{dc}) \\ ½(S_9V_{dc}-S_{10}V_{dc}) \\ ½(S_{11}V_{dc}-S_{12}V_{dc}) \\ ½(S_{13}V_{dc}-S_{14}V_{dc}) \\ ½(S_{15}V_{dc}-S_{16}V_{dc}) \\ ½(S_{17}V_{dc}-S_{18}V_{dc}) \end{array}\right\} \quad (4.13)$$

Where, S_1, S_2, S_3…. S_{18} the state of the switches from the eighteen pulse commutation logic gates. The nine-phase inverter works based on the eighteen-step sequence of the switches. The switch sequence can be done based on the back-EMF zero crossing sequence using the truth table above table 4.3.

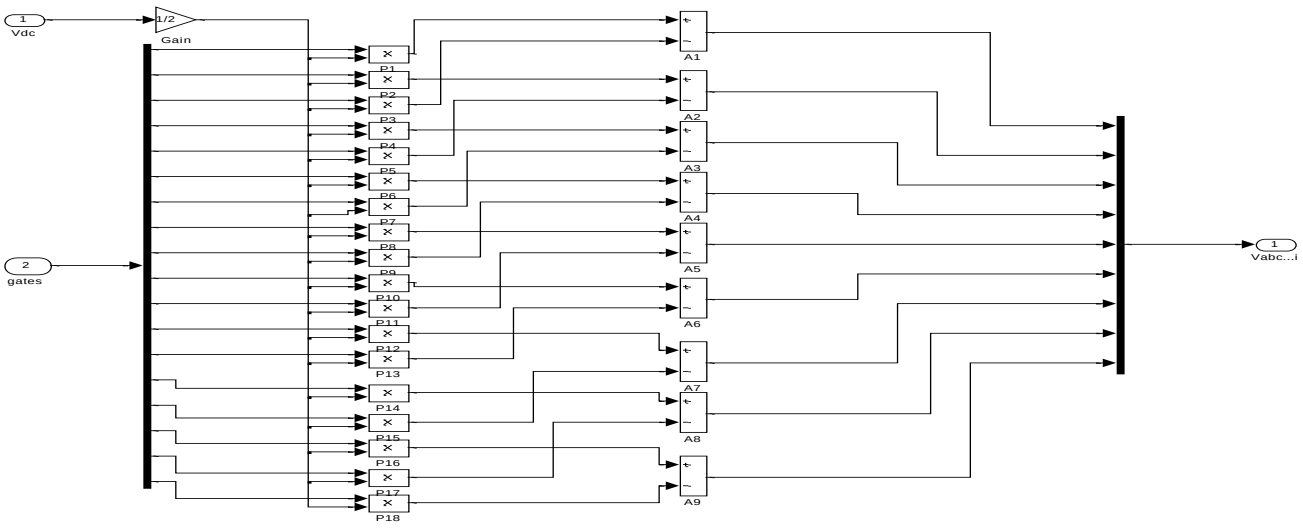

Fig. 4.10 Nine-phase inverter-function block-diagram (logical control of nine phase inverter)

4.5 Eighteen-step Commutation logics for the machine

The operating status of the switches in the voltage source inverter in figure 4.8 can be represented by switching states. Using table 4.1 and nine phase BLDC back-EMF waveform described above the switching sequence of the inverter developed for 160^0 conduction mode in Table 4.1, switching state '1' denotes that the ON state switch and 0 denotes for OFF state switches. in an inverter leg is on and the inverter terminal voltage V is positive (while '0' indicates that the inverter terminal voltage is zero due to the conduction of the lower switch. There are thirty-two possible combinations of switching states in the VSI as listed in Table 4.3. if any of lower-leg switches of the nine-phase inverter is 1 (ON) the terminal voltage of that leg is negative-half of the DC-bus voltage $(-Vdc/2)$ and if any of the upper-leg switches of the nine-phase inverter is 1 (ON) the terminal voltage of that leg is positive-half of the DC-bus voltage $(+Vdc/2)$ based on this principle of working and using the above tables the sensorless control of the nine-phase BLDC motor model is designed.

The machine is used an electronic commutation to control the speed and torque of the machine. The sequence of distribution of gate signals depends on the feedback from the motor rotor position of the motor. The position of the motor is sensed during every $\frac{\pi}{9} = 20$ electrical degree. According to the position of the rotor pulses to the 18 switches driving the BLDC machine. Here, the commutation sequence is developing using sensorless techniques called the zero crossing of the back-EMF detection method. After determining the position signals the commutation logic are generated, which drive the inverter switches. This model can generate exact square wave switching pattern. Thus, generating signals for 18 switches. At each instant, out of nine phases eight -phases conduct, and one of the nine phase are not conduct or remain unpowered. Here, in the figure 4.11 shows the eighteen-pulse generator based on the back-EMF sequence of the motor.

Table 4.3 eighteen-step switching sequences (state) of the nine-phase inverter switches based on the back-EMF sequence for the first 180^0 rotation

Step	Rotor Position Ele.dgree	The Eighteen Inverter Switches and states (**0** for **OFF** state and **1** for **ON** state)																	
		S_1	**S_2**	**S_3**	**S_4**	**S_5**	**S_6**	**S_7**	**S_8**	**S_9**	**S_{10}**	**S_{11}**	**S_{12}**	**S_{13}**	**S_{14}**	**S_{15}**	**S_{16}**	**S_{17}**	**S_{18}**
1	350^0-10^0	0	0	0	1	0	1	0	1	0	1	1	0	1	0	1	0	1	0
2	10^0-30^0	1	0	0	1	0	1	0	1	0	1	0	0	1	0	1	0	1	0
3	30^0-50^0	1	0	0	0	0	1	0	1	0	1	0	1	1	0	1	0	1	0
4	50^0-70^0	1	0	1	0	0	1	0	1	0	1	0	1	0	0	1	0	1	0
5	70^0-90^0	1	0	1	0	0	0	0	1	0	1	0	1	0	1	1	0	1	0
6	90^0-110^0	1	0	1	0	1	0	0	1	0	1	0	1	0	1	0	0	1	0
7	110^0-130^0	1	0	1	0	1	0	0	0	0	1	0	1	0	1	0	1	1	0
8	130^0-150^0	1	0	1	0	1	0	1	0	0	1	0	1	0	1	0	1	0	0
9	150^0-170^0	1	0	1	0	1	0	1	0	0	0	0	1	0	1	0	1	0	1
10	170^0-190^0	0	0	1	0	1	0	1	0	1	0	0	1	0	1	0	1	0	1

The ZCD method is based on detecting the instance at which the back-EMF in the unexcited phase crosses zero. Here, in order to produce maximum torque, the inverter must be commutated every 20 electrical degrees by detecting ZC of back-EMF on the floating coil of the motor, so that current is in phase with the back-EMF. This zero crossing triggers a timer, so that the next sequential inverter commutation occurs at the end to this timing interval. The conducting interval for each phase is 160 electrical degrees. Therefore, any eight phases conduct currents at any time, leaving the ninth phase floating. The commutation logic specifies the time intervals during which the switches should be ON and OFF to average the DC bus voltage applied there by controlling the speed.

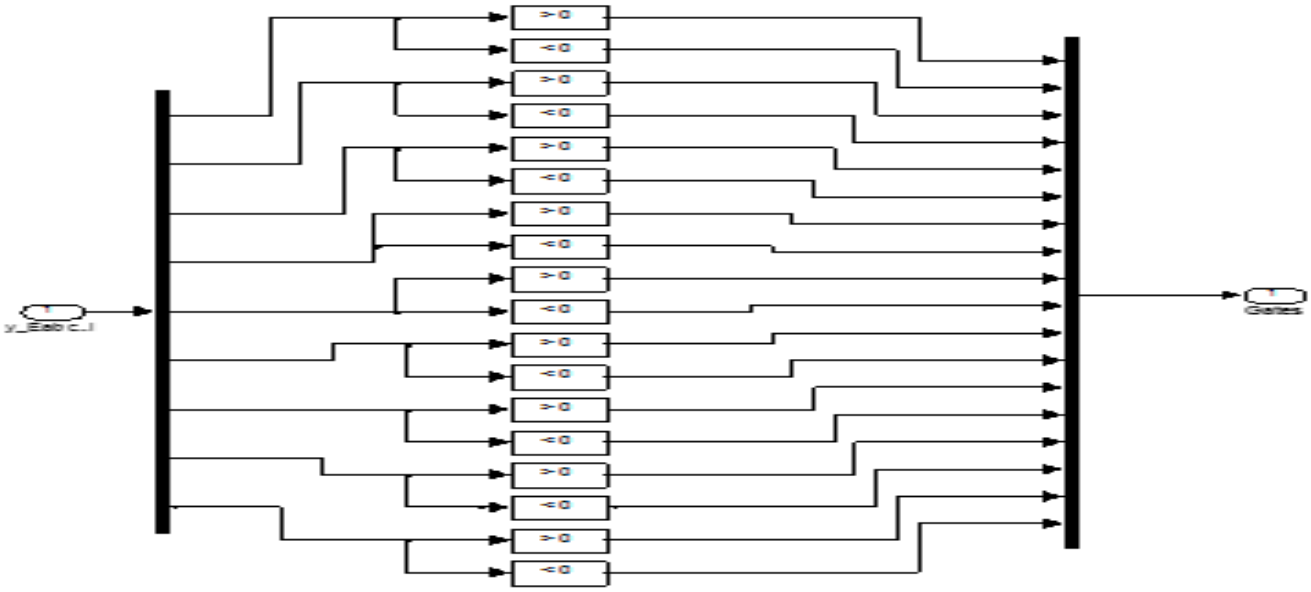

Fig. 4.11 Back- EMF ZCD for eighteen-step commutation logic

Therefore, based on the above back-EMF sequence and the switching state Table 4.3 we can control equivalently as using rotor position sensor in addition using the above table and switching sequence the MATLAB eighteen-step commutation Simulink block and MATLAB code developed for proper function of the sensorless control of the machine in the following chapter.

4.6 Speed control of the Nine-Phase BLDC motor

4.6.1 The open-loop analysis motor based

One of the difference between DC motor and BLDC motor is implied under, the BLDC motor, the stator windings are energized sequentially to rotate the rotor of the motor. And also, there is no physical connection between the stator and the rotor.

Therefore, the open loop transfer function $\boldsymbol{G(s)}$ of the Nine-phase BLDC motor using s-domain is obtained from the previous chapter the open-loop transfer function is given by (Eq.3.64) and rewritten here below in equation 4.3 and the output characteristics of the open-loop analysis is shown in the next chapter using MATLAB/Simulink.

$$G(s) = \frac{\omega_m(s)}{V_{pn}(s)} = \frac{15.9236}{1.235\times10^{-6}\times s^2+0.0251\times s+1} \tag{4.3}$$

4.6.2 The closed-loop PI speed controller of the motor

The speed of BLDC motor has direct relationship between the DC voltage or the phase voltage, that means the motor speed can be controlled by controlling the amplitude to varied the supplied Vdc to voltage source inverter. For inverter controlled BLDC motor drives, the inverter can be controlled by either PWM techniques with constant DC-link voltage or pulse amplitude modulation modulates the inverter power devices Using 160-degree modulation techniques and controls the amplitude of DC-link voltage. And the general block diagram representation of PAM based speed control of the machine is given in figure 4.12 and the proposed PAM speed controller basically has four parts;

- Nine-phase BLDC motor
- DC-link voltage source (DC to DC) / (AC-DC) voltage source.
- Nine-phase VSI (Plant)
- PI-Controller (proportional-integrator

For PAM control, 160-degree commutation control is used in general and the DC-link voltage is adjusted according to the error between speed and its reference.

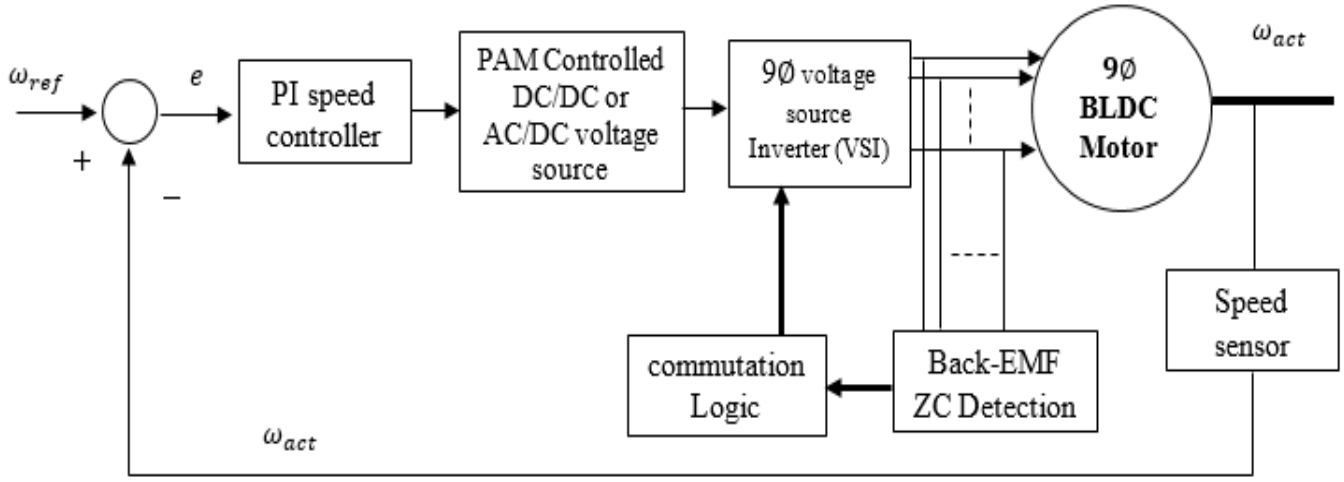

Fig. 4.12 Overall closed-loop speed controller block diagram

After the motor sensorless control he model of the PI speed control of the BLDC motor is required in order to control the motor for different speed and different motor speed. The speed of BLDC motor ha direct relationship between the DC voltage or the phase voltage, that means the motor

speed can be controlled by controlling the amplitude to varied the supplied Vdc to voltage source inverter. The general closed loop PI control of the motor block diagram is given below.

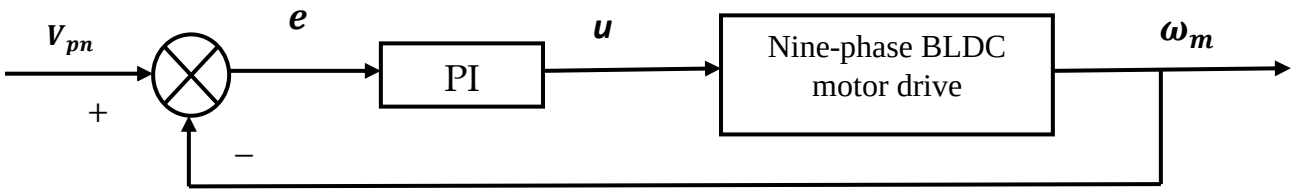

Fig. 4.13 closed loop PI control block diagram of the motor

The proportional-integral(PI) controller is about the most common and useful algorithm in control of speed control of BLDC motor. In most case, feedback loops are controlled using the PI algorithm. The main reason why feedback is very important in systems is to be able to attain a set point irrespective of the disturbances or any variation of any form. The PI controller always designed to correct error(s) between measured proses value(s) and set value(s) in a system. A simple illustration on how PI works is given below: Consider the characteristics of parameters-proportional(P) and integral(I), and derivative(D) controls, as applied to the diagram below in figure 4.8.

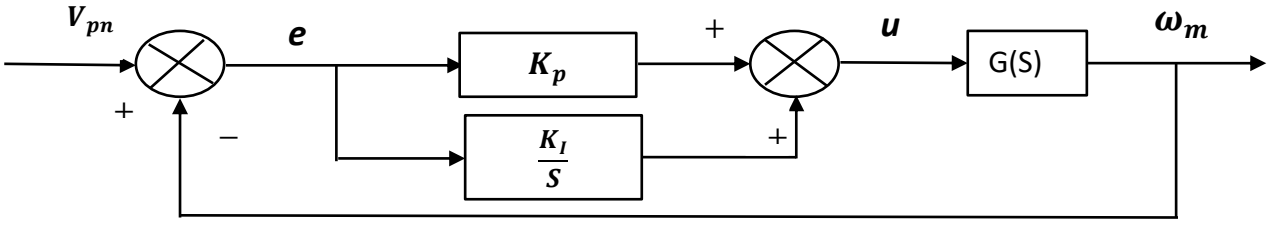

Fig. 4.14 closed-loop PI control of the motor

Considering the figure 4.14, variable, e is error, and it is the difference between the desired input value voltage (V_{pn}) and the actual output the output speed of the rotor (ω_m). In closed loop, *e* will be sent to the PI controller, and the controller will perform the proportional and integral and derivative computation on the error signal. Thereafter, the signal, u which is the output of the controller is now equal to the sum of [the product of proportional gain, Kp and magnitude of the error(e)] and [the product of the integral gain, Ki and the integral of the error(e)].

$$U=K_p e+K_i \int e dt \quad (4.4)$$

Next, by adding the transfer function of the nine-phase BLDC motor from the above open loop transfer function obtained in equation (3.39) in the place of G(S) the above closed loop block-diagram can be modified as follows. And the DC-link voltage is given 300 volts.

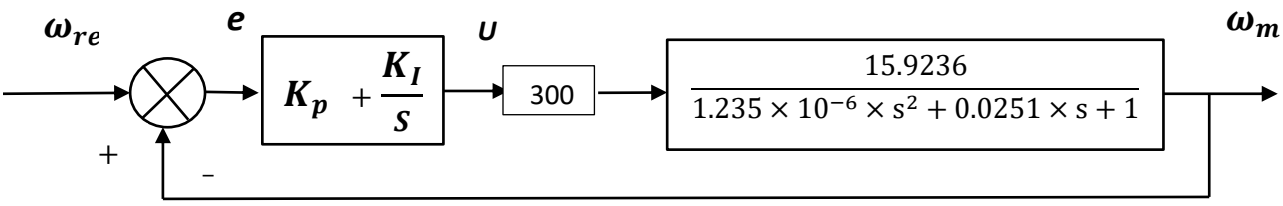

Fig. 4.15 closed-loop PI control with the motor transfer function

The signal value, u is the set continuously fed to the plant with every corresponding new output (ω_m), being obtained as the proses continues. The output, ω_m is set back and subsequently new error signal, ***e*** is found and the same process repeats itself on and on. After using different methods of tuning the speed is controlled the tuning of the proportional suitable and stable output is achieved. All the tuning and the result of the simulation will be discussed in the following chapter five using MATLAB/Simulink. And also in the following chapter sensorless control of the machine based on the back-EMF model and closed loop speed control of the system explained.

CHAPTER 5

MATLAB SIMULATION AND RESULT DISCUSSION

5.1 Introduction

MATLAB Simulink environment is a software package that utilizes the computational tools of MATLAB to analyze complex dynamic systems. The program is capable of solving both linear and nonlinear processes so it is perfectly suited to simulating multiphase synchronous machines. The first step in modeling a controller is to create a block diagram representation of its algorithm. This can be constructed from existing blocks in the Simulink library or from those created by the user. Once the block diagram has been developed it can be simulated using any number of different solvers. These compute the internal state variables of the blocks by solving their respective Ordinary Differential Equations. Choosing the appropriate solver can significantly decrease the computation time and improve the accuracy of the simulation. This decision is largely dependent on whether the controller model is implemented in discrete time using z variables, or continuous time using time domain t variable or the Laplacian S variable.

5.2 Simulation of sensorless control of the nine-phase BLDC motor

5.2.1 Simulink Modeling of nine-phase BLDC motor

The nine-phase BLDC motor model can be constructed using mathematical equations of the machine and back-EMF waveform sequences of the motor derived from the above chapters three and four. Once the block diagram has been developed it can be simulated using any number of different solvers. These compute the internal state variables of the by solving their respective Ordinary Differential Equations. The nine-phase BLDC motor parameter the given by the following table 5.1

Table 5.1 Nine-phase BLDC Motor parameters [37]

Motor parameters	**Values**
Per phase resistance (R)	0.7 ohm
Per phase inductance (L)	0.52mH
Per mutual inductance (M)	0.21mh
Moment of inertia (J)	0.0025 kgm^2
Number of poles(P)	2
Back-EMF constant (Ke)	0.0175 V/rad/sec
Torque constant (Kt)	1.2 Nm/A
DC-bus voltage (Vdc)	300V

The motor model and simulation based on the mathematical equation of the motor and using MATLAB code presented here I this chapter. The Simulink model of the motor and its drive is modeled using MATLAB Simulink in order to see the characteristics and the appropriate model of the motor. The overall Simulink model of the nine-phase BLDC motor is given in the figure below 5.1. The Simulink model of the nine-phase BLDC motor drive divided by four main different blocks,

I. Nine-phase BLDC Motor model
   - Voltage equation block
   - Back-EMF equation block
   - Mechanical equation block
   - Electromagnetic torque block

II. Nine-phase voltage source inverter blocks

III. Switching pulse block (the eighteen-step pulse generator)

IV. The back-EMF sequence generator block

Figure 5.1 Depicts the complete Simulink model of nine-phase permanent magnet brushless DC motor (PMBLDC motor) drive both the motor model and the nine-phase inverter model of the motor. The detail of each blocks of the Simulink model of figure 5.1 presented in Appendix A.

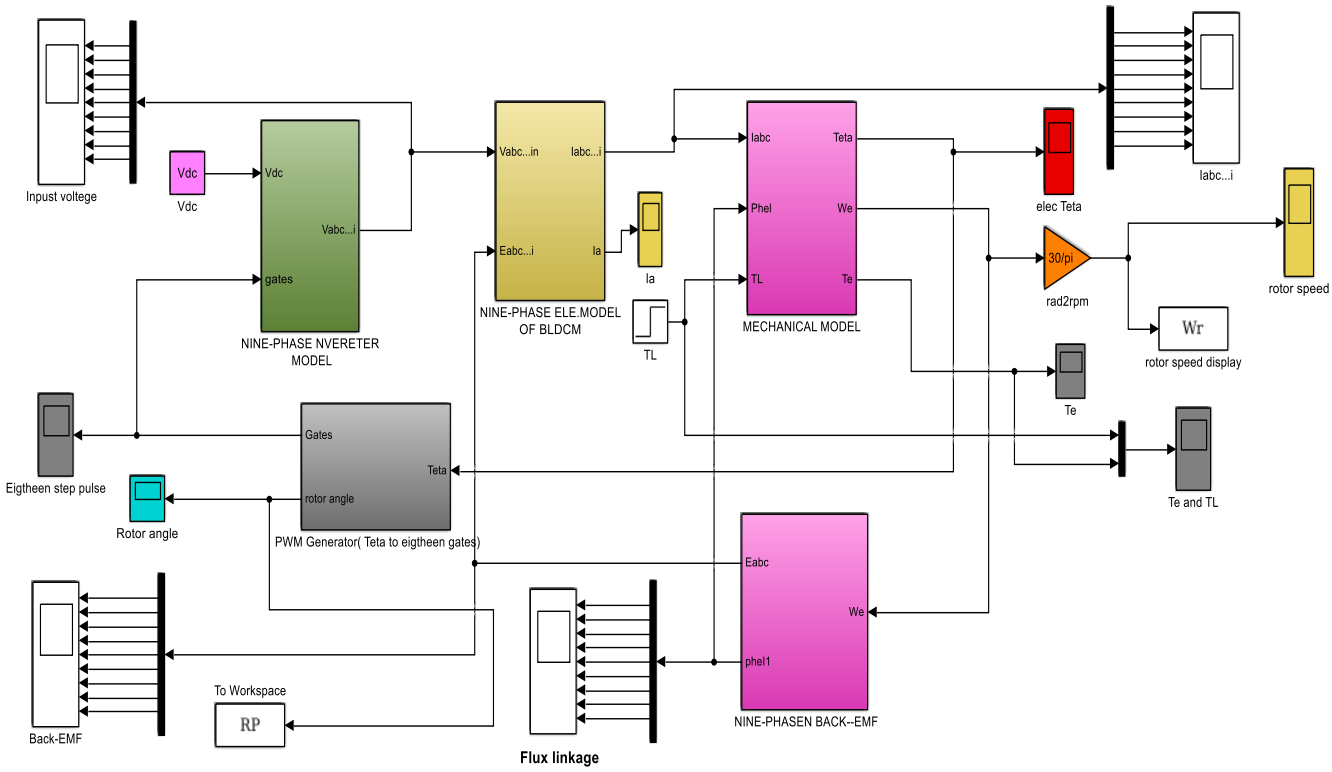

Fig. 5.1 Simulink model for sensorless control of nine-phase BLDC motor

5.2.2 Simulink model of voltage equation of BLDC motor

Simulink model of electrical torque produced by the machine, using the back-EMF and the nine-phase stator-current produced by the machine stator winding Simulink model of the nine-phase BLDC motor drive. Fig 5.2 shows Simulink model of phase a winding voltage and current equation of the motor, for the reaming phases (b to i) also has been done similar manner.

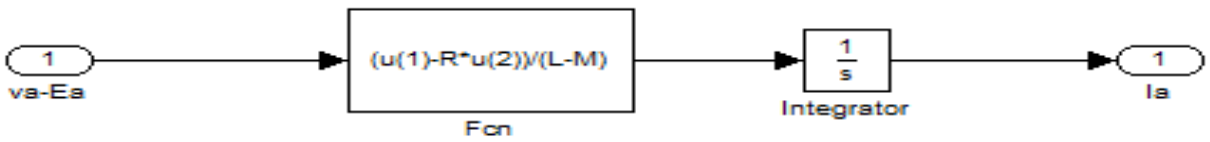

Fig. 5.2 Simulink model of voltage equation for stator winding phase-a

5.2.3 Simulink model of Electromagnetic torque produced

The torque and rotor speed relationship equation developed in the previous chapters also developed using MATLAB Simulink. And the Simulink model of the mechanical equation related to the electrical torque also modeled together in the figure 5.3 below.

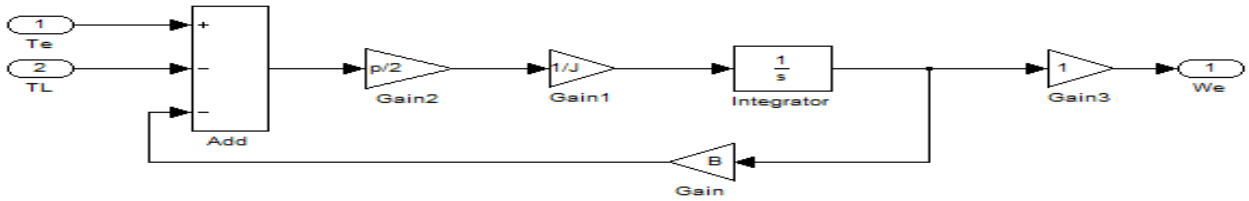

Fig. 5.3 Simulink model torque equation

5.2.4 Simulink model of the nine-phase inverter

The nine-phase inverter used in the Simulink model is done by the inverter function and the eighteen step switches developed in the previous chapter the MATLAB Simulink model of the nine-phase inverter Simulink is modeled based on the switching sequence is given in the figure 5.4 below. switching sequence inverter function done by using the rotor position information of the motor. Modeling of switching sequence based on the back-EMF sequences for each eighteen step of the machine the function of the model is summarized by Table 4.3.

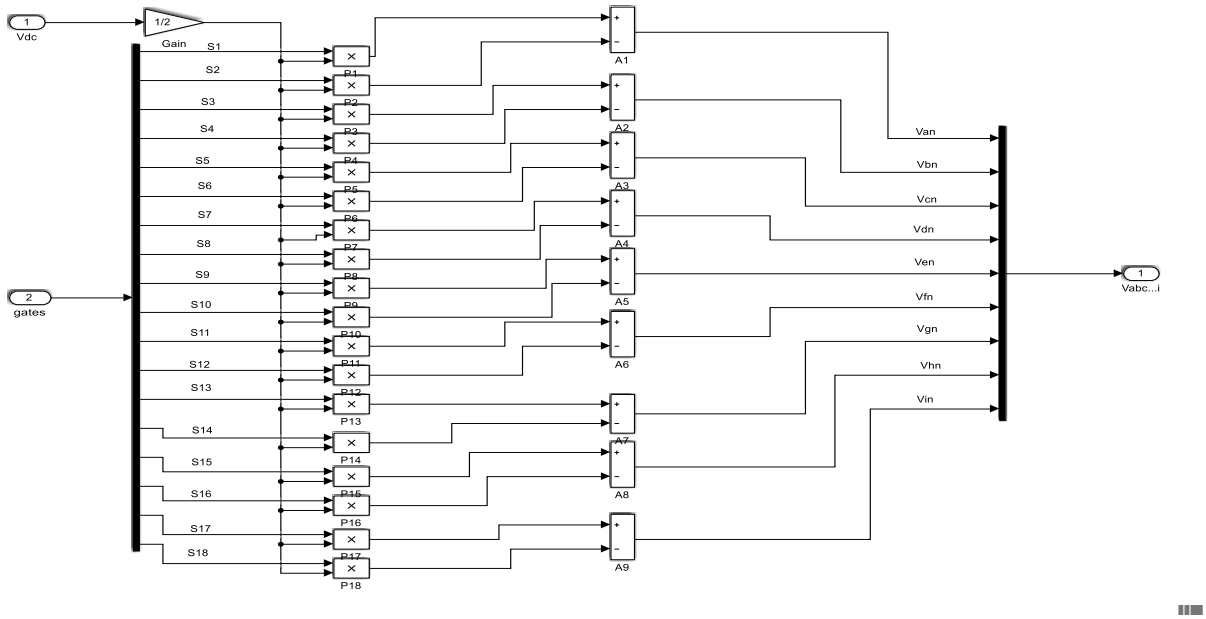

Fig. 5.4 Nine-phase inverter function Simulink modeling

5.3 Simulation Result and Discussion

The Simulation result of a sensorless control of nine-phase BLDC motor based on the back-EMF waveform sequence was carried out to assess its performance. The nine-phase BLDC motor used has the parameters given in Table 5.1

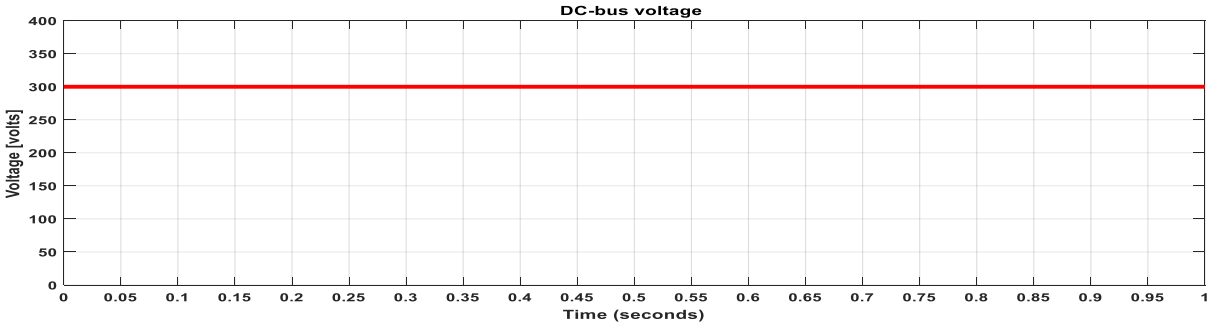

Fig. 5.5 DC-bus Voltage supplied to the nine-phase inverter

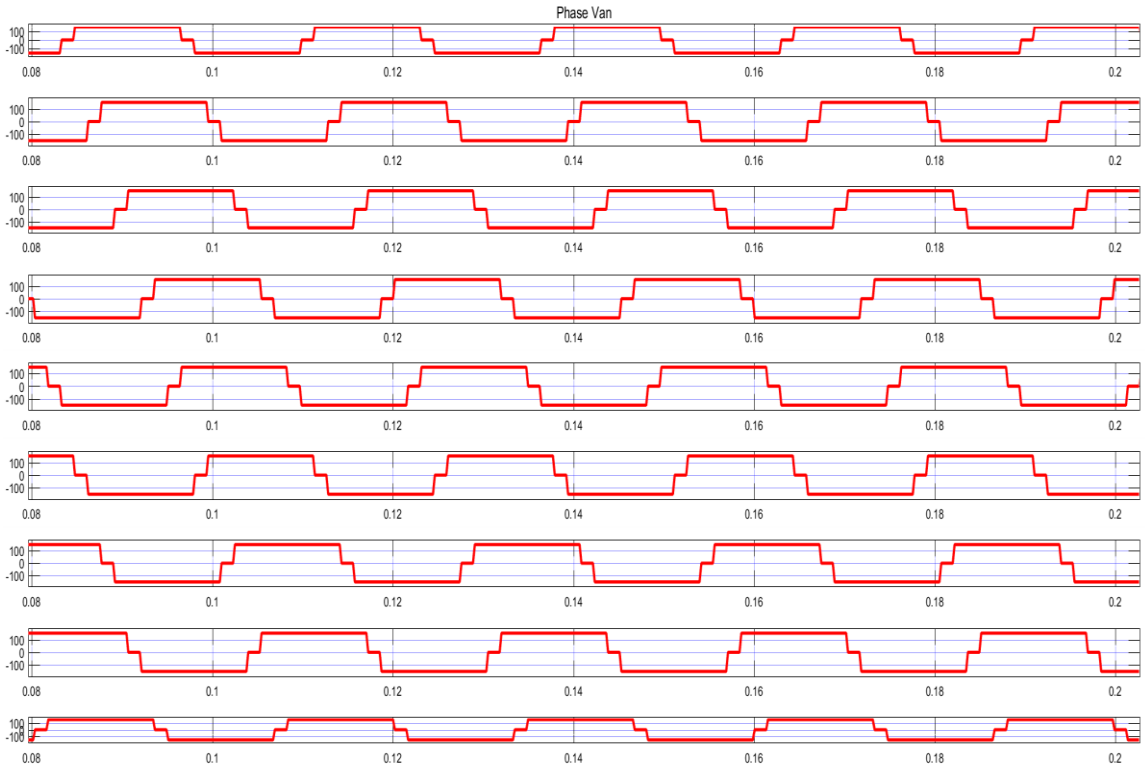

Fig. 5.5-a Nine-phase controlled VSI terminal voltages for No-load

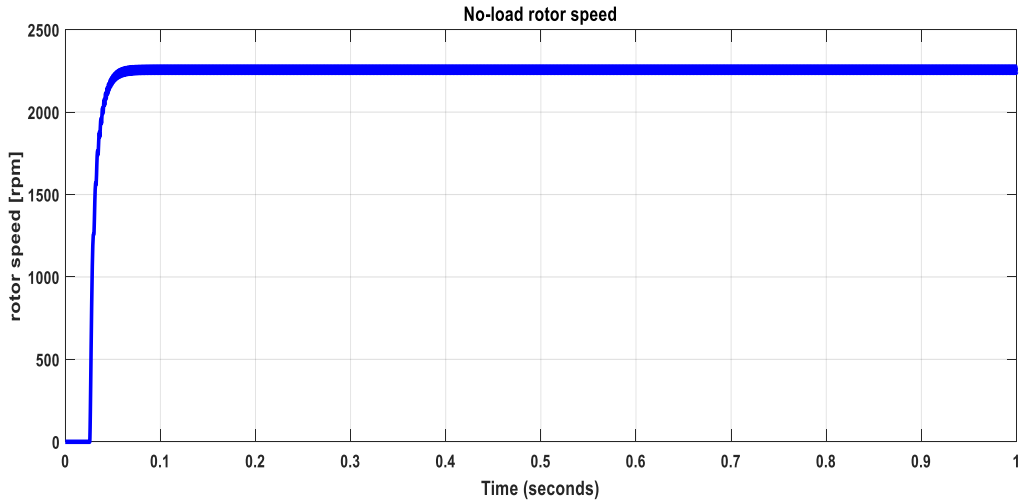

Fig. 5.6 No-load open-loop speed response of the motor

The result of the open loop simulation as shown the response of the speed outputs good almost it has 0.01sec rise time and the settling time 0.07sec and the maximum peak value is also almost constant after settling time.

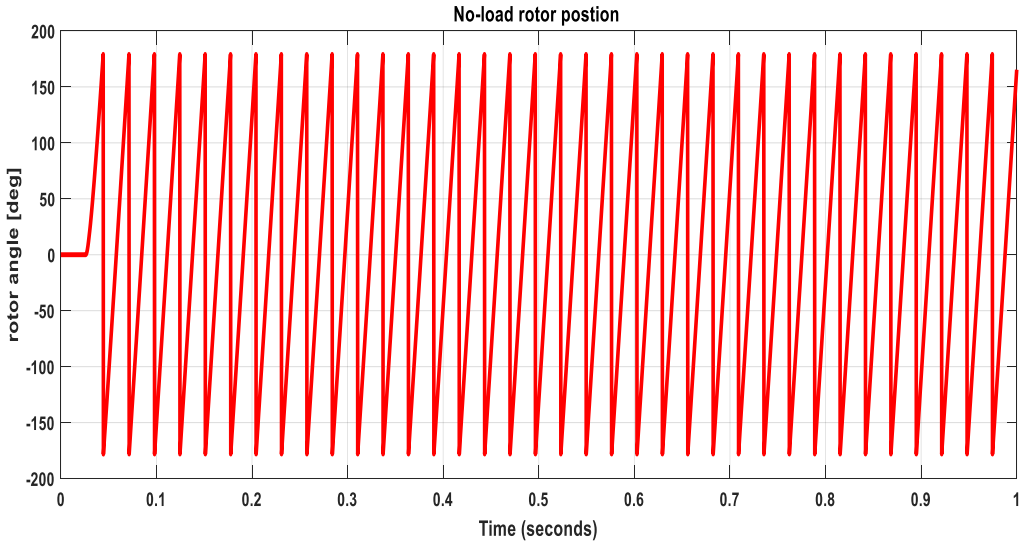

Fig. 5.7 Actual rotor position for no-load

Figure 5.7 shows the actual rotor position, as can be observe from the figure if the angle is reach at 2π rad or 360^0 it turns back to 0 until the simulation time is end with the constant frequency.

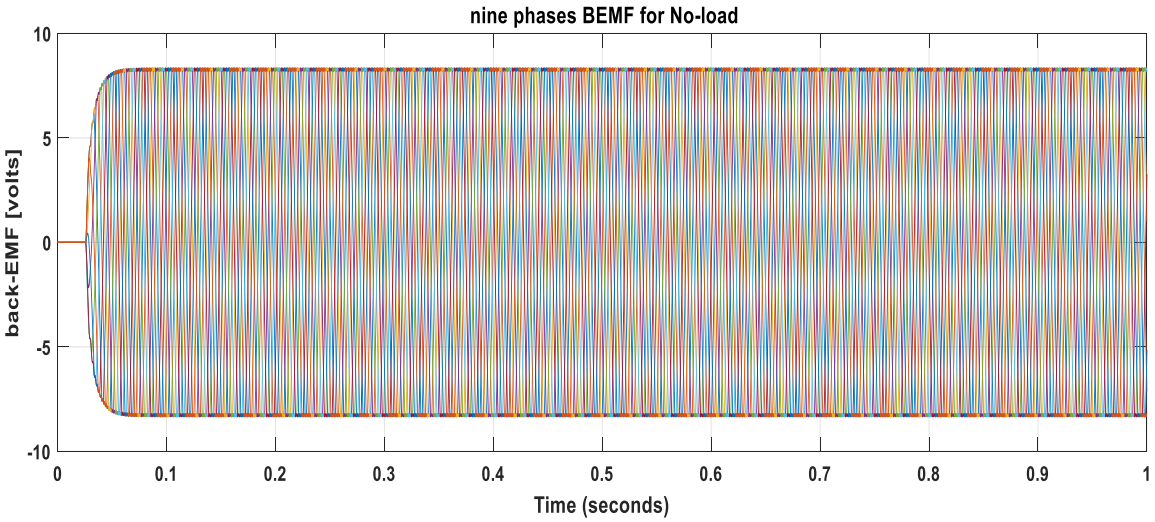

Fig.5.8 nine-phase Back-EMF output without load

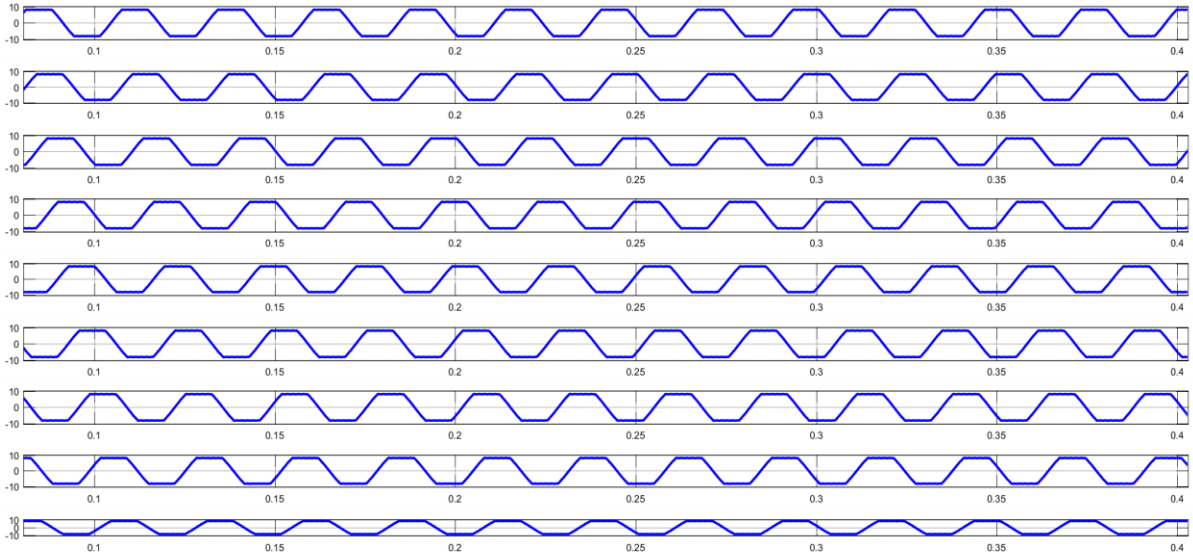

Fig.5.9 Individual nine phases Back-EMF output without load

From the above back-EMF zoom output shows every time within 40^0 periods the back-EMF of one phase is goes from high to low or low to high.

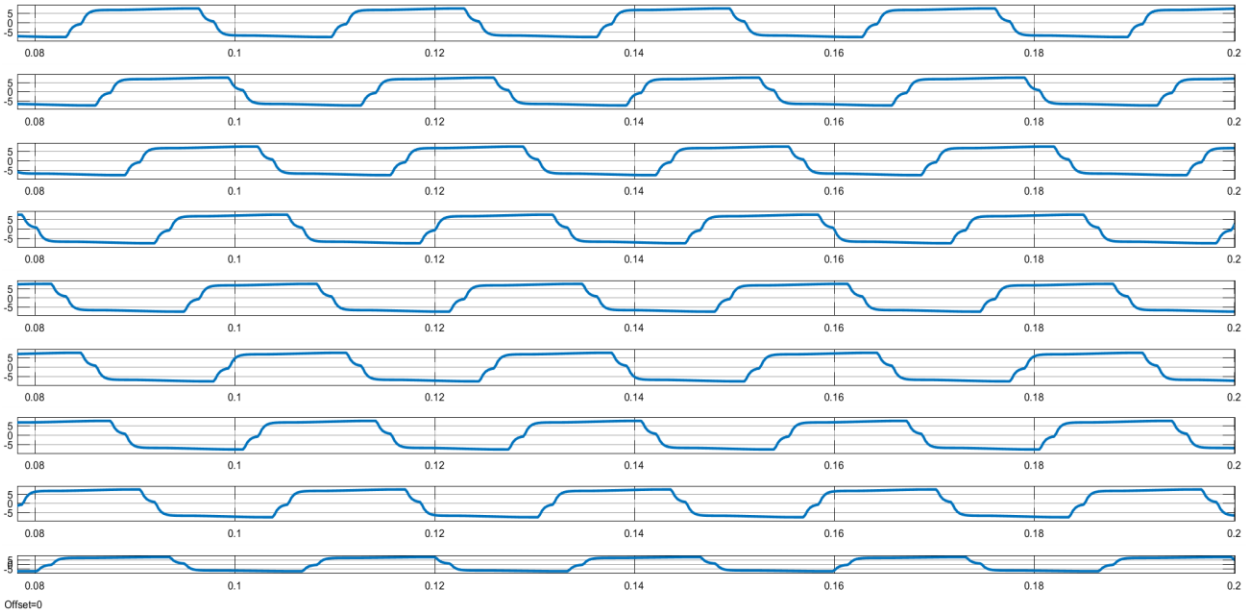

Fig. 5.10 controlled nine-phase stator current without load

From simulated figure 5.10 the stator phase current of the nine phase BLDC motor controlled based on the back-EMF wave sequences for no-load condition the frequency of phase current produced is constant which is almost 30Hz.

The next simulation shows the open-loop response of the system when load torque(TL=4Nm) is applied at 0.5 second the load torque and the response of the simulation is given in the figre 5.21 and fig.5.22 respectively.

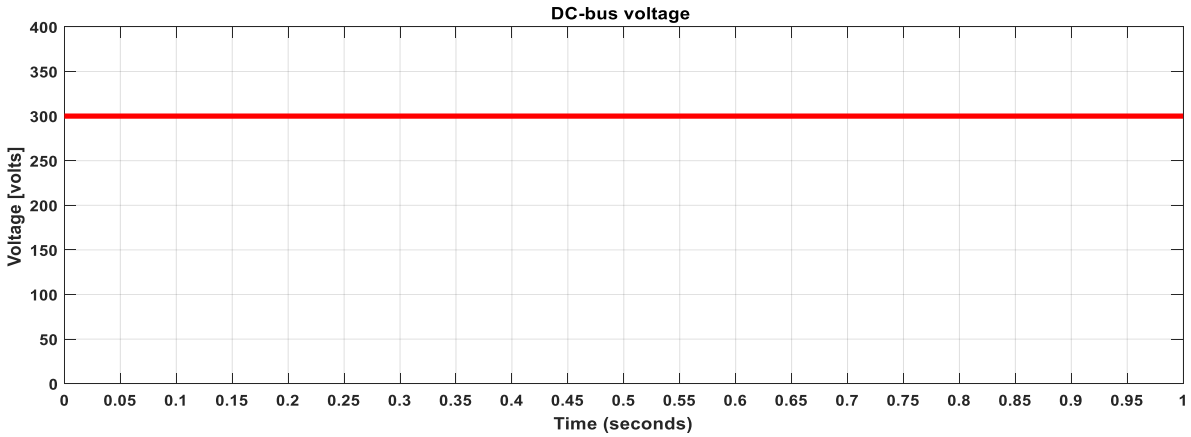

Fig. 5.11 DC-bus Voltage supplied to the nine-phase inverter

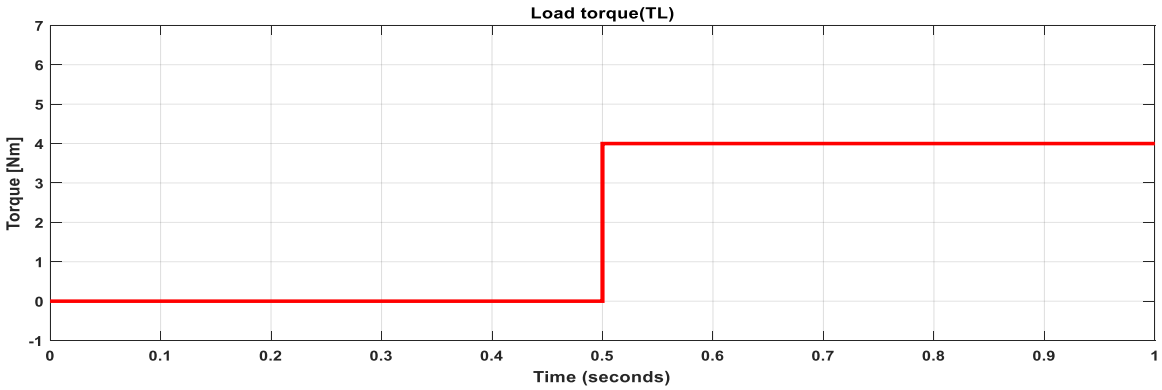

Fig. 5.12 Load torque applied (0 f0r 0.5 sec and 4Nm aftre 0.5sec)

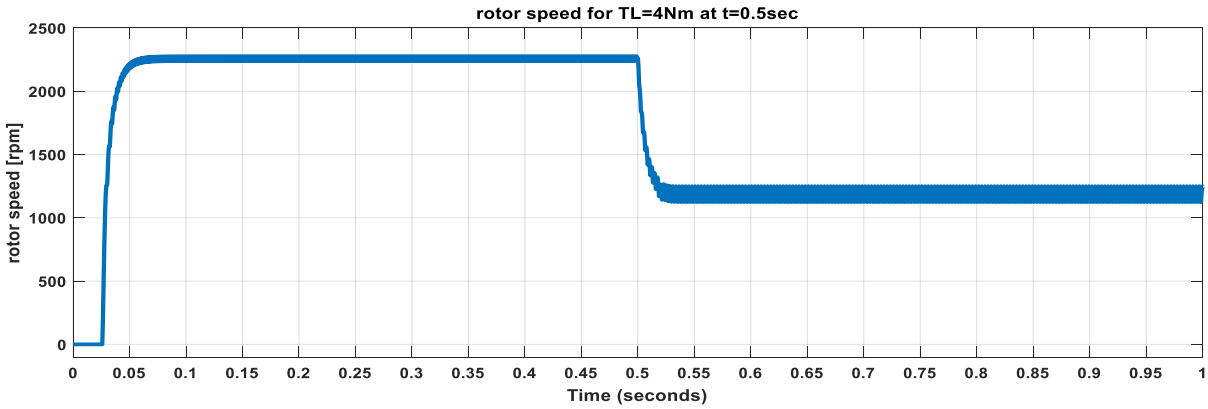

Fig. 5.13 output speed of the motor with load torque (TL) at 0.5 sec

The output speed of the motor with load torque (TL) at 0.5 sec the rising time is 0.015sec and the maximum speed produced is 2265rpm at and the minimum speed is 1127rpm after 0.55sec. fall time for speed response 15.108ms.

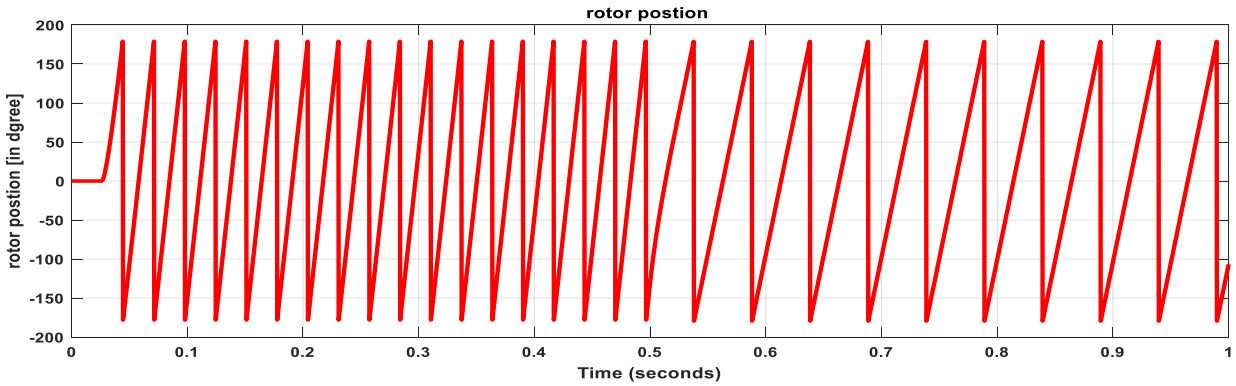

Fig. 5.14 actual rotor positions

from the figure above the speed response is shown that at the time of the load torque applied the speed of the motor is decreased and almost half of the no-load speed, as the load is a disturbance variable for the system the speed is decreased by some amount of speed in order to get constant speed the speed control must be applied.

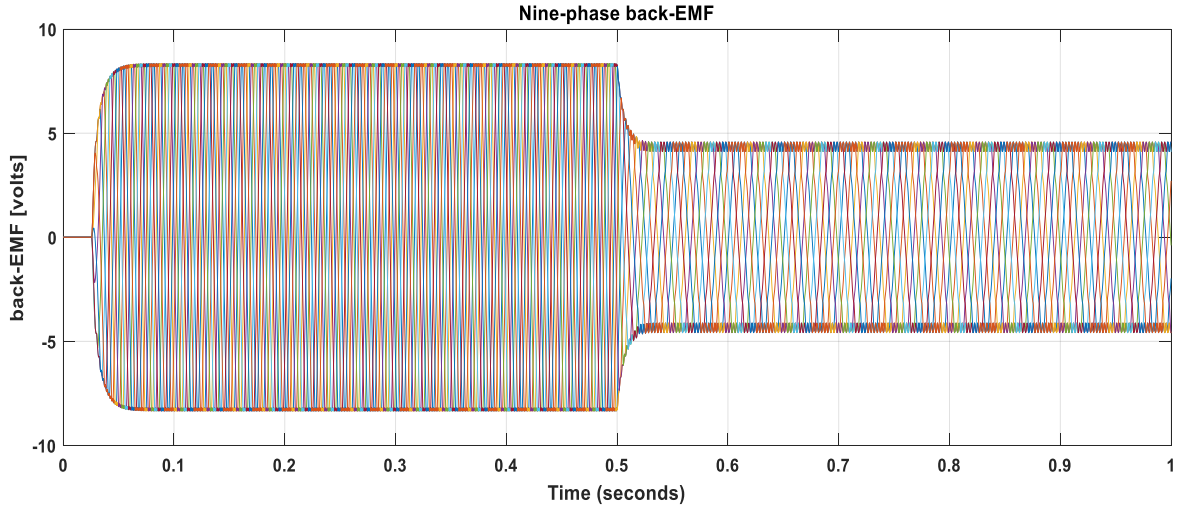

Fig. 5.15 Nine-phase Back-EMF produced with load at 0.5 sec

The back-EMF is also the function of the rotor speed from the above figure.5.15 we can see that the amplitude of the back-EMF is decreased when the time of the load torque is applied due to the decreasing of the rotor speed.

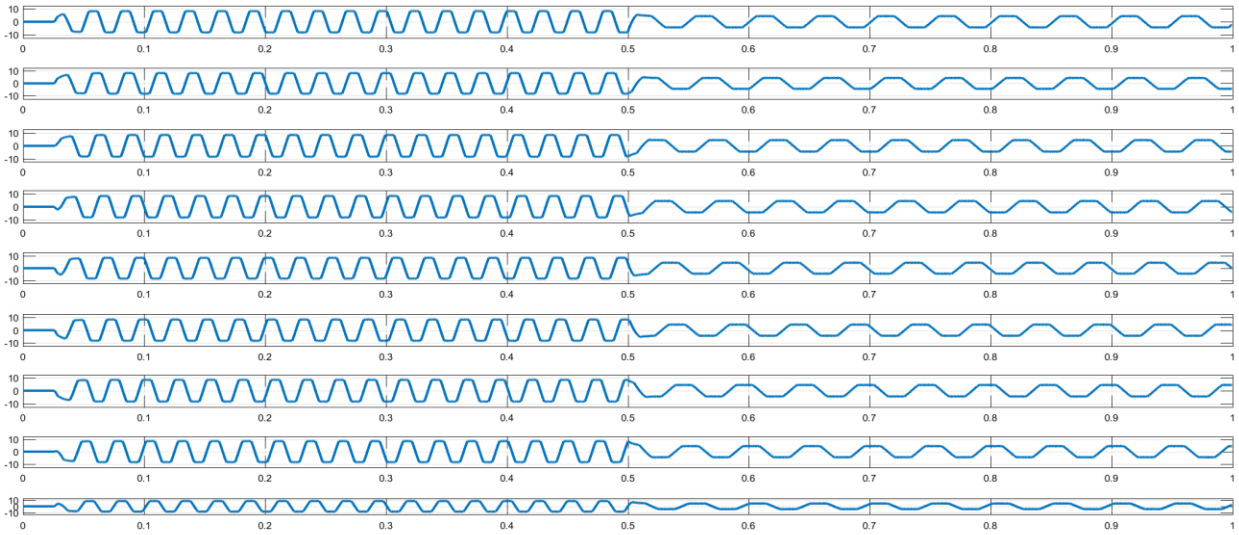

Fig. 5.16 Nine-phase individual Back-EMF output with load

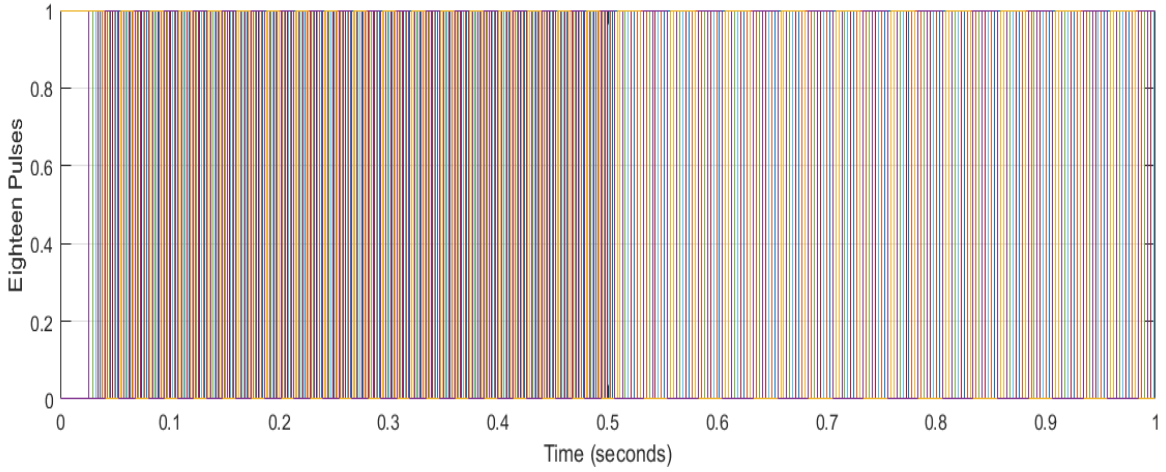

Fig. 5.17 Eighteen-pulses commutation logic output pulses

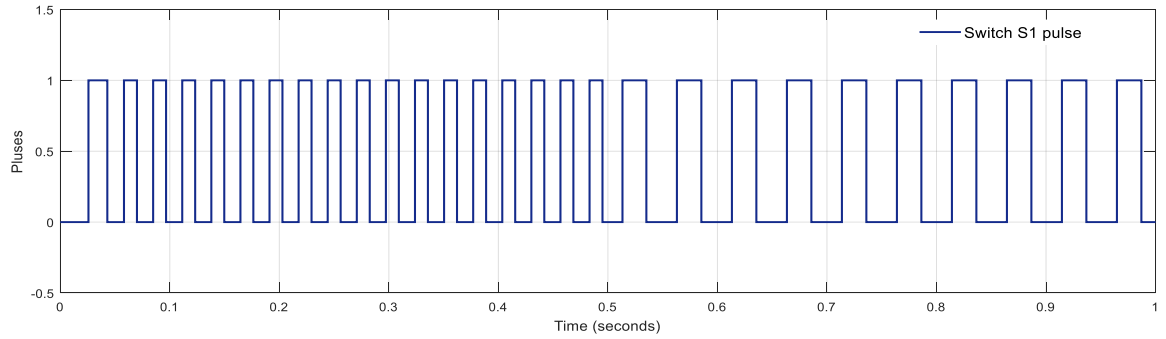

Fig. 5.18 Commutation logic generated Pulses for switch S_1 with load applied 0.5 sec

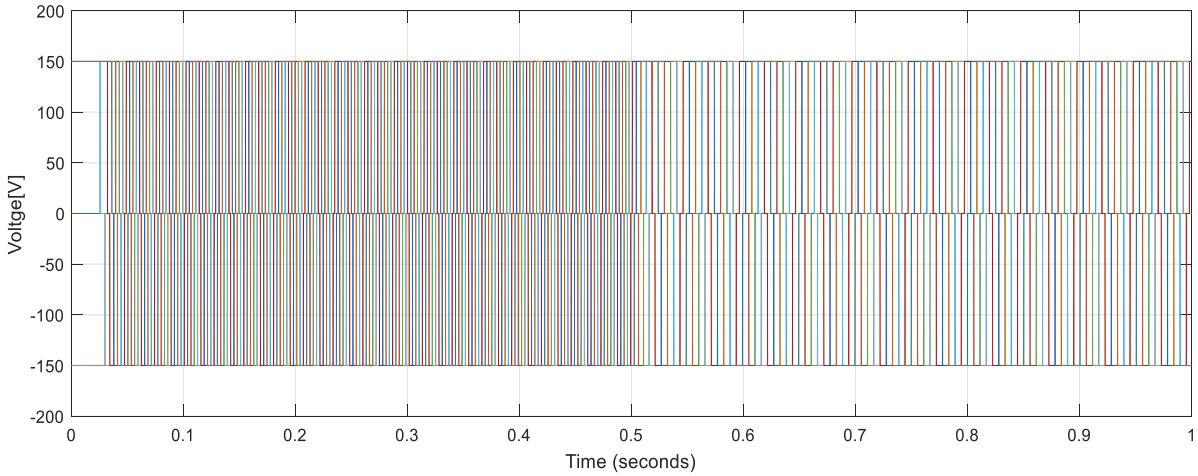

Fig. 5.19 Nine-phases VSI output voltage

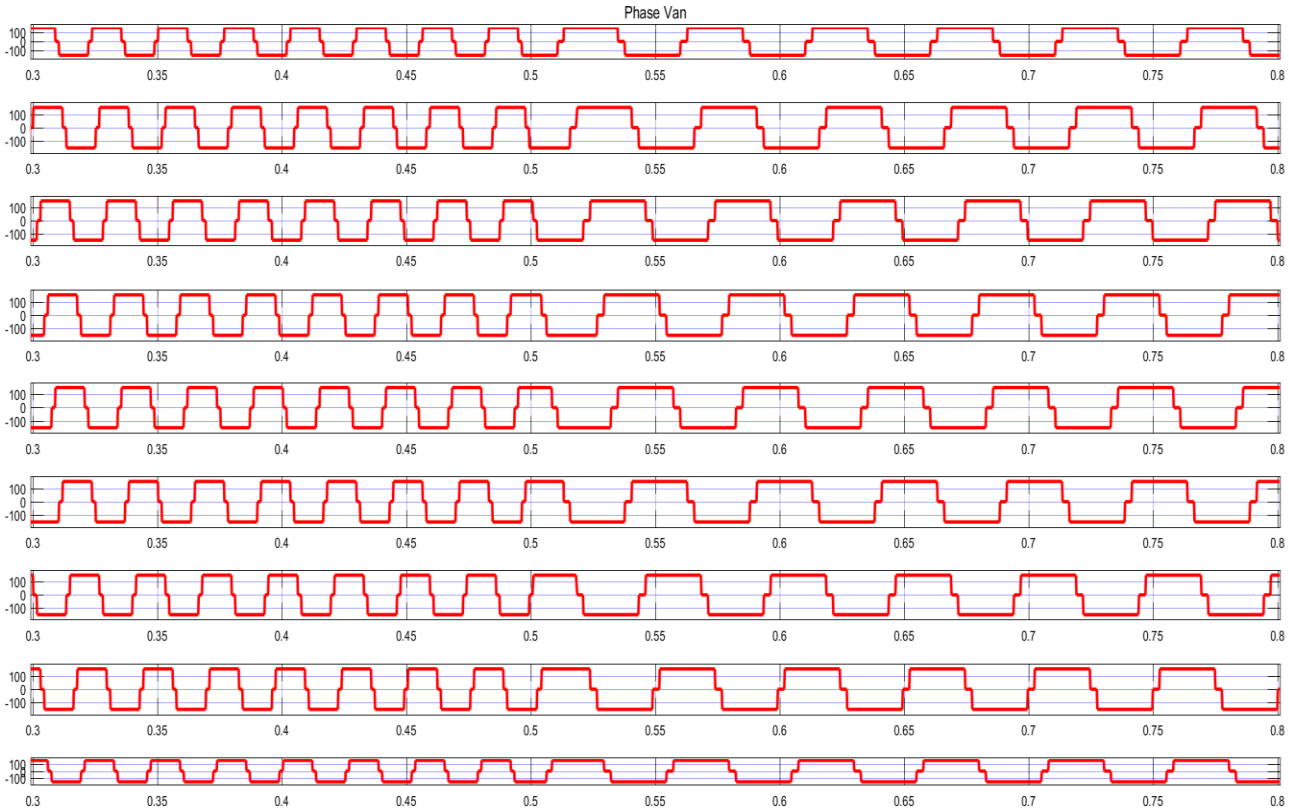

Fig. 5.20 Individual nine-phases VSI output voltage for 0.8sec

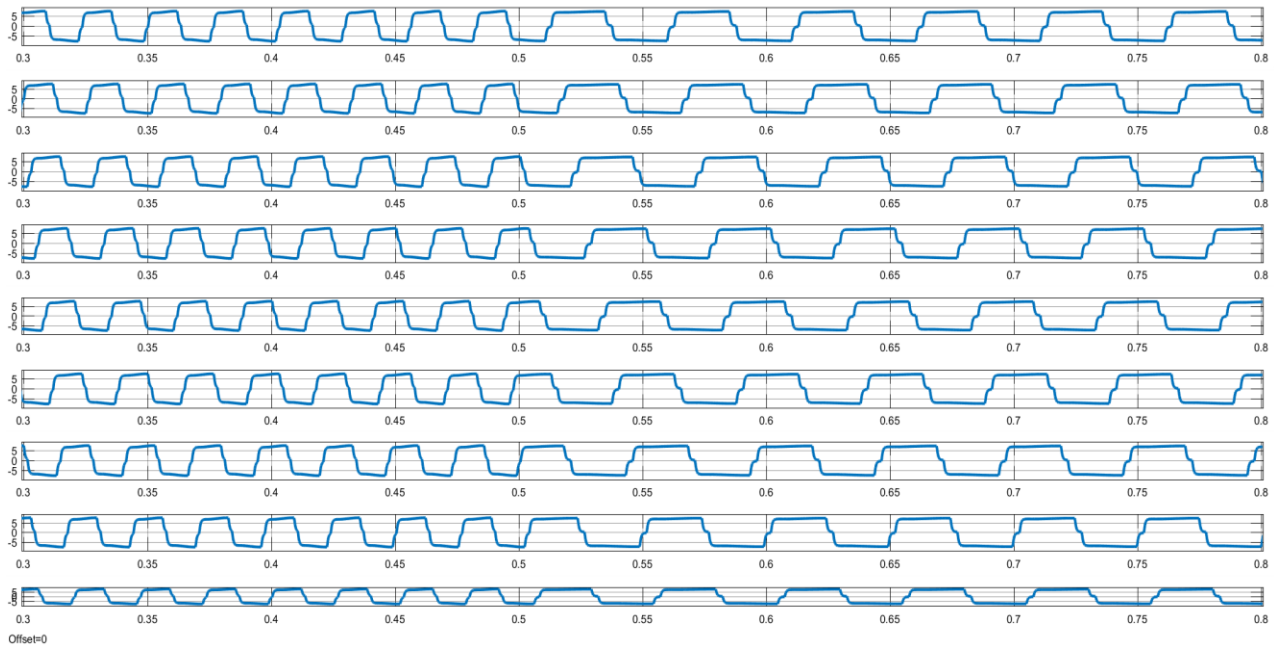

Fig. 5.21 controlled stator winding phase current of the motor with load applied at 0.5sec.

From the figure 5.20 and figer 5.21 after the load applied the frequancy of the stator both wave form is decrease and the phase current waveform based on the the controlled termnal voltage out put of the nine-phase BLDCM. And also the amplitudes of both phase current and voltage are constant. From the figure 5.21 amlutude is 7A and the rise time is 0.0026sec. and the amplitude of the phase voltage from the figure 5.20 is 148.7V voltage and the frequancy of both phase curent and voltage is 30Hz.

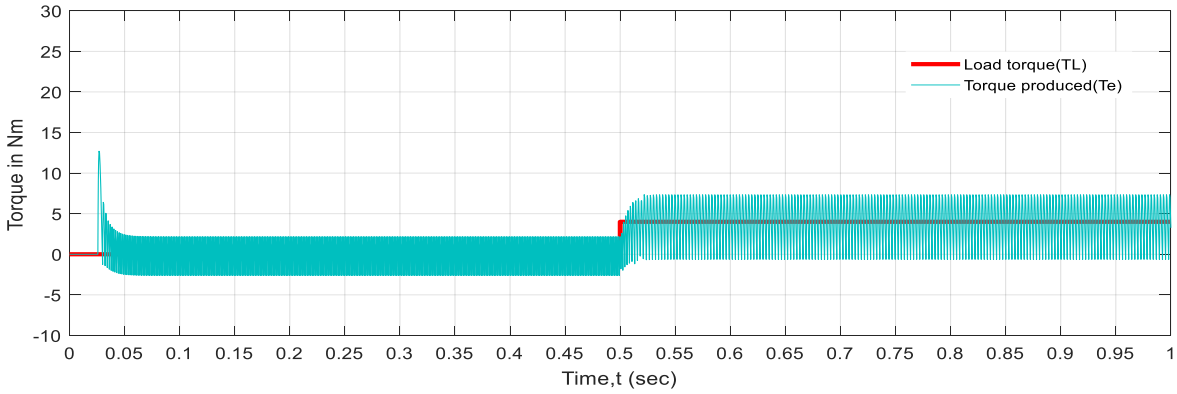

Fig. 5.22 electrical torque produced and load torque applied at 0.5sec

From torque produced by the motor shown in figure 5.22 the starting torque is 12.7Nm at 0.027sec, mean torque produced is 2.019Nm and the rising time of the torque produced is 0.0034 second and the fall time is 0.006sec.

5.4 Simulation of speed control of nine-phase BLDC motor

5.4.1 Simulation of open-loop response of the motor

With the aid of the nine-phase BLDC motor modeling and the parameters of the motor given in the above table 5.1 provided, the open loop analysis is done by considering the stability factors and making the necessary plots for this analysis. Using the open loop, the transfer equation (3.39) and the parameters of the motor given above we can developed MATLAB-m files for open lope m-files Nopenloop.m. equation 3.37 and equation 3.39 from chapter four rewritten here in below.

$$\mathbf{G(s)} = \frac{\boldsymbol{\omega_m}}{\mathbf{V_{an}}} = \frac{\mathbf{1/K_e}}{\boldsymbol{\tau_m \tau_e s^2 + \tau_m s + 1}}$$

$$\mathbf{G(s)} = \frac{\boldsymbol{\omega_m(s)}}{\mathbf{V_{pn}(s)}} = \frac{\mathbf{15.9236}}{\mathbf{1.235 \times 10^{-6} \times s^2 + 0.0251 \times s + 1}}$$

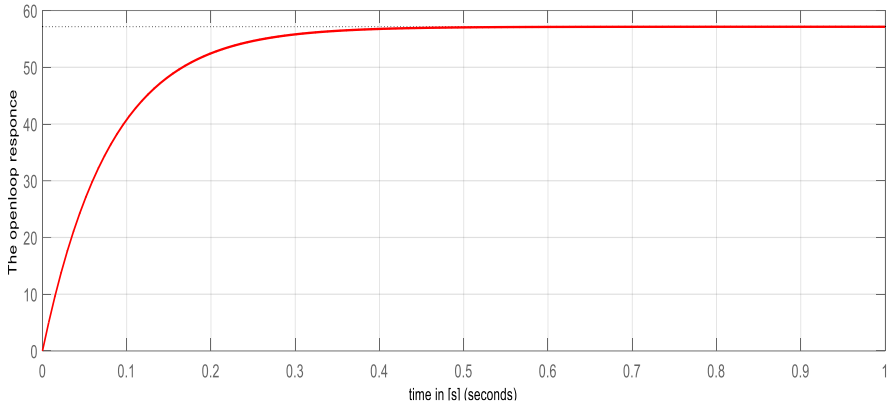

Fig. 5.23 Open-loop plant step-response of the system

Similarly, here the open loop performance of the motor is investigated and the result is satisfactory for the above model observed the output.

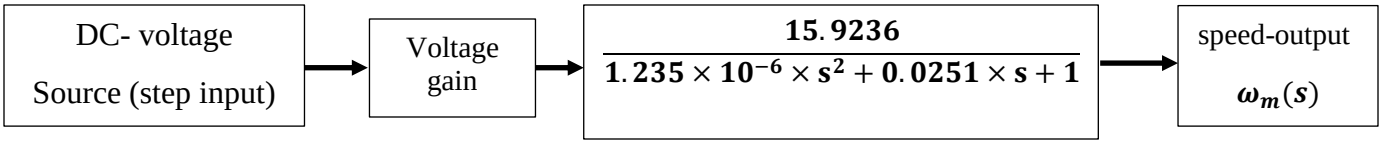

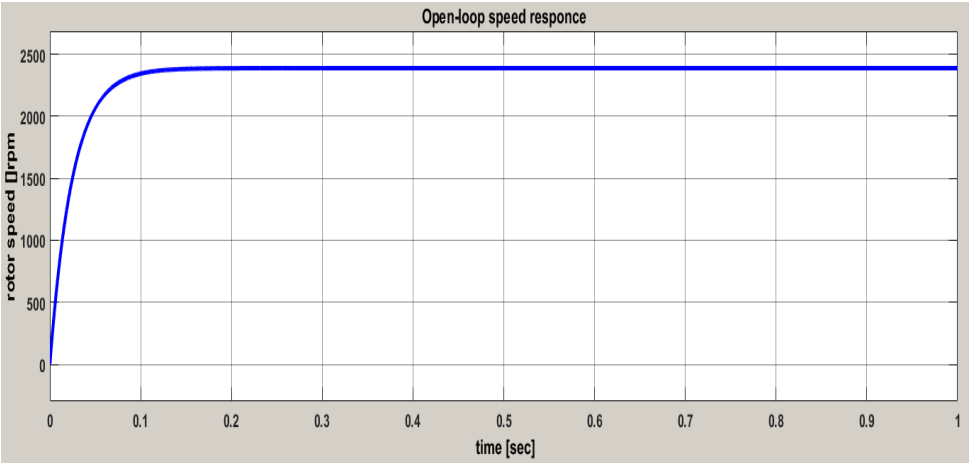

Fig. 5.24 Open-loop Simulink speed response in rpm for 1sec

5.4.2 closed-loop PI speed control simulation of nine-phase BLDC motor

From chapter 4 we have seen the general way of the PID speed control of the motor based on the open loop transfer function and the PI controller the speed can be tuned in the required speed point.

This speed control using Proportional-Integrator(PI) closed loop controller is implemented here for the nine-phase BLDC motor. the result of the modeling and the result of the closed loop simulation is presented as follows. Output of the PI controller adjust the pulse amplitude modulation (PAM) of the controlled voltage source.

The general block diagram representation for PI speed control of the motor is given as follows

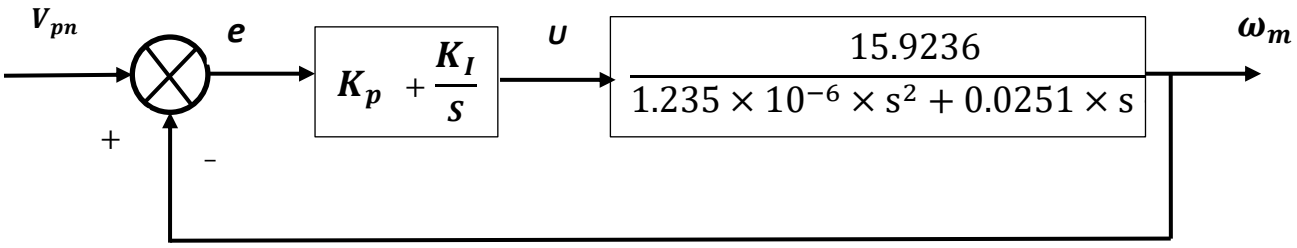

Fig. 5.25 Closed loop **PI** speed control block of motor using the transfer function

Based on the rule and the result of the open loop speed control of the motor the closed loop proportional (K_p) and the integral (K_I) constant is tuned in order to get the desired speed required. The closed loop simulation done one using MATLAB/ Simulink software.

The MATLAB Simulink block is as follows

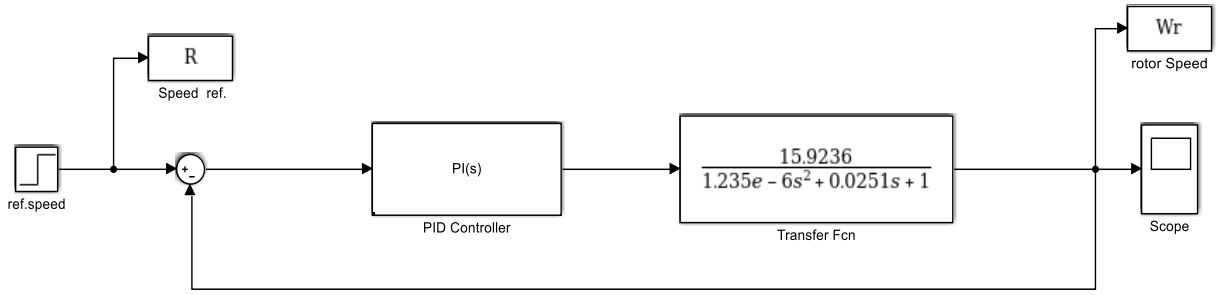

Fig. 5.26 Closed loop PI speed control Simulink model of the motor

The result of the Simulink is presented as follows

The reference speed in the Simulink is used for 0.5 sec the speed is 2000rpm and for the next 0.5sec to 1 sec the speed became 1000rpm and from the Simulink block the display of the speed of scope1 is shown the reference speed (Wr).

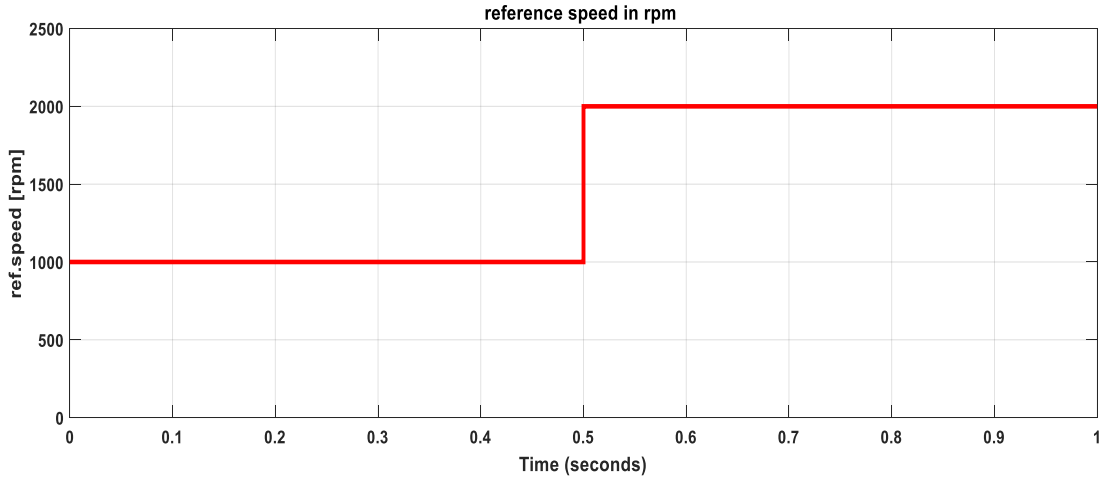

Fig. 5.27 reference speed (1000rpm for 0.5 sec and for the next 0.5sec 2000rpm)

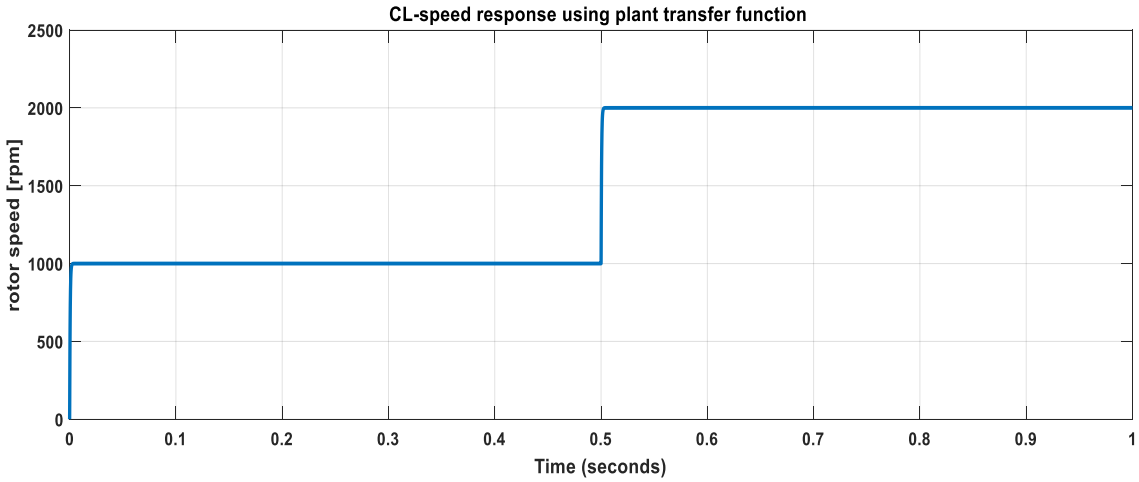

Fig. 5.28 PI speed response of the motor for the given reference speed given in fig. 5.27

The second closed loop control is using PI controller and the whole-time domain Simulink model of the motor.

The tuned proportional constant Kp and Ki for closed loop speed controller are given below:

$k_p = 3.0214$ and $k_i = 0.0204$.

The design criteria (desired output) for the closed-loop PI speed controller

- Rising time less than 0.01sec and
- Settling time less than 0.05sec.

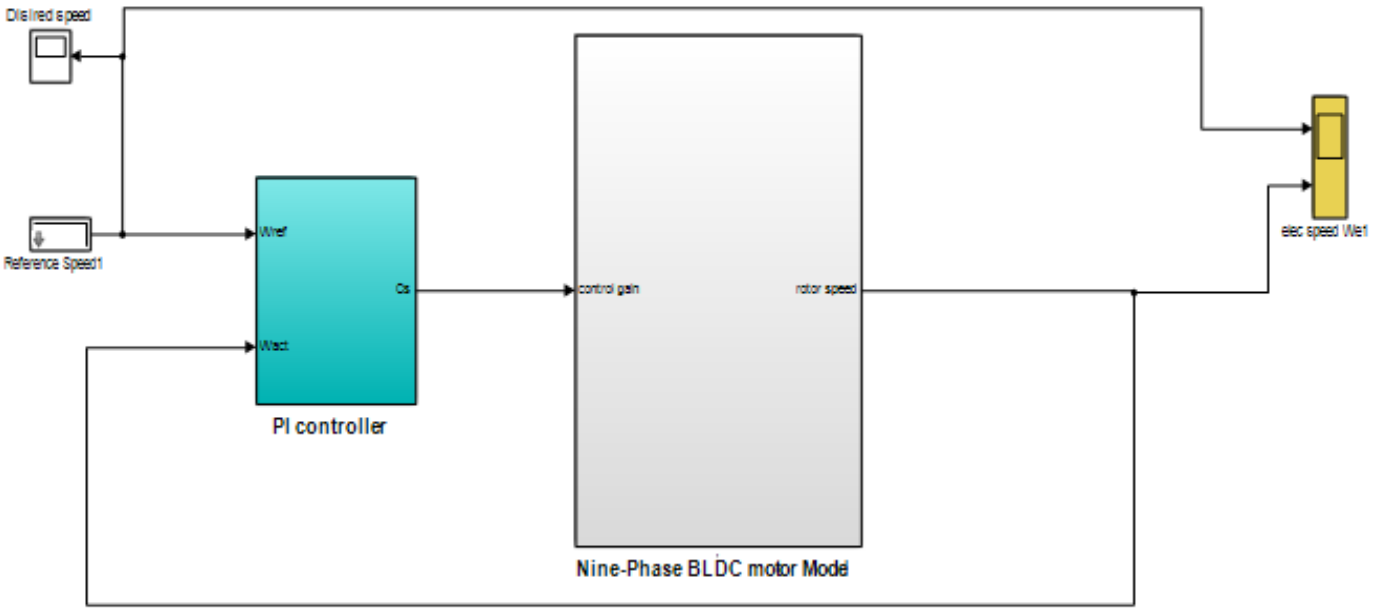

Fig. 5.29 Simulink model for PI speed controller of the Nine-phase BLDC motor

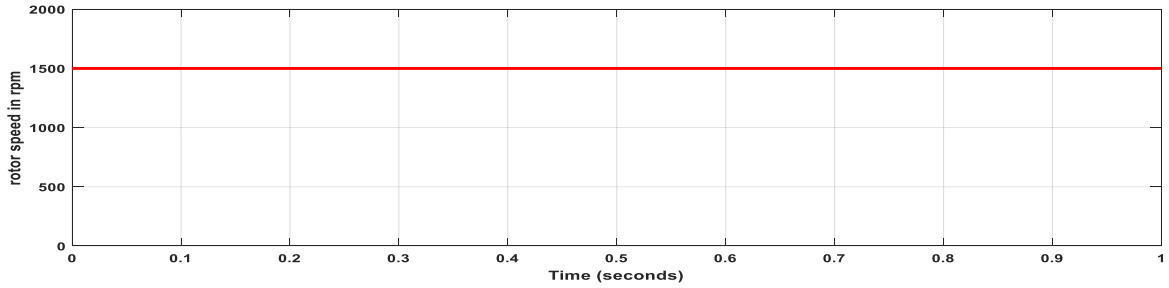

Fig 5.30 speed reference input given (1500 rpm constant speed)

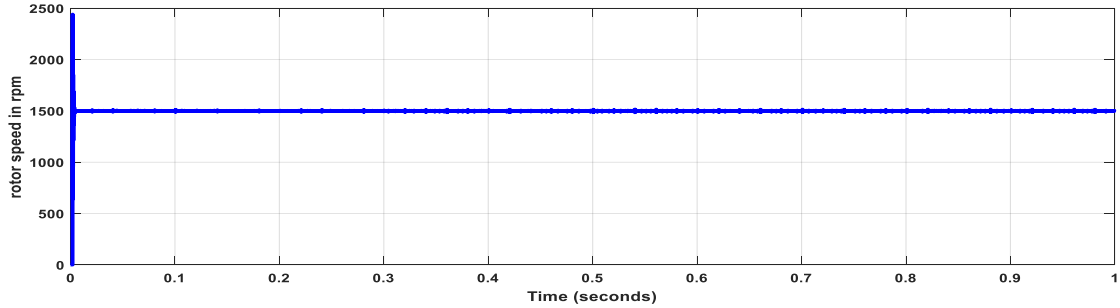

Fig. 5.31 closed loop speed response of the motor for the above reference speed

The closed-loop speed simulated result shows in the figure 5.31 the settling time is very short and acceptable which is 0.005sec and its rise time is 0.0026sec. Form, for above closed-loop PI Simulink model the result of the simulation for different speed level shown below, first the reference input speed is given in the figure 5.32:

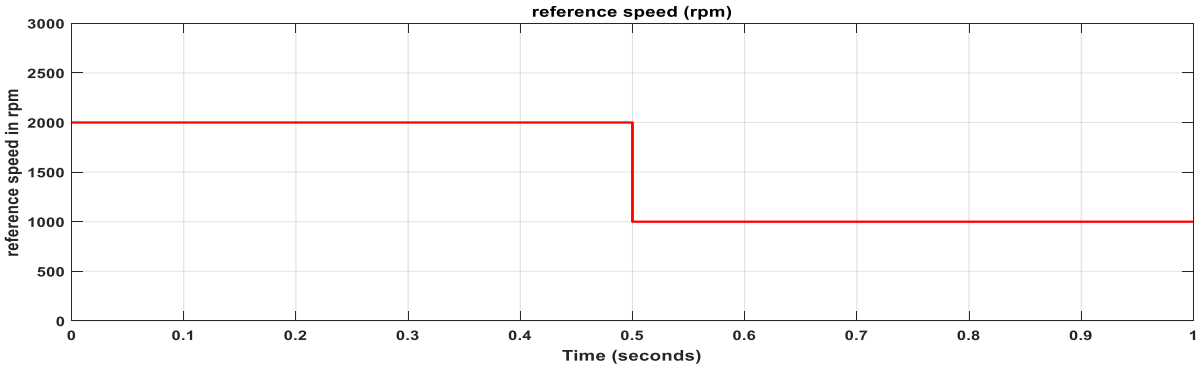

Fig. 5.32 Reference speed (2000rpm for 0.5sec and 1000rpm after 0.5sec) to the controller The response of the system for the above desired speed is given below

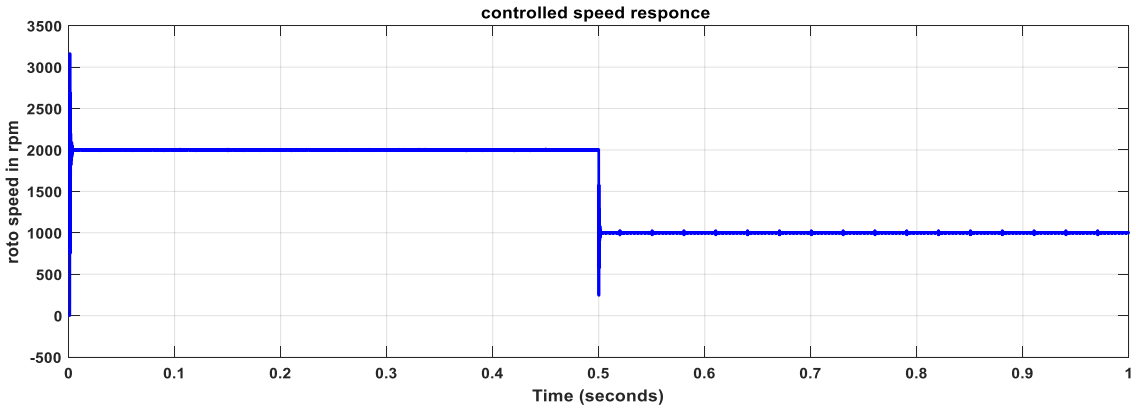

Fig. 5.33 Speed response of the simulation for the above reference speed

The response of the closed-loop control of the system motor for different speed range for the given desired speed is shown as follows;

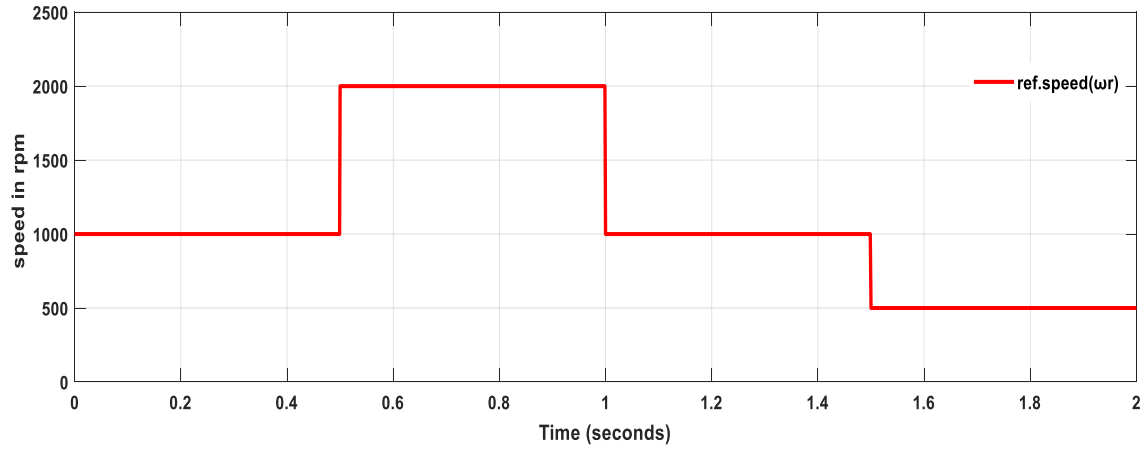

Fig. 5.34 speed reference given to the motor

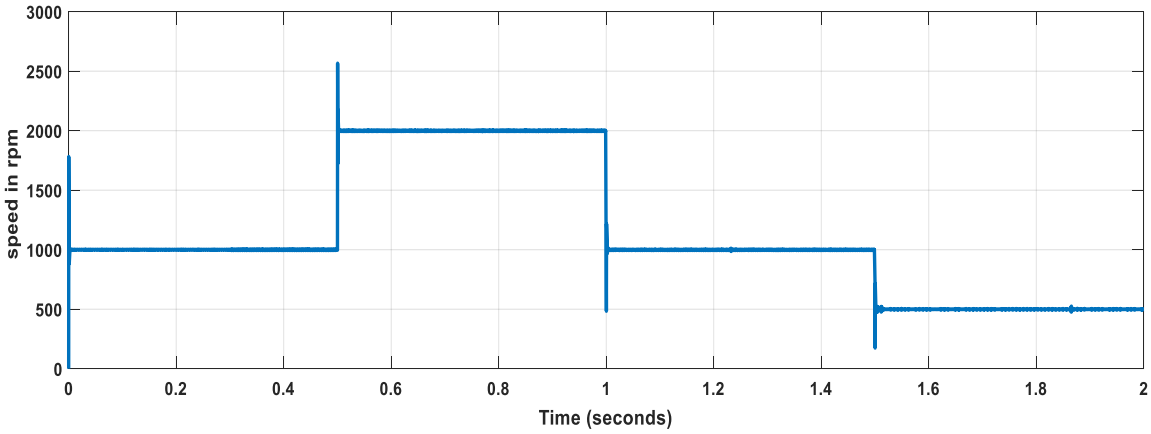

Fig. 5.35 PI- control speed response of the motor for different speed

Therefore, the controller result is shown in the above is very satisfactory and the settling time is also very fine. The only drawbacks of the controller are the overshoot intransient point or time for the problem we can add the differentiator controller became PID using this proportional-integrator-differentiator controller we can eliminate the overshoot and the overshoot oscillation time is very short which is less than 0.005sec.

CHAPTER 6

CONCLUSION AND RECOMMENDATION

6.1 Conclusion

In this thesis, design and simulation of sensorless control for nine-phase BLDC motor using Back-EMF waveform zero-cross detection method and closed-loop speed control of nine-phase BLDC motor has been done. Based on the back-EMF sequence produced in the stator winding phases the rotor position of the motor equally monitored as using sensor. using back-EMF waveform sequence produced nine-phases BLDC motor, switching sequence of nine-phase VSI gates has been controlled effectively. This method is feasible due to the unique and simplified structure of BLDC motor. The principle of sensorless control using back-EMF method for BLDC motor are also elaborated. Nine-phase BLDC motor and nine-phase voltage source inverter has been modeled and simulated with the help of MATLAB/Simulink software.

In this work, for speed control of the motor PI controller is implemented and simulated. The result of speed controller has shown good performance with no-load condition and with load conditions. where the simulated results shown that the raising time is 0.01sec before adding the PI control. After, PI controller added the rising time of the speed response enhanced to 0.0026sec and the settling time of the speed response becomes to 0.005sec. The transient response oscillation time is very short which is less than 0.005sec. From the simulated result, one can observe that the PI speed controller shown effective result. Hence, this work can be applied areas such as electrical air conditioner controller, electric vehicles drive and industrial drive applications.

6.2 Recommendation

In this work, it is believed that there are a lot of ideas for further research studies. Some possible directions are the following:

- Sensorless vector control can be needed for high and precise application of the motor because using that method we can even now the very low and stand still position of the motor.

- If high performance initial rotor estimation technique is applied or good performance of open loop motor starting is applied for switching to closed loop.
- If the appropriate parameter identification is done for the motor for appropriate operation of the closed loop.
- If intelligent estimation and control technique apply, the system performance can be improved.

References

[1] L. Parsa and H. Toliyat, "*Fault-tolerant five-phase permanent magnet motor drives*," in Conf. *Rec. IEEE IAS Annu. Meeting, Oct. 2004, pp. 1048–1054*

[2] MousaviS.M.H,Mirbaghere S M,Sefid S.S.S.G, "Simulation of New Multiphase BLDC motor Drive " *IEEE International conference on Power electronics Drives and Energy System 2012 PP 1-5*

[3] T.Y Kim, B.K Lee, C.Y Won" Modeling and Simulation of multiphase BLDC motor drive System for Autonomous under water vehicle" *IEEE International Conference on Electric machines & drives" vol 2 may 2007 pp 1366-1371*

[4] T. Sebastian, G. Slemon, and M. Rahman, "Modelling of permanent magnet synchronous motors," *Magnetics, IEEE Transactions on, vol. 22, pp. 1069-1071, 1986.*

[5] Leila Parsa, and Hamid A. Toliyat, 'Five-Phase Permanent-Magnet Motor Drives', *IEEE transactions on industry applications, vol. 41, no. 1, january/february 2005*

[6] *David C. White and Herbert H. Woodson, "Electromechanical Energy Conversion", John Willey and Sons, Inc. New York, 1959, pp. 545-602*

[7] Mengesha mamo wogari*, Olorunfemi Ojo**, Fellow, "*Nine-Phase Interior Permanent Magnet Motor for Electric Vehicle*" Fellow *IEEE*

[8] Rockhill, A.A.; Lipo, T.A. *"A Simplified Model of a Nine Phase Synchronous Machine Using Vector Space Decomposition", Power Electronics and Machines in Wind Applications (PEMWA) 2009.*

[9] Hyung-Min Ryu, Ji-Woong Kim, and Seung-Ki Sul "*Synchronous Frame Current Control of Multi-Phase Synchronous Motor, Part I. Modeling and Current Control based on Multiple d-q space concept under Balanced Condition*" Conference record of the annual congress, IEEE Ind. Appl. Society, 2004

[10] Ensoo Jung, Hyunjae Yoo, Seung-Ki Sul, Hong-Soon Chi, and Yun-Young Choi, "Nine-phase Permanent Magnet Motor Drive System for Ultra High-Speed Elevator", conference record of IEEE Energy Conversion Congress and Exposition, September, 2010.

[11] Rockhill, A.A.; Lipo, T.A. "A Simplified Model of a Nine Phase Synchronous Machine Using Vector Space Decomposition", Power Electronics and Machines in Wind Applications (PEMWA) 2009.

[12] *M. A. Abbas, R. Christen, and T. M. Jahns, "Six-phase voltage source inverter driven induction motor," IEEE Trans. Ind. Appl., vol. IA-20, no. 5, pp. 1251–1259, Sep./Oct. 1984.*

[13] *K. N. Pavithran, R. Parimelalagan, and M. R. Krishnamurthy, "Studies on inverter-fed five-phase induction motor drive,"IEEE Trans. Power Electron., vol. 3, no. 2, pp. 224–235, Apr. 1988.*

[14] *E. Andrese and K. Bieniek, "6-phase induction motors for current-source inverter drives," in Conf. Rec. IEEE IAS Annu. Meeting, Philadelphia,PA, 1981, pp. 607–618.*

[15] "Multiphase Electric Machines for Variable-Speed Applications" *Emil Levi, Senior Member, IEEE*

[16] P. Ferraris and M. Lazzari, "Phase numbers and their related effects on the characteristics of inverter fed induction motor drives," inConf. Rec. IEEE IAS Annu. Meeting, Mexico City, Mexico, 1983, pp. 494–502.

[17] S. Williamson and A. C. Smith, "Pulsating torque and losses in multiphase induction machines," *IEEE Trans. Ind. Appl., vol. 39, no. 4, pp. 986–993, Jul./Aug. 2003.*

[18] A. Boglietti, R. Bojoi, A. Cavagnino, and A. Tenconi, "Efficiency analysis of PWM inverter fed three-phase and dual three-phase induction machines," *inConf. Rec. IEEE IAS Annu. Meeting, Tampa, FL, 2006, pp. 434–440.*

[19] G. K. Singh, K. Nam, and S. K. Lim, "A simple indirect field-oriented control scheme for multiphase induction machine," *IEEE Trans. Ind. Electron., vol. 52, no. 4, pp. 1177–1184,*

[20] E. A. Klingshirn, "High phase order induction motors—Part I— Description and theoretical considerations,"IEEE Trans. Power App. Syst., vol. PAS-102, no. 1, pp. 47–53, Jan. 1983.

[21] H. A. Toliyat, S. P. Waikar, and T. A. Lipo, "Analysis and simulation of five-phase synchronous reluctance machines including third harmonic of airgap MMF," IEEE Trans. Ind. Appl., vol. 34, no. 2, pp. 332–339, Mar./Apr. 1998.

[22] R. O. C. Lyra and T. A. Lipo, "Six-phase induction machine with third harmonic current injection," inProc. ElectrIMACS, Montreal, QC, Canada, 2002, CD-ROM, Paper 304.

[23] F. Locment, E. Semail, and X. Kestelyn, "Optimum use of DC bus by fitting the back-electromotive force of a 7-phase permanent magnet synchronous machine," in Proc. Eur.

[24] C. E. Coates, D. Platt, and V. J. Gosbell, "Performance evaluation of a nine-phase synchronous reluctance drive," inConf. Rec. IEEE IAS Annu. Meeting, Chicago, IL, 2001,

[25] X. Kestelyn, E. Semail, and D. Loriol, "Direct torque control of a multiphase permanent magnet synchronous motor drive: Application to a five-phase one," *in Proc. IEEE IEMDC, San Antonio, TX, 2005,pp. 137–143.*

[26] J. W. Kelly, E. G. Strangas, and J. M. Miller, "Multi-phase inverter analysis," *inProc. IEEE IEMDC, Cambridge, MA, 2001, pp. 147–155.*

[27] Bonfe, M.; Bergo, M. A "Brushless Motor Drive with Sensorless Control for Commercial Vehicle Hydraulic Pumps" *In Proceedings of the IEEE International Symposium on Industrial Electronics (ISIE 2008), Cambridge, England, July 2008; pp. 612-617.*

[28] **"**3-Phase BLDC Motor Control with Hall Sensors using 56000/E Digital Signal Controllers " *Application Note; AN1916, Freescale Semiconductor: TX, USA, 2005*.

[29] Shen, J.X.; Iwasaki, S. *"Sensorless Control of Ultrahigh-Speed PM Brushless Motor using PLL and Third Harmonic Back EMF." IEEE Trans. Ind. Electron. 2006, 53, 421-428.*

[30] Shen, J.X.; Zhu, Z.Q.; Howe, D. *"Sensorless Flux-Weakening Control of Permanent-Magnet Brushless Machines using Third Harmonic Back EMF". IEEE Trans. Ind. Appl. 2004, 40,*

[31] Nagaraj B, Subha S, Rampriya B. "Tuning algorithms for PID controller using soft computing techniques". *IJCSNS Int J Comp Sci 2008;8(4):278–8*1

[32] P Pillay and R. Krishnan "Application characteristics of permanent magnet synchronous and brushless dc motors for servo drives" *IEEE Trans Ind Appl vol 27 no 5, pp 986-996 sep/oct*

[33] P. Pillay and R. Krishnan, "Modeling of permanent magnet motor drives,"*IEEE Trans.Ind. Electron., vol. 35, no. 4, pp. 537–541, Nov. 1988.*

[34] Oludayo J.Oguntoyinbo " PID control of BLDC motor and robot trajectory planning and simulation with MATLAB/simulation"

[35] "3-Phase Sensorless BLDC Motor Control with Back-EMF Detection Using Zero Crossing" 56F805 Manual Designer Reference Freescale

[36] Yen-Shin Lai "Efficiency comparison of PWM-controlled and PAM-controlled sensorless BLDCM drives for refrigerator application"

[37] Priyanka c.p, Sija gonpinathan "Model and simulation analysis of Eleven phase BLDC motor" vol. 2 ,Desmber 2013

Appendix

Appendix A- MATLAB Simulink model block

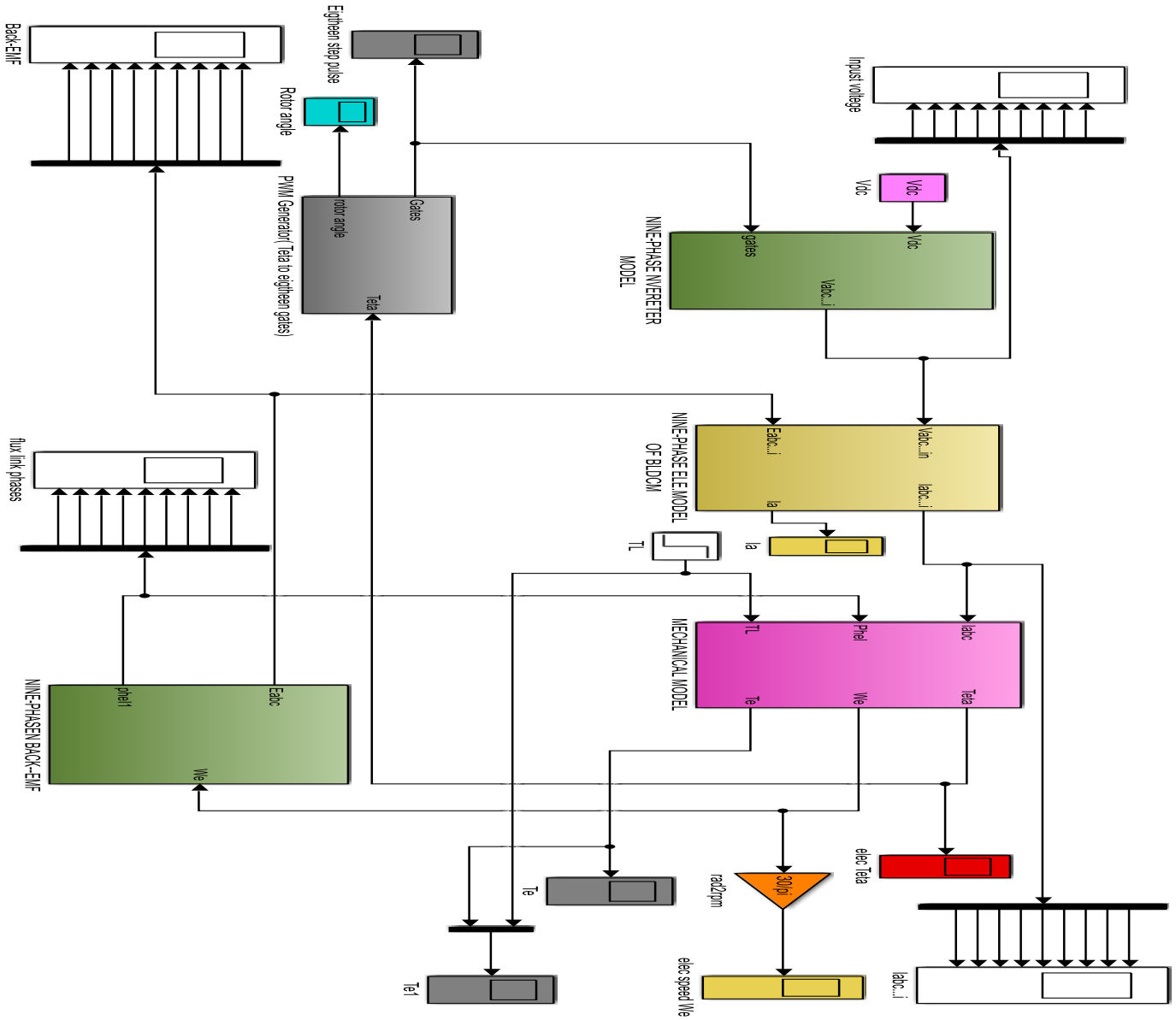

Fig. a) General Simulink model of nine-phase BLDC motor drive

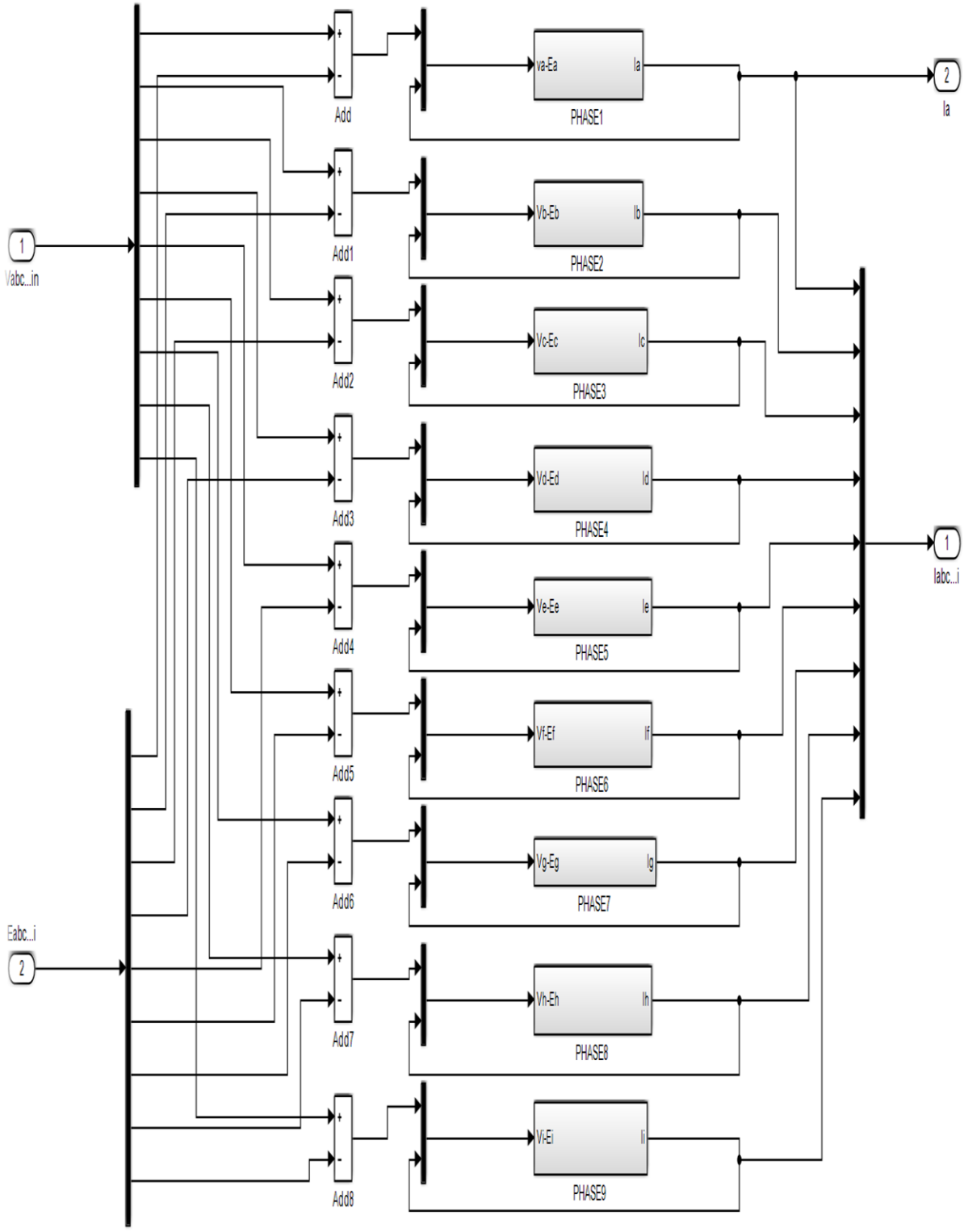

Fig. b) the nine-phase electrical modeling of the motor

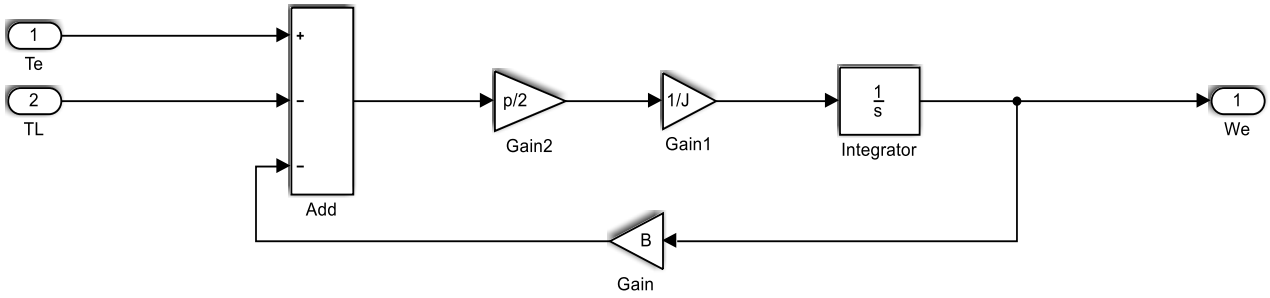

Fig. c) Mechanical torque equation Simulink block of the motor

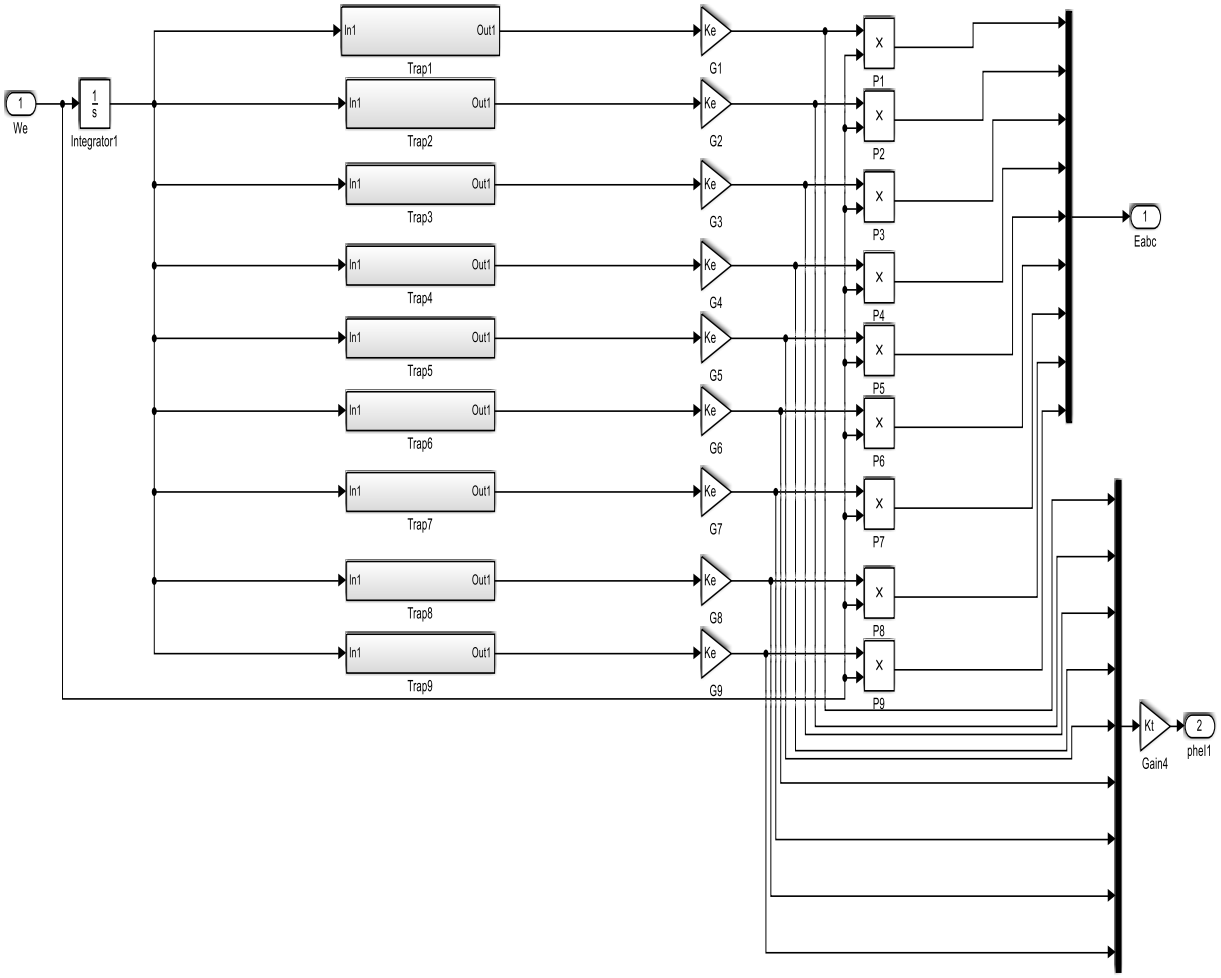

Fig. d) The nine-phase Back-EMF calculation Simulink block

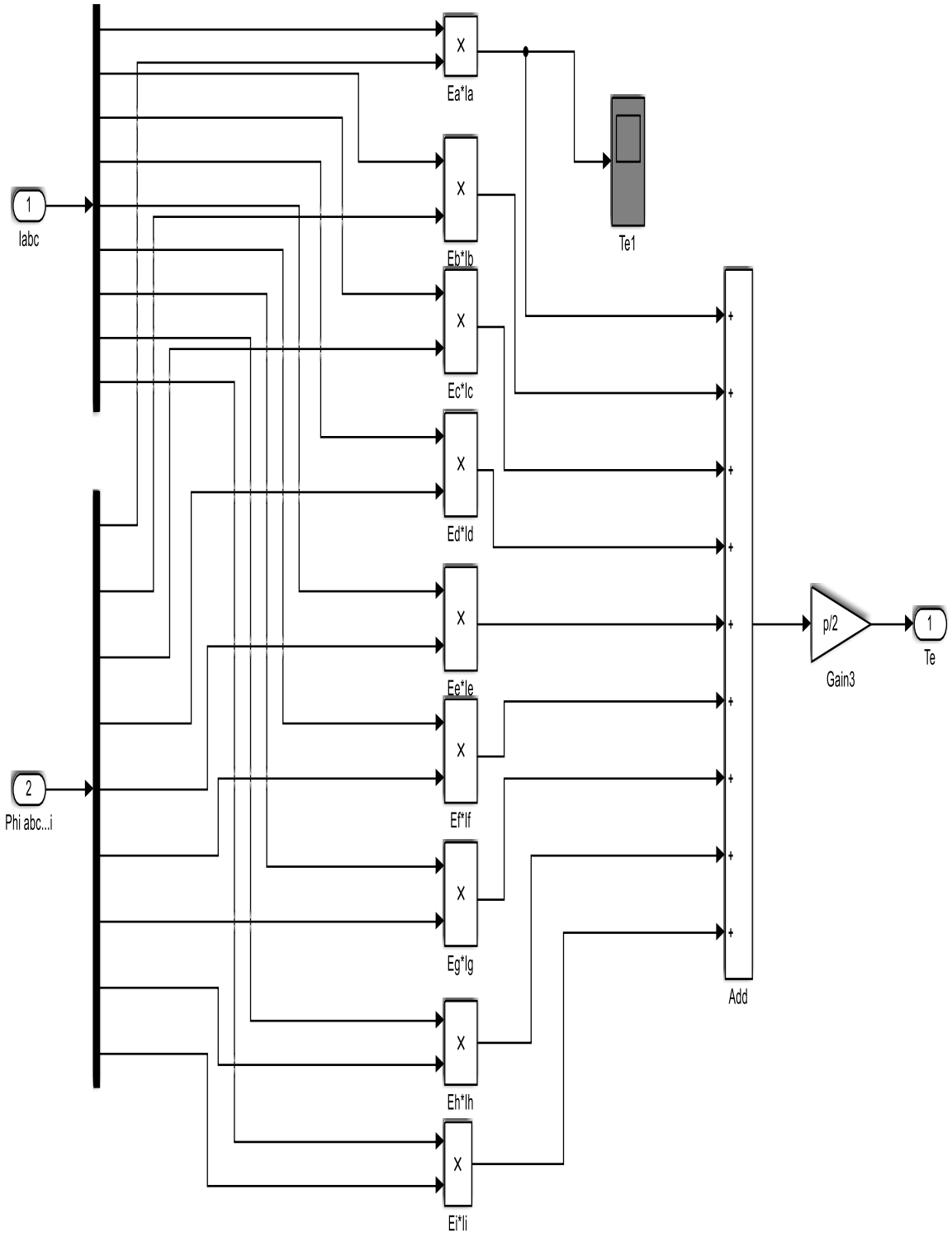

Fig. e) Simulink model of electrical torque produced by the motor

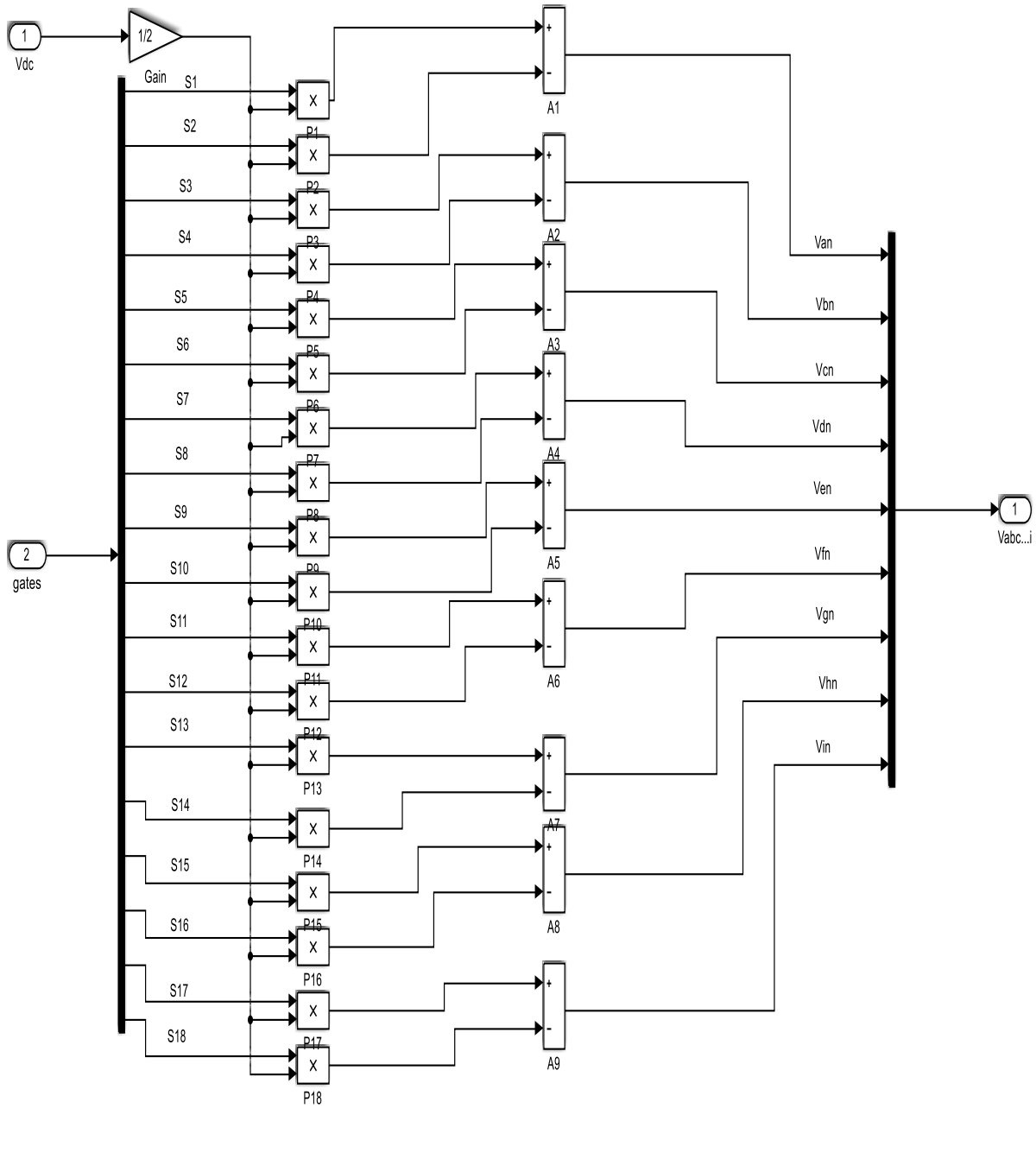

Fig. f) Simulink model of eighteen-step nine phase invertor function block

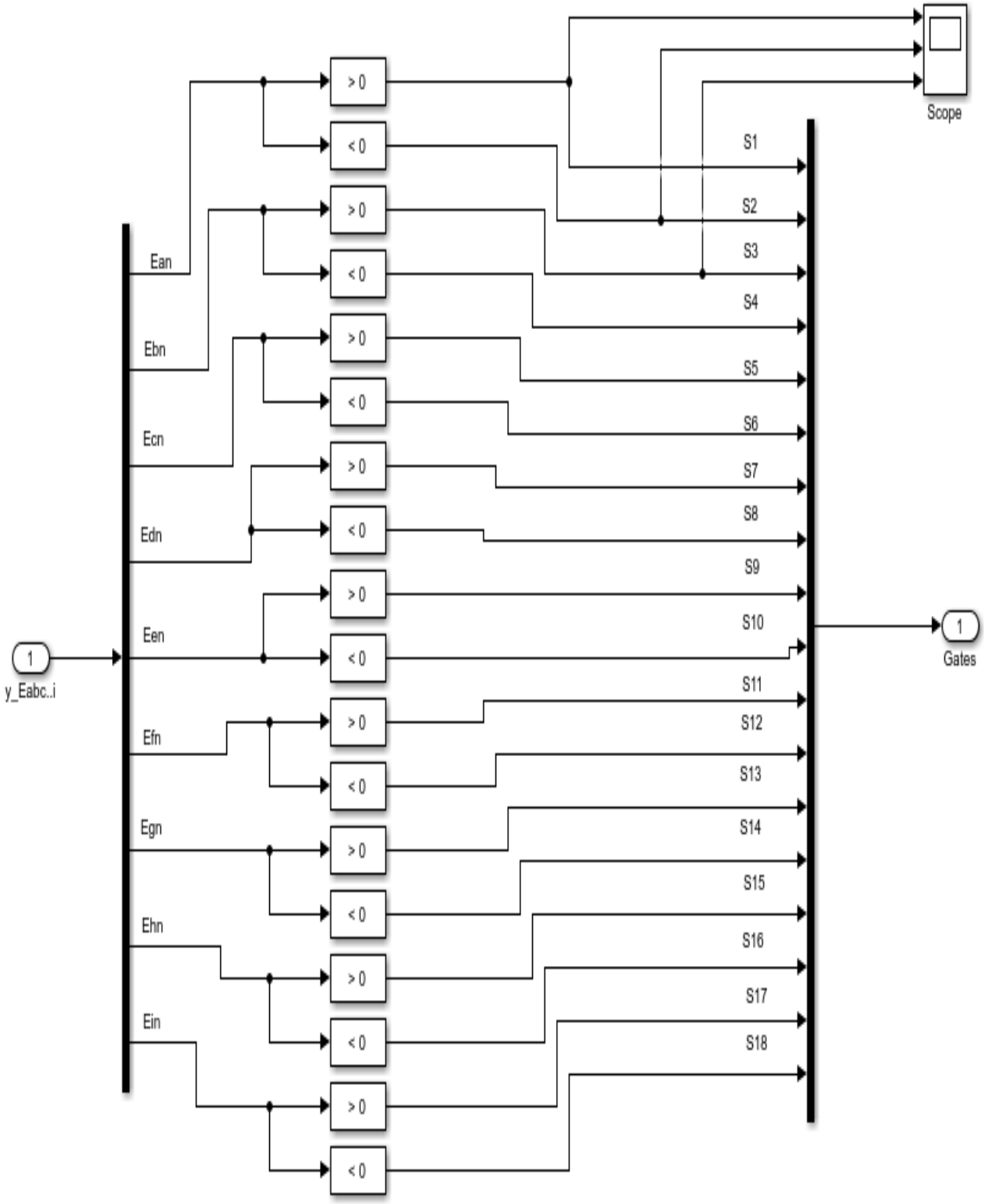

Fig. g) Simulink model of eighteen-step pulse generator function Simulink block

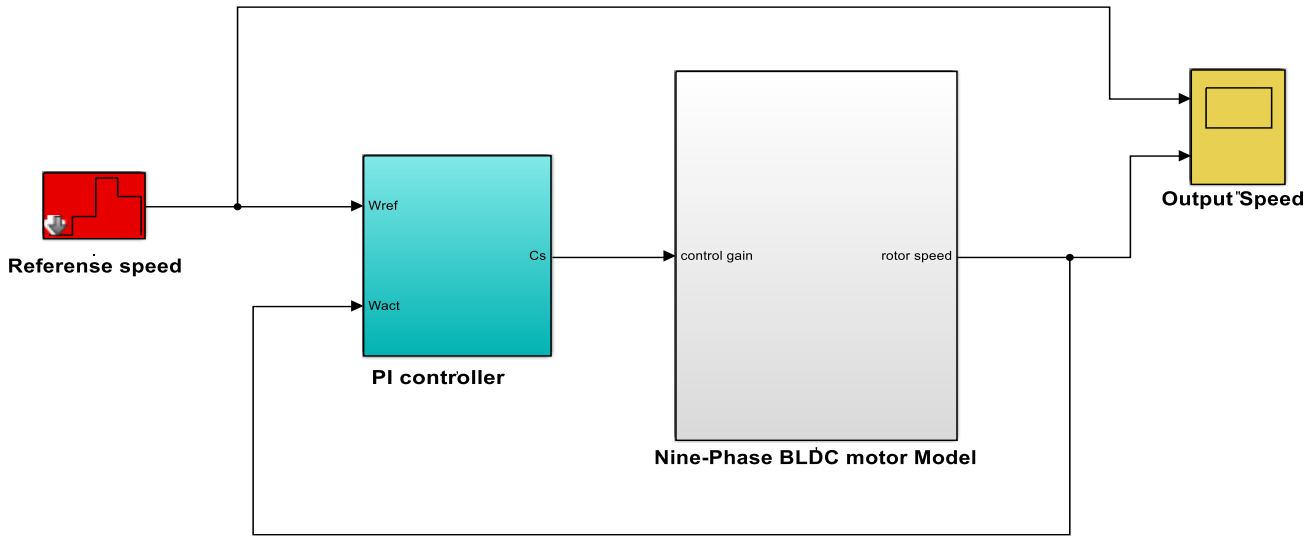

Fig. h) the overall closed loop PI Control Simulink block

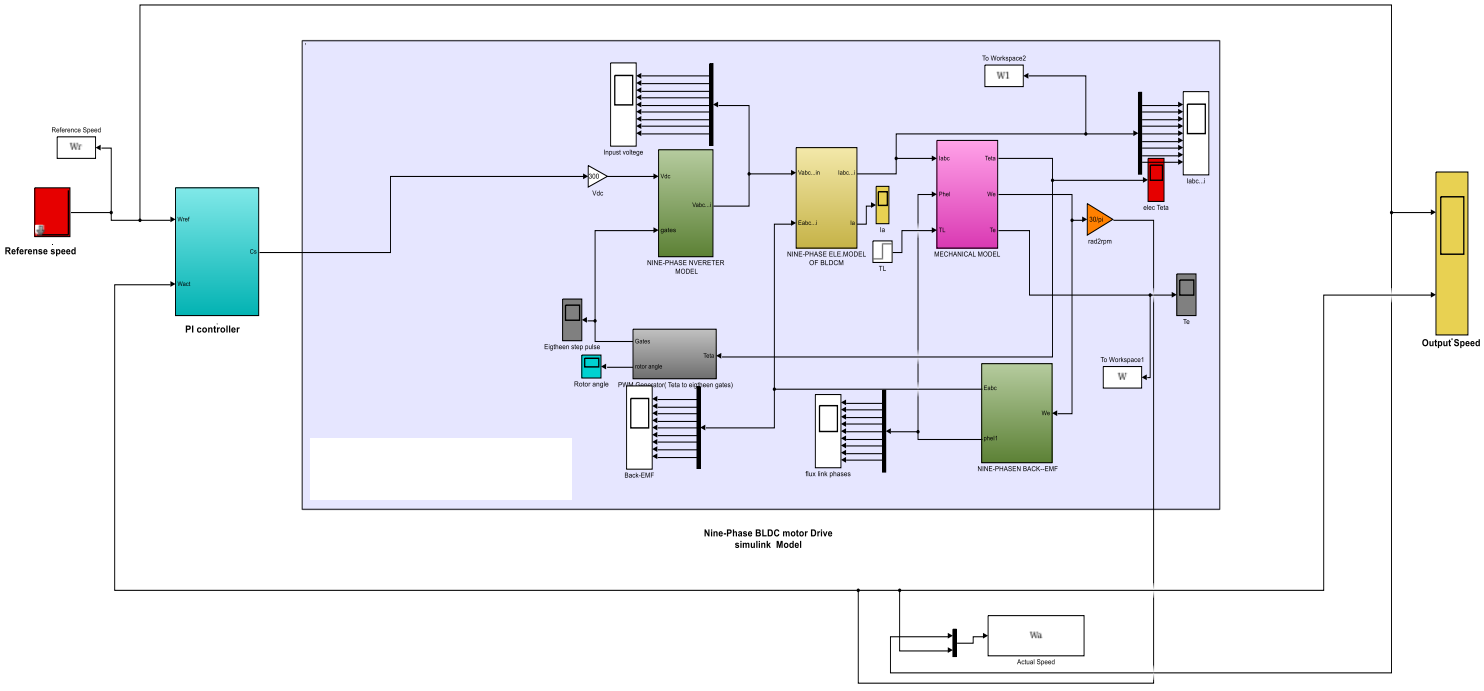

Fig. i) Expanded closed-loop PI Control Simulink model block

Appendix-B MATLAB codes used in the paper

A) Parameters of the of the model

Nphaseparas.m

```
% The parameters of the BLDC Motor
R=0.7;          % Resistance of the stator winding
L=0.00052;      % elf Inductance of the stator winding
M=0.00021;      % mutual Inductance of the stator winding
J=0.00025;      %Inertia of the motor (kg.m2)
B=0.00005;      %Friction constant
ke=0.0175;      % Back-EMF constant in(V/rpm)
kt=1.0;         %Torque constant (Nm/A)
p=2;            % Magnetic poles of the PM
TL=4;           % load torque in Nm
Vdc=300;        % Dc voltage source
```

And evaluated parameters

Nevaluatedparas.m

```
%
% Start code
% Evaluated constants para not give
%
Nphaseparas
te=L/(8*R);    % In the case of BLDC motor each time 8 phase is contributed
tm=(8*R*J)/(ke*kt); % similarly 8 phase is active and one phase turned off
%
% End code
```

B) Back-EMF sequence to eighteen-pulse generator MATLAB function used for 160^0 operating mode in the paper

emfL.m

```
% Back-EMF sequence to eighteen-pulse generator
function y=emfE(u)
```

```
if(u>-180)&&(u<=-160)
    y=[-1;1;1;1;1;0;-1;-1;-1];
elseif(u>-160)&&(u<=-140)
    y=[-1;0;1;1;1;1;-1;-1;-1];
elseif(u>-140)&&(u<=-120)
    y=[-1;-1;1;1;1;1;0;-1;-1];
elseif(u>-120)&&(u<=-100)
    y=[-1;-1;0;1;1;1;1;-1;-1];
elseif(u>-100)&&(u<=-80)
    y=[-1;-1;-1;1;1;1;1;0;-1];
elseif(u>-80)&&(u<=-60)
    y=[-1;-1;-1;0;1;1;1;1;-1];
elseif(u>-60)&&(u<=-40)
    y=[-1;-1;-1;-1;1;1;1;1;0];
elseif(u>-40)&&(u<=-20)
    y=[-1;-1;-1;-1;0;1;1;1;1];
elseif(u>-20)&&(u<=0)
    y=[0;-1;-1;-1;-1;1;1;1;1];
elseif(u>0)&&(u<=20)
    y=[1;-1;-1;-1;-1;0;1;1;1];
elseif(u>20)&&(u<=40)
    y=[1;0;-1;-1;-1;-1;1;1;1];
elseif(u>40)&&(u<=60)
    y=[1;1;-1;-1;-1;-1;0;1;1];
elseif(u>60)&&(u<=80)
    y=[1;1;0;-1;-1;-1;-1;1;1];
elseif(u>80)&&(u<=100)
    y=[1;1;1;-1;-1;-1;-1;0;1];
elseif(u>100)&&(u<=120)
    y=[1;1;1;0;-1;-1;-1;-1;1];
elseif(u>120)&&(u<=140)
    y=[1;1;1;1;-1;-1;-1;-1;0];
elseif(u>140)&&(u<=160)
    y=[1;1;1;1;0;-1;-1;-1;-1];
elseif(u>160)&&(u<=180)
    y=[0;1;1;1;1;-1;-1;-1;-1];
end
```

Open loop simulation for speed control and different stability checking code used

```
% This the S-domain analysis or step response of Nine phase macchine

% Start code

close all;

clear all;
```

```
clc
% include all costants parametrs
Nphaseparas
% include evaluated constants
Nevaluatedparas
% Transfer function
G=tf([1/ke],[te*tm tm 1])
% Plots the step response diagram
figure;
step(G,1);
title('open loop step response diagram');
xlabel('time in [s]');
ylabel('The openloop responce');
grid on;
```